# Optical Control of Signal Transduction and Other Cellular Processes

by

Kalyn Anette Brown

B.S. Biochemistry, Indiana University, 2010

Submitted to the Graduate Faculty of

The Dietrich School of Arts and Sciences in partial fulfillment

of the requirements for the degree of

Doctor of Philosophy

University of Pittsburgh

2016

UNIVERSITY OF PITTSBURGH

The Dietrich School of Arts and Sciences

This dissertation was presented

by

Kalyn Anette Brown

It was defended on

October 2, 2015

and approved by

W. Seth Horne, PhD, Associate Professor, Chemistry

W. Seth Childers, PhD, Assistant Professor, Chemistry

Parth Roy, PhD, Associate Professor, Bioengineering and Pathology

Dissertation Advisor: Alexander Deiters, PhD, Professor, Chemistry

**Optical Control of Signal Transduction and Other Cellular Processes**

Kalyn Anette Brown, PhD

University of Pittsburgh, 2016

Nature uses precise spatio-temporal control to maintain proper cellular function. Being able to replicate this control is an important step in investigating proteins. The research presented here uses photo-labile "caging" groups and light to control protein function including signaling cascades, protein localization and dimerization. Cell signaling is an essential process that allows cells to respond to extracellular stimuli. Four kinases, ERK2, p38α, JNK1 and PAK1, were targeted to optochemically control signal transduction. ERK2, p38α, and JNK1 are MAP kinases that are implicated in cell proliferation, apoptosis, motility, and differentiation. PAK1 is a serine/threonine kinase that affects focal adhesion dynamic and action reorganization. Incorporation of a photocaged lysine into the ATP binding pocket of PAK1 allowed for optical control of PAK1 kinase activity and paxillin focal adhesions. Ras GTPases are membrane bound molecular switches involved in various pathways that convert stimuli into a cellular response. Membrane localization of Ras GTPases is determined by the C-terminal CaaX domain. Within the CaaX domain, cysteine residues are modified by the addition of a farnesyl group and two palmitoyl groups. Ultimately, photochemical control of membrane localization by CaaX domain signaling was used to determine the kinetics of CaaX domain processing. Src family tyrosine kinases are involved in cell proliferation, cytoskeletal alterations, differentiation, survival,

adhesion, and migration and are localized to the membrane through the modification of a SH4 domain with myristoylation and palmitoylation. Optochemical control of SH4 domain mediated membrane localization was not achieved. Finally, the dimerization of FKBP12 and FRB was photochemically controlled by the development of a photo-cleavable rapamycin dimer. Rapamycin heterodimerizes FKBP12 and FRB and has been exploited as a research tool in a wide array of cellular processes. Photochemical control of protein localization and dimerization allows for precise spatial and temporal control over these processes, which will lend to the development of useful biological tools.

## TABLE OF CONTENTS

## LIST OF TABLES

## LIST OF FIGURES

# PREFACE

I would like to thank my advisor, Dr. Alexander Deiters, for his support during my graduate career. I would also like to thank my committee, Dr. W. Seth Horne, Dr. W. Seth Childers, and Dr. Partha Roy for their time and suggestions and the staff in the Chemistry Department at the University of Pittsburgh for being welcoming and helpful. I would also like to say thank you to the staff in the Chemistry Department at North Carolina State University for their support. I would also like to acknowledge the members of the Deiters Lab who were an invaluable part of my time in the lab. James, Alex, and Meryl, I am honored to have gone through the experience with the three of you. To the ladies of the Deiters Lab, each of you made the good times the best and the bad times better.

Most importantly, I would like to thank my parents, Rod and Lyn. Your love and endless support has been the backbone of my education. I would have never made it from Richmond to Bloomington to Raleigh to Pittsburgh without you both. Thank you moving me multiple times. Thank you being the best through my worst and never giving up when I really wanted to stop. I will never be able to repay you for everything you have done for me.

# 1.0 UNNATURAL AMINO ACID MUTAGENESIS AND PHOTOCHEMICAL CONTROL

## 1.1 UNNATURAL AMINO ACID MUTAGENESIS

In order to control protein function, the methodology of unnatural amino acid mutagenesis can used with photocaged amino acids. Unnatural amino acid mutagenesis allows for the genetic incorporation of amino acid analogs into proteins that can introduce new function. These functions can include bioorthogonal reactive handles, IR or NMR probes, fluorescent side chains, heavy atom side chains for structure determination and photolabile side chain for optochemical control.[1]

### 1.1.1 History of Unnatural Amino Acid Mutagenesis

Biosynthetic incorporation of unnatural amino acids first occurred in 1989. This was achieved through the chemical mis-aminoacylation of suppressor yeast tRNAs. When this tRNA-UAA was combined with the other necessary components for translation from *E. coli* cells, incorporation of the unnatural amino acid (UAA) at the TAG amber stop codon was achieved *in vitro*.[2] While it was an important milestone in the UAA incorporation field, there were limitations to this approach. The tRNA aminoacylation yield was only 45% and the incorporation efficiency was only 15-20%. The low yields of these reactions required large amounts of starting

materials in order to obtain relevant protein quantities. In 1995, Schultz, Dougherty, Lester and co-workers achieved the first incorporation of an UAA in cells through injection of the aminoacylated suppressor yeast tRNA and mRNA containing a TAG stop codon into *Xenopus* oocytes.[3] This method was used to incorporate tyrosine and phenylalanine analogs at three specific positions within the nicotinic acetylcholine receptor to investigate their importance in ligand binding.

Beginning in 2001, genetic incorporation of UAAs emerged. The Schultz lab adapted a tyrosyl-tRNA and tyrosyl-tRNA synthetase (TyrRS) pair from *Methanococcus jannaschii* for amber stop codon suppression in *E. coli*.[4] The tRNA was mutated in order to reduce recognition by endogenous *E. coli* synthetases and the TyrRS was randomized at 5 essential amino acid-recognition sites in close proximity to the Tyr OH group; a selection was performed to identify a synthetase that specifically recognized the UAA, *o*-methyl-L-tyrosine and charges the cognate suppressor tRNA. By transforming *E. coli* with DNA that encoded the suppressor tRNA, the mutant TyrRS, and the gene of interest, dihydrofolate reductase containing a TAG mutation, the biosynthetic machinery of *E. coli* produced dihydrofolate reductase with o-methyl-L-tyrosine incorporated. The *M. jannaschii* pair has been extensively used in *E. coli*.[1,5] In each of these examples, a library of mutant TyrRSs were subjected to a selection for the specific recognition of o-nitrobenzyl-o-tyrosine and sulfotyrosine, respectively.

Incorporation of UAAs in eukaryotes has also been achieved. The yeast genetic code has been expanded with a tyrosyl-tRNA/TyrlRS pair from *E. coli*,[6] a pyrrolysyl-tRNA/PylRS from *Methanosarcina barkeri*,[7] and a leucyl-tRNA/LeuRS from *E. coli*.[8] The first example of expression of proteins with UAAs in mammalian cells was in 2002 using a suppressor tRNA from *Bacillus stearothermophilus* and a TyrlRS from *E. coli* to encode 2-iodo-L-tyrosine.[9] A

*Bacillus subtillis* suppressor tRNA and trypotophanylRS have also been using to incorporate 5-hydroxytryptophan, a fluorescent probe, into mammalian cells.[10]

In 2008, the *Methanosarcina mazei* pyrrolysyl-tRNA synthetase and tRNA pair was used for unnatural amino acid mutagenesis.[11] Pyrrolysine is the 22$^{nd}$ amino acid and is incorporated in response to a UAG codon in archaea by a dedicated tRNA and pyrrolysyl-tRNA synthetase (PylRS).[12] This natural amber suppression system was adapted to several UAAs, in a similar way as the TyrRS and LeuRS enzymes were engineered previously. Initial UAAs that were encoded using mutant PylRS enzymes were N$^{\varepsilon}$-benzyloxycarbonyl-L-lysine,[11] krzyN$^{\varepsilon}$-acetyl-L-lysine,[13] and *o*-nitrobenzyl-oxycarbonyl-N$^{\varepsilon}$-L-lysine.[14,15]

In 2009, the Deiters and Chin labs used the *M. bakeri* PylRS/tRNA pair to incorporate a photocaged lysine (**PCK**, Figure 1).[16] The PylRS was mutated at five positions and three rounds of positive and negative selection yielded a synthetase (PCKRS) with mutations (M241F, A267S, Y271C, and L274M) that specifically enabled incorporation of **PCK**.

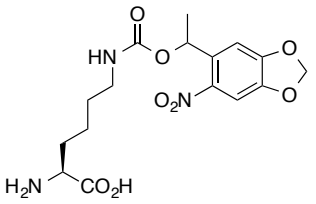


**PCK**

**Figure 1:** Structure of the photocaged lysine PCK.

In order to successfully incorporate unnatural amino acids into mammalian cells, the suppressor tRNA, the corresponding aminoacyl tRNA synthetase (RS), the unnatural amino acid, and the DNA encoding the protein of interest containing the TAG mutation must all be present (Figure 2**A)**. When added to the growth media of mammalian cells, the UAA will be transported into the cell. Plasmid DNA encoding the suppressor tRNA and the RS is transfected into cells

and the endogenous cellular machinery expresses the tRNA and RS for incorporation and expression of the protein of interest. The RS, evolved for the UAA (shown in red), will specifically charge the suppressor tRNA (shown in blue) with the unnatural amino acid (shown in blue). The evolved RS is orthogonal to all endogenous tRNAs and the suppressor tRNA is orthogonal to all endogenous RSs. The acylated suppressor tRNA than delivers the UAA in response to the UAG codon that was introduced into the mRNA of the protein of interest, enabling site-specific incorporation into the growing polypeptide chain at the desired residue.

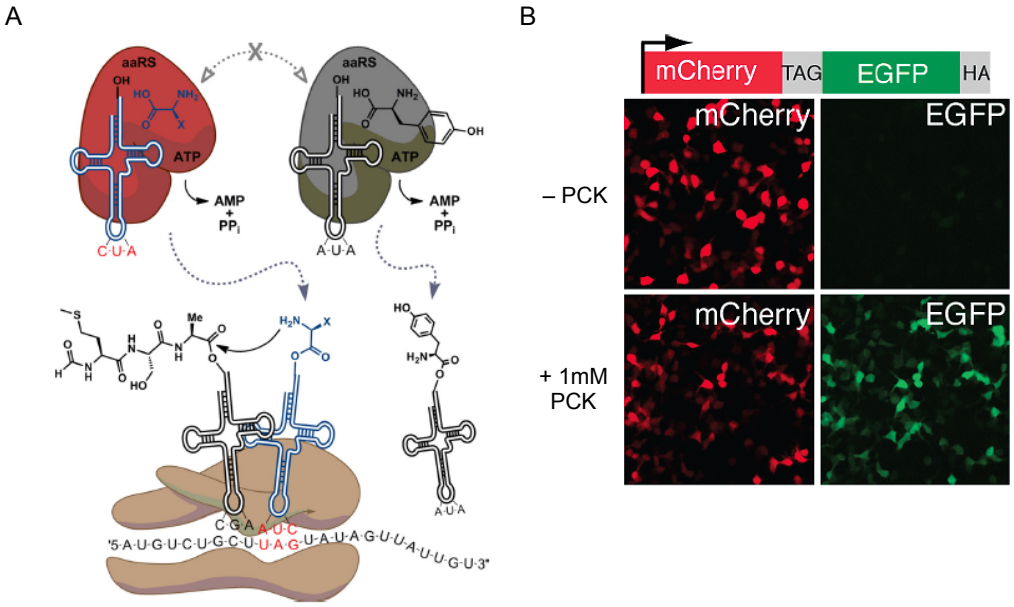


**Figure 2: A)** Schematic of unnatural amino acid incorporation. This research was originally published in Journal of Biological Chemistry. Young, T.S and Schultz, P.G. Beyond the Canonical 20 Amino Acids: Expanding the Genetic Lexison. *Journal of Biological Chemistry*. 2010; 285:11039-11044. © the American Society for Biochemistry and Molecular Biology. **B)** Incorporation of PCK into a reporter plasmid. Adapted with permission from Gautier, A. *et. al.* 2010, *132*. Copyright 2010 American Chemical Society.

**PCK** incorporation was validated by using a reporter construct in human embryonic kidney (HEK293T) cells (Figure 2**B**) that only shows EGFP fluorescence after suppression of TAG codon. EGFP fluorescence is only observed in the presence of **PCK**, demonstrating a high specificity of the mutant synthetase for the UAA over any of the endogenous amino acids. These results were further confirmed by MS/MS analysis.

The field of unnatural amino acid mutagenesis is rapidly expanding. Most recently this has include the incorporation of UAAs into mouse tissue, *C. elegans*, and *D. melanogaster*.[17-20]

## 1.2 PHOTOCHEMICAL CONTROL

Nature has developed precise spatial and temporal control of biological processes on the unicellular and multicellular level. Processes such as DNA replication,[21] cell signaling,[22] molecular transport,[23] and protein biosynthesis[24] depend on the location of proteins, DNA, and other biomolecules and the timing of their activity and interactions. In trying to elucidate the mechanisms of cellular processes, it is crucial to examine them with conditional activation that allows for spatiotemporal control comparable to that of the natural system.[25,26] Light is a unique external regulatory element that can be used to control biological processes with high resolution. The simplicity and accuracy of timing, location, and amplitude associated with light exposure makes it an ideal non-invasive technique for use in biology.[25,27-29]

### 1.2.1 Methods for Photochemical Control

Photochemical control of proteins can be achieved through the application of multiple methodologies (Figure 3). These methodologies include optogenetic approaches such as the use of LOV domains, phytochromes/cryptochromes, and channelrhodopsins as well as the use of photoremovable protecting groups or "caging groups".[30,31] Caging groups can be added to a

critical position within the protein (or to small molecule effectors) to render the molecule inactive until the group is removed through light exposure, typically UV light of ≥365nm.

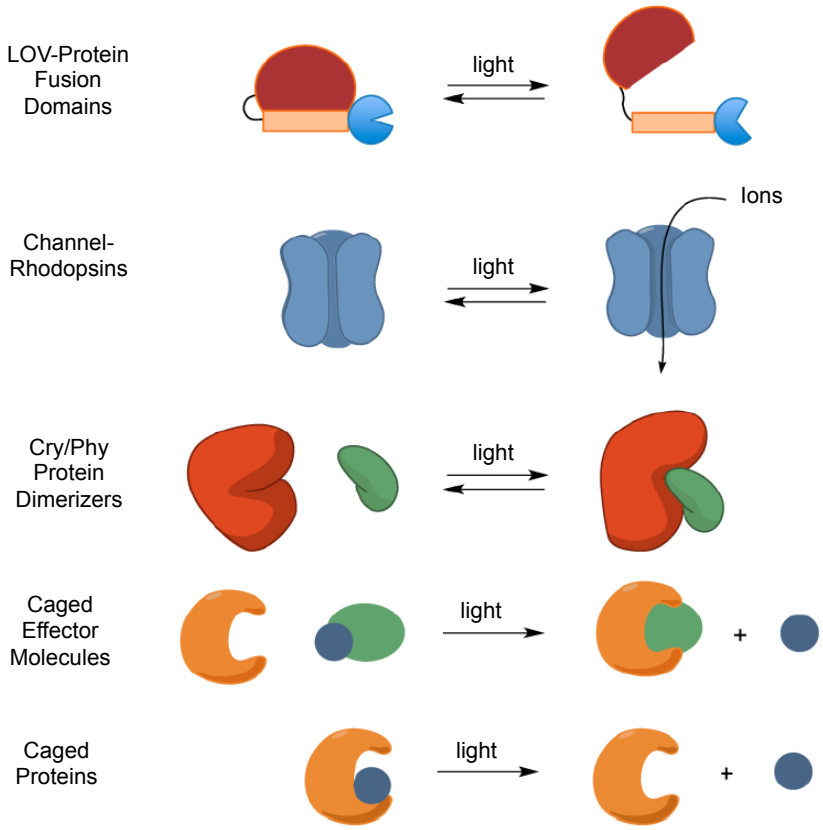


**Figure 3:** Schematic of methods for photochemical control of biological processes. Adapted with permission from Baker, A. S.; Deiters, A. *ACS Chemical Biology* 2014, *9*, 1398. Copyright 2014 American Chemical Society.

### 1.2.1.1 Optogenetic Approaches

Optogenetic approaches include the use of photo-responsive proteins that are found in Nature. These include light-oxygen-voltage (LOV) sensitive domains, channelrhodopsins, phytochromes, and cryptochromes. These approaches have been used to control various cellular functions including transcription, DNA recombination, post-translational modifications, cytoskeleton dynamics, signaling, and localization (Table 1).

**Table 1**: Functions that have been controlled by LOV domains, phytochromes, and crytochromes. Reprinted by permission from Macmillan Publishers Ltd: Nature Chemical Biology, Gautier, A.; Gauron, C.; Volovitch, M.; Bensimon, D.; Jullien, L.; Vriz, S., How to control proteins with light in living systems. 2014, *10* (7), 533-41, copyright 2014.

| Light target | Light-gated module | Biochemical output | Targeted feature |
|---|---|---|---|
| FAD CRY | CRY2-Gal4BD transcription factor | CIB1-Gal4AD binding | Transcription initiation |
| FAD CRY | CRY2-CreN recombinase | CIBN-CreC binding | Recombination |
| FAD CRY | Tale-CRY DNA binding | CIB1-VP64 binding | Transcription initiation |
| FAD CRY | Tale-CRY DNA binding | CIB1-Sin3IDx4 binding | Histone acetylation |
| FMN LOV2 | DHFR(x2)-LOV2 DHRF | TH-folate synthesis | Nucleotide biosynthesis |
| FMN LOV2 | LOV2-TAP Trp repressor | DNA binding | Gene expression |
| FMN LOV2 | Lov-Rac1 small GTPase | GTPase | Actin dynamics |
| FMN FKT1 | FKT1-VP16AD transcriptional activator | GI-Gal4BD binding | Transcription initiation |
| FMN FKT1 | FKT1-Rac1 small GTPase | G1Cher-CAAX binding | Actin dynamics |
| FMN LOV2 | LOV2-degron-targeted protein | Ubiquitination | Protein degradation |
| FMN LOV | mPAC adenylate cyclase[a] | cAMP | Signaling |
| FAD VVD-LOV | Gal4-vivid transcription factor | DNA binding | Gene expression |
| FAD BLUF | bPAC adenylate cyclase[a] | cAMP | Signaling |
| Bilin PHY | PHY-Gal4BD transcript. factor | PIF-Gal4AD binding | Transcription initiation |
| Bilin PHY | PHY-Cdc42 small GTPase | PIF-WASP binding | Actin dynamics |
| Bilin PHY | PHY-mCherry-CAAX mb. anchor | PIF -YFP binding | Protein trafficking |
| Bilin PHY | PHY-mCherry-CAAX mb anchor | iSH-YFP-PIF PI3K activation | Signaling |

The LOV domain is found in all kingdoms of life and was first discovered in plants. It is a photoreceptor kinase that uses a flavin mononucleotide to bind a conserved cysteine residue within the kinase. Photoexcitation of the LOV domain induces a structural change that allows for activation.[32] The LOV domain has also been used to control the activity of dihydrofolate reductase, zinc finger transcription factors, GTPases, and tryptophan repressors.[29-31]

One recent application of the LOV domain is the optical control of organelle transport.[33] This was first demonstrated with peroxisomes. A peroxisome-targeting domain fused with red fluorescent protein (RFP) and a LOV domain containing a caged peptide that binds ePDZb1 was designed along with a second fusion protein containing the ePDZb1, GFP, and kinesin (Figure 4**A)**. Kinesin is a motor protein that moves along microtubules. Expression of these proteins in

COS-7 cells showed localization of the PEX-LOV fusion protein to the center of the cell before light exposure presumably because the PEX-LOV protein was localized to peroxisome due to the peroxisome-targeting moiety. After a brief irradiation with blue light, the ePDZb1-binding peptide was exposed due to conformational change of the LOV domain (Figure 4**A**) and the peroxisome became bound to kinesin. This allowed for the transport of the peroxisomes to the outer edge of the cell (Figure 4**B)**. Peroxisomes did not move before irradiation with blue light. This indicated that LOV domains are capable of temporal control of peroxisome localization within cells.

Furthermore, peroxisome transportation could be controlled spatially (Figure 4**C)**. The colored rectangles were irradiated with blue light sequentially and the movement of the peroxisomes was analyzed (Figure 4**D)**. After irradiation, the peroxisomes moved towards the outer edge of the cells, but only from the areas that were exposed to blue light. Peroxisomes in the non-irradiated areas did not move from their initial locations. This demonstrated the ability for the LOV domain in this system to be used to spatially control protein localization within cells.

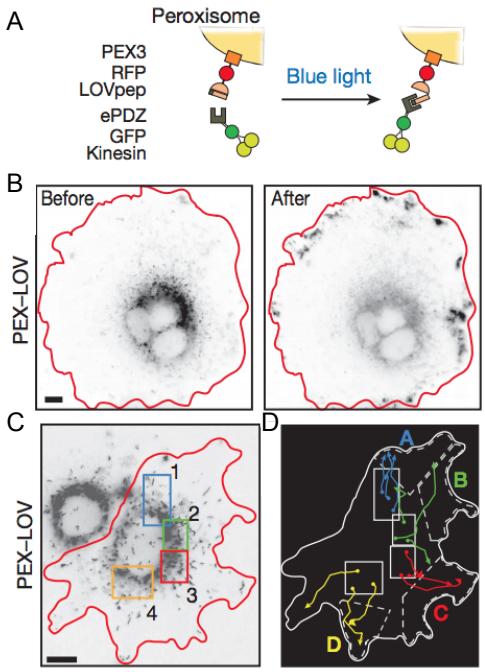


**Figure 4**: **A)** Schematic of experimental design for peroxisome transport using a LOV domain. **B)** Cellular localization of peroxisomes before and after illumination with blue light. **C)** Spatial irradiation of cells with PEX-LOV D) Movement of peroxisomes after spatial irradiation. Adapted by permission from Macmillan Publishers Ltd: Nature, van Bergeijk, P.; Adrian, M.; Hoogenraad, C. C.; Kapitein, L. C., Optogenetic control of organelle transport and positioning. 2015, *518* (7537), 111-4, copyright 2015.

This experimental design proved to be modular, as the researchers were able to control the localization of recycled endosomes and mitochondria temporally and spatially. The ability to control protein localization within the cell with tight spatiotemporal control will lend to the study of how organelle function is affected by their position as well controlling cellular processes like movement and signaling.

Channelrhodopsins contain a blue light-sensing chromophore that opens to form a pore upon exposure; this pore is then available for a flux of ions. The first channelrhodopsin was discovered in 2002 and was found to conduct multiple mono and divalent cations.[34] Within three years, channelrhodopsins were introduced into neuronal cells to change the charge potential. This approach has been successful in the study of neuron function,[35] and was featured as the Nature Methods method of the year in 2011.[36] Since the discovery of channelrhodopsins, multiple

modifications including codon optimization, amino acid mutations and trafficking mutations have been made.[37] Along with these mutations, variations in the activation wavelength and kinetics have been introduced. Channelrhodopsins can now be activated with wavelengths from 450 to 550 nm and can vary in the time of deactivation from seconds up to 30 minutes.

Phytochromes (Phy) and cryptochromes (Cry) are proteins that undergo conformational changed through absorptions of a photon. This structural change allows for the binding of a phytochrome interaction factor (PIF) and a cryptochrome-interact basic-helix-loop-helix protein (CIB), respectively.[30] This technology has been used to control transcription, Cre recombinase, histone acetylation, actin dynamics, signaling, and membrane localization.[30,31]

One application of the Phy technology is shown in Figure 5.[38] Upon irradiation with light of 650 nm, PIF and Phy interact (Figure 5**A**). Phy was localized to the membrane using a CaaX domain and YFP was fused to PIF (Figure 5**B**). When this system was expressed in mammalian cells, the membrane localization of YFP could be controlled by 650 nm irradiation (Figure 5**C**). Membrane localization was reversed when light with 750 nm was used and alternating light irradiations led to repeated localization of YFP fluorescence to the membrane and the cytoplasm.

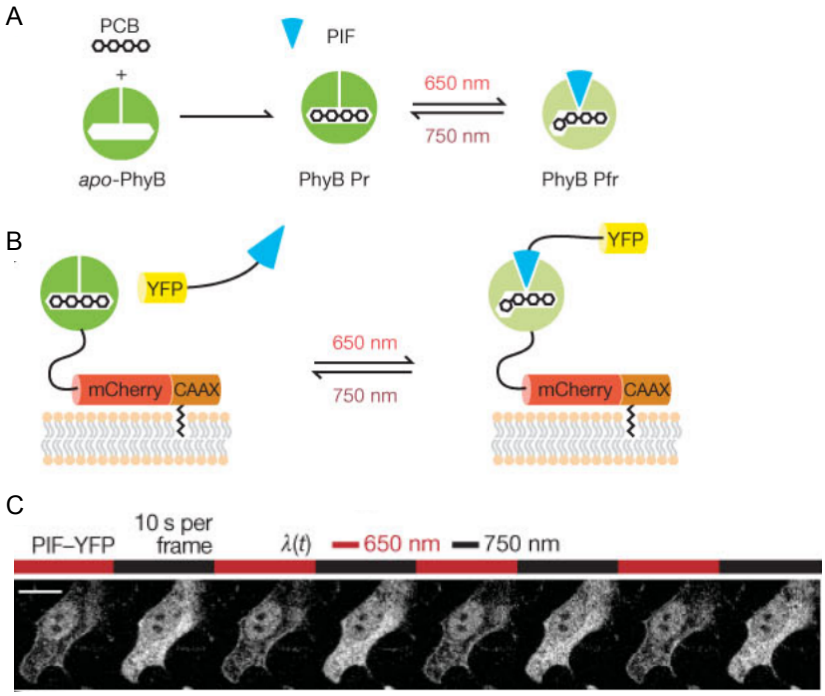


**Figure 5**: **A)** Phy and PIF interaction triggered by 650 nm light. **B)** Schematic of YFP membrane localization using Phy and PIF domains. **C)** Fluorescence microscopy of YFP localization when cell was irradiated with 650 nm and 750 nm light. Reprinted by permission from Macmillan Publishers Ltd: Nature, Levskaya, A.; Weiner, O. D.; Lim, W. A.; Voigt, C. A., Spatiotemporal control of cell signaling using a light-switchable protein interaction. 2009, *461* (7266), 997-1001, copyright 2009.

Using this conditional membrane localization, kinase activity was controlled (Figure 6). The membrane bound Phy was used to optically recruit Tiam, a Rac activator, through a PIF fusion (Figure 6**A**). The activation of Rac was observed by the development of lamellipodia (Figure 6**B**).

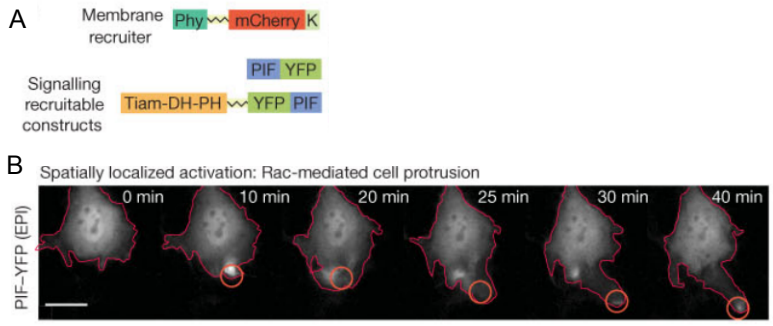


**Figure 6**: **A)** Schematic of membrane bound Phy and Tiam-PIF. **B)** Protrusion of mammalian cells through the activation of Rac by the membrane localization of Tiam. Tiam is localized to the membrane by the Phy-PIF interaction and subsequent activation of Rac is observed by the development of cellular lamellipodia. Reprinted by permission from Macmillan Publishers Ltd: Nature, Levskaya, A.; Weiner, O. D.; Lim, W. A.; Voigt, C. A.,

Spatiotemporal control of cell signalling using a light-switchable protein interaction. 2009, *461* (7266), 997-1001, copyright 2009.

Membrane localization has also been controlled with crytochrome domains (Figure 7). Here, the Cry domain was fused to a red fluorescent protein and its binding partner, CIB, was fused to a membrane localized green fluorescent protein (Figure 7**A**).[39] Before stimulation with blue light, red fluorescence can be seen throughout the cell (Figure 7**B**). After stimulation, the red fluorescence is localized at the membrane through an induced interaction of Cry and CIB.

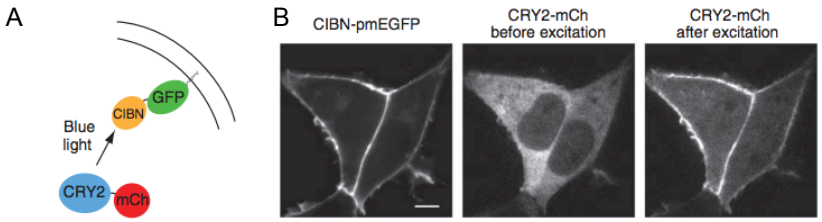


**Figure 7: A)** Schematic of membrane localization using a Cry and CIB domain. **B)** Localization of red fluorescent protein only after stimulation with blue light. Reprinted by permission from Macmillan Publishers Ltd: Nature Methods, Kennedy, M.; Hughes, R.; Peteya, L.; Schwartz, J.; Ehlers, M.; Tucker, C., Rapid blue-light-mediated induction of protein interactions in living cells. 2010, *7* (12), 973-U48, copyright 2010.

Cryptochrome technology has also been applied to conditional transcriptional activation using light-inducible transcription effectors (LITE, Figure 8).[40] A transcription activator-like effector (TALE), which recognizes a specific DNA sequence, is fused to a Cry domain and upon irradiation recruits a CIB-transcription factor fusion protein, activating the gene downstream (Figure 8**A**). This was demonstrated by designing a LITE for the *Grm2* gene and following the mRNA and protein levels in response to illumination (Figure 8**B**, Figure 8**C**). Before light stimulation, only background levels of mRNA (Figure 8**B**) and protein (Figure 8**C**) were observed. However, after irradiation with 466 nm light, both were increased by 2.5- and 7-fold, respectively.

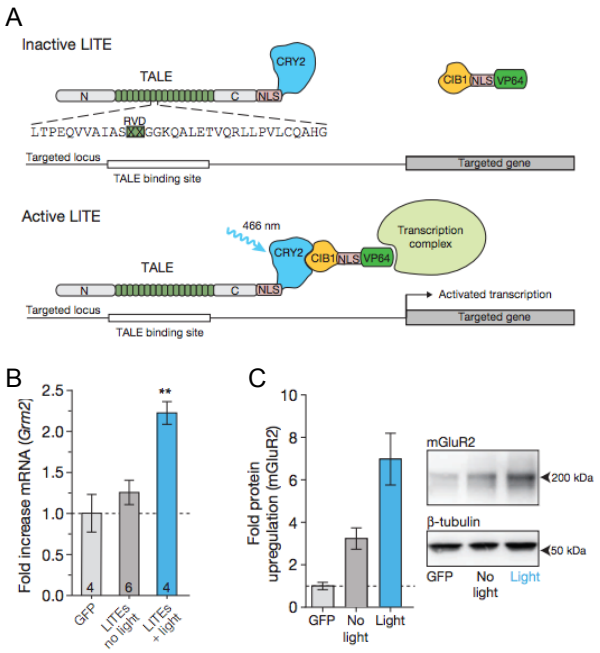


**Figure 8**: **A)** Schematic of light-inducible transcription effectors (LITE) **B)** mRNA expression changes and **C)** protein level changes of *Grm2* in response to LITE. Reprinted by permission from Macmillan Publishers Ltd: Nature, Konermann, S.; Brigham, M. D.; Trevino, A. E.; Hsu, P. D.; Heidenreich, M.; Cong, L.; Platt, R. J.; Scott, D. A.; Church, G. M.; Zhang, F., Optical control of mammalian endogenous transcription and epigenetic states. 2013, *500* (7463), 472-6, copyright 2013.

While these methods have been used successfully to control a wide range of biological processes, they require fusions of the photoresponsive proteins and the protein of interest. This can be difficult to implement and may not be possible for all proteins.

### 1.2.1.2 Photocaged Small-molecules

For proteins that are activated or deactivated through a small molecule interaction, the small molecule can be modified with a caging group to provide photochemical control. Small molecules that have been popular targets are agonists of inducible gene expression systems such as ecdysone,[41] IPTG,[42] doxycycline,[43] and toyocamycin.[44] The small molecules act as transcriptional and translational modulators and are functional in bacterial and mammalian cells. There are also small molecule effectors that can work at the post-translational level of protein

synthesis, e.g., photocaged rapamycin analogs.[45,46] These will be described in detail in Chapter 5.

#### 1.2.1.3 Photocaged Proteins

Caged proteins can be generated in multiple ways, including non-specific modification of amino acid residues, protein synthesis, and unnatural amino acid incorporation.[47,48] Protein ligation to form photocaged amino acids uses semisynthetic methods (Figure 9**A**).[49] For example, Smad2 (shown in orange in Figure 9**A**) minus the last five amino acids fused with the Smad-binding domain (SBD) of the Smad anchor for receptor activation (SARA) (shown in blue and gold)-maltose binding protein (MBP) was expressed in bacteria. The SBD-SARA-MBP fusion was necessary for increased stability of the Smad2. The last five amino acids with two phosphates, a carboxyfluorescein, and a quencher were synthetically prepared and the two parts were then ligated together to form the photocaged Smad2 complex.[50] The presence of the C-terminal caging group inhibited the homotrimerization of the SBD-SARA fusions. After irradiation, green fluorescence is present due to the removal of the quencher (Figure 9**B**) and homotrimerization can occur. A second caged Smad2 was designed without the phosphates on the peptide. When both of these were introduced into mammalian cells, there was very little fluorescence seen before irradiation (Figure 9**B**). After irradiation, fluorescence is seen and the localization of each Smad2 can be observed. The phosphorylated Smad2 was found in the cytoplasm and the nucleus, while the nonphosphorylated variants were found exclusively in the cytoplasm, supporting previous studies.

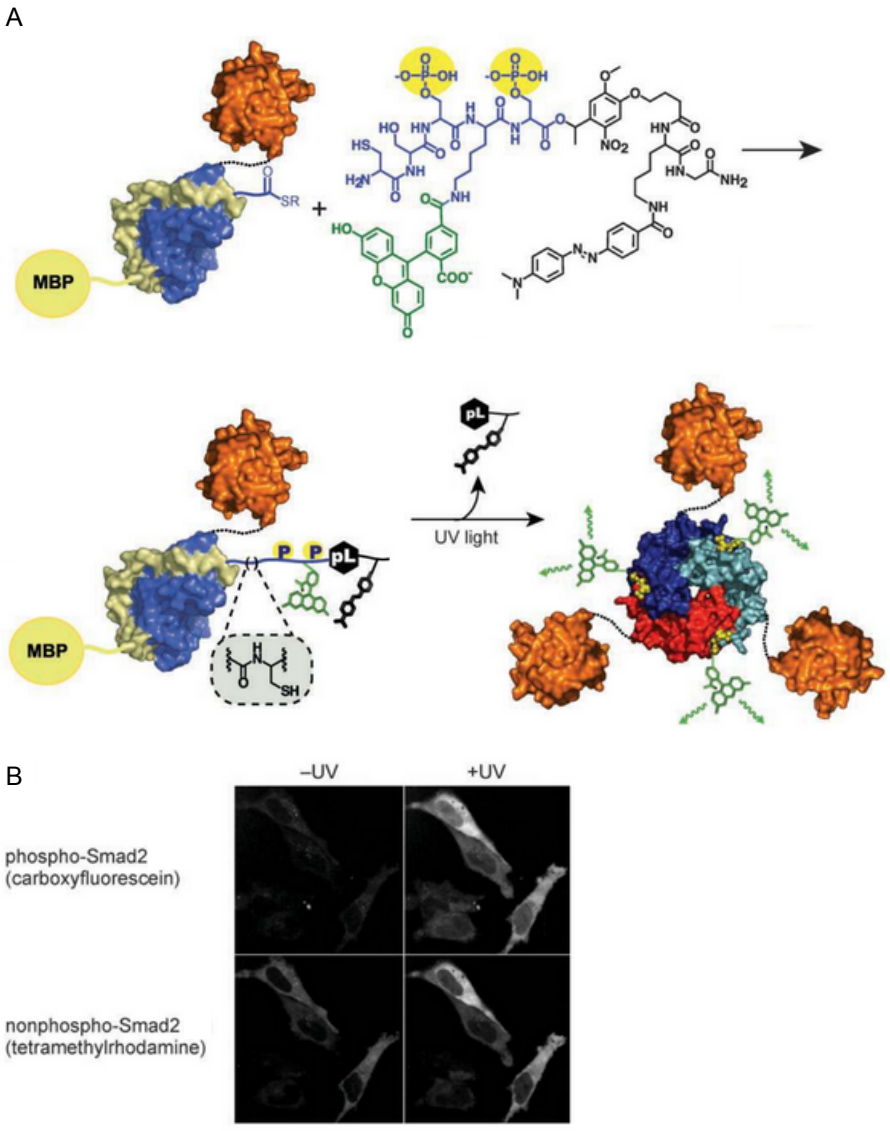


**Figure 9**: **A)** Generation of caged Smad2 through expressed protein ligation and decaging. **B)** Observed fluorescence of caged Smad2 complexes before and after UV irradiation and cellular localization. Hahn, M. E., Pellois, J. P., Vila-Perello, M. & Muir, T. W. Tunable photoactivation of a post-translationally modified signaling protein and its unmodified counterpart in live cells. *Chembiochem* 8, 2100-2105, doi:10.1002/cbic.200700404 (2007). Copyright 2007.

An example of generating photocaged amino acids using chemical modification was published by Ghosh and coworkers.[51] They applied α -bromo-(2-nitrophenyl)acetic acid to covalently modify a serine or cysteine side chain of cofilin (Figure 10). Cofilin is inactivated through a phosphorylation target of by LIM-kinase. The modification of S3 with α-bromo-(2-nitrophenyl)acetic acid generates a photocaged cofilin that is recognized as a phosphorylated serine and cofilin remained inactive. Upon irradiation and caging group removal, serine is

immediately phosphorylated and inactivated again. Site directed mutagenesis of S3 to cysteine produces a constitutively active cofilin that can also be caged. Upon treatment with α-bromo-(2-nitrophenyl)acetic acid a caged cofilin is generated and with irradiation, a constitutively active cofilin is generated as the cysteine side chain cannot be phosphorylated to inactivate cofilin. This was used to determine that cofilin assists in the formation of actin polymers and also contributes to the directionality of cell movement.[52] Before the use of photocaging to conditionally control cofilin, these questions were unanswered.

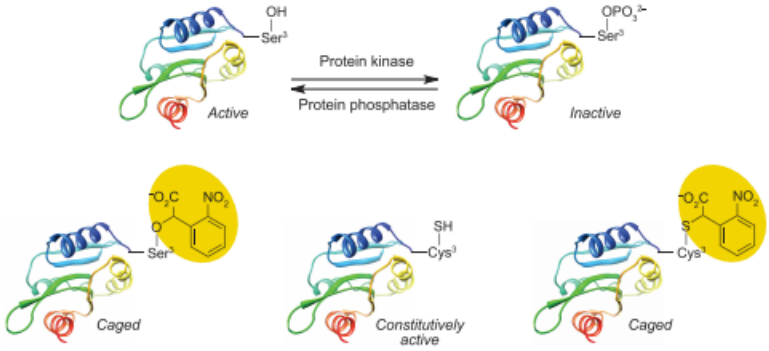


**Figure 10**: Schematic of cofilin deactivation by phosphorylation and the various forms of cofilin that were generated by Ghosh and coworkers. Adapted with permission from Lee, H. M., Larson, D. R. & Lawrence, D. S. Illuminating the chemistry of life: design, synthesis, and applications of "caged" and related photoresponsive compounds. *ACS Chem Biol* 4, 409-427, doi:10.1021/cb900036s (2009). Copyright 2009 American Chemical Society.

### 1.2.1.4 Photocaged Unnatural Amino Acids

Unnatural amino acids for the photochemical control of protein function include *o*-nitrobenzyl derivatives of tyrosine,[53,54] serine,[55] cysteine,[19,56-58] and lysine (**PCK**).[7,14,16]

The caging of proteins in cells through UAA incorporation has several distinct advantages over other optogenetic approaches. First, the caging group is very small (150-250 Da) and induces

little to no perturbation to the overall protein structure, enabling precise optical control of distinct functions. Second, the positioning of the caged amino acid can be determined based on protein structure or protein mechanistic information, thus obviating the need for extensive rounds of trial-and-error and protein engineering. However, the location of the caged amino acid must be at a position within the protein that will not interrupt caged protein expression and folding. Third, light exposure removes the caging group and generates the native, wild type protein. Irradiation with >360 nm light has been shown to cause no or minimal damage to biological systems. [59,60]

The incorporation of **PCK** was used to photochemically control protein localization using a nuclear localization signal (NLS), Figure 11**A**.[16] Within the NLS, a key lysine residue, that shows a decrease in nuclear localization when mutated to an aparagine,[61] was mutated to a TAG codon. An NLS-**PCK**-GFP fusion is expressed, showing fluorescence distributed throughout the cell, indicating inactivity of the caged NLS (Figure 11**B**). After UV irradiation, the native lysine is restored due to decaging and the NLS becomes fully active, as seen by the complete nuclear localization of GFP (Figure 11**B**). Because the starting point of translocation is known due to the timepoint of irradiation, the kinetics of nuclear import can be determined (Figure 11**C**). It was found that translocation from the cytoplasm to the nucleus had a half-time of ~20 seconds. Kinetic analysis of this specific NLS had not been performed until this investigation. Other analyses of bipartite NLSs have been performed when they are fused with various proteins of interest.[62] These studies were done by injecting cells with the NLS-tagged proteins and the half-time appears to be much longer compared to when the caged NLS was used.

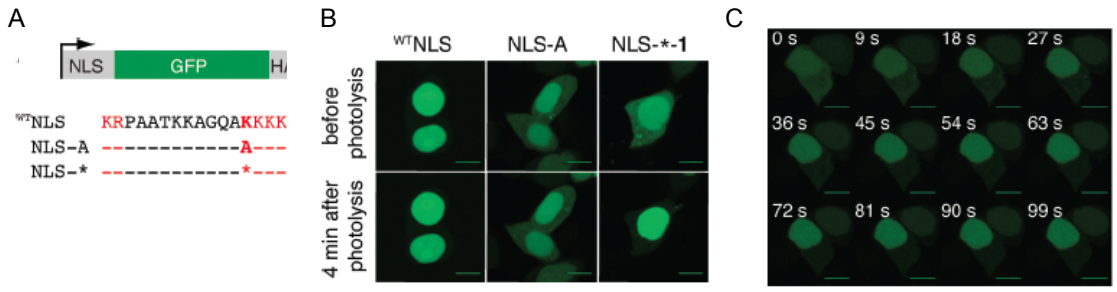


**Figure 11: A)** Nuclear localization sequence and position of the TAG mutation for incorporation of PCK. **B)** Cellular phenotype of wtNLS, NLS-A (alanine mutant) and NLS-PCK (denoted by * in figure) before and after irradiation. **C)** Time course of NLS-PCK translocation after UV irradiation. Adapted with permission from Gautier, A.; Nguyen, D.; Lusic, H.; An, W.; Deiters, A.; Chin, J. *J Am Chem Soc* 2010, *132*, 4086. Copyright 2010 American Chemical Society.

The site-specific incorporation of **PCK** and related caged amino acids enables the expression of photocaged proteins directly in mammalian cells.[54,58,63-65] This allows for tight spatiotemporal control of that protein and the cellular process to which it contributes. The work presented in this dissertation will use **PCK** and the above described unnatural amino acid mutagenesis to explore kinase signaling, membrane localization, and other cellular processes.

## 2.0 OPTICAL CONTROL OF SIGNAL TRANSDUCTION

Protein phosphorylation is an important post-translational modification that occurs on approximately 30% of cellular proteins.[66] Phosphorylation is catalyzed by kinases through transfer of the γ-phosphate from ATP or GTP to their protein target. This modification generates a conformational change that alters function or protein-protein interactions. Recognizing that this was an important aspect of cellular signaling, in 2002, the human kinome project was generate.[67] Manning and coworkers used sequence comparisons to evaluate the genome and found 518 potential kinases. This revealed the vast number of protein kinases throughout mammalian cells that are responsible for a vast array of cellular responses including, proliferation, differentiation, metabolism, cell structure and apoptosis.[67]

Conditional control of kinases has been an important research topic. Activation of kinases with light instead of traditional approaches such as genetic knockouts or small molecule inhibitors allows for precise temporal control of activation and limits the ability of the cell to adapt to the stimulation.[68-70] This unambiguous spatially and temporally controlled activation of kinases allows for the study of downstream targets, the kinetics of phosphorylation, feedback loops, and the resulting cellular response. Controlling kinases with light also allows for sub network control of the signaling pathways. Kinases throughout the pathway can be optochemically controlled to allow for insights into the function and feedback of each kinase.

Wu and coworkers developed a photoactivatable Rac1 using the LOV domain (Figure 12**A**).[71] Before irradiation, Rac1 is unable to bind with its downstream effector PAK1. The photoactivatable Rac1 was expressed in mammalian cells and used to investigate the motility of cells upon activation (Figure 12**B**). Upon irradiation, indicated by the yellow dot in Figure 12**B**, the closest cellular edge expanded while the opposite edge retracted. The red area, showing the new leading edge, and the purple area, which shows the original opposite edge, indicates that within 5 minutes of irradiation Rac1 is functional. Conversely, when the dominant negative variant of Rac1 is used with the photoactivatable LOV domain, the opposite cellular polarity is seen. Using the LOV domain allows for the reversible activation of Rac1, which can be used to study the motility of cells. The photoactivatable Rac1 was used to determine that Rac1 activation alone was adequate to induce cell polarity and movement, as well as to elucidate that PAK1 plays a role in aiding the development of protrusions. When PAK1 was inhibited with an inhibitory domain peptide, no membrane protrusions were observed upon activation of Rac1 with light. In contrast, myosin does not contribute to Rac1 induced protrusions, but it was found that cell motility directionality is diminished when myosin is inhibited. Finally, the use of a photoactivatable Rac1 was used to determine that RhoA is inhibited upon activation of Rac1. This had been disputed in the literature previously and the ability to spatially and temporally induce Rac1 activity allowed for the observation, through a RhoA biosensor, that Rac1 inhibits RhoA.

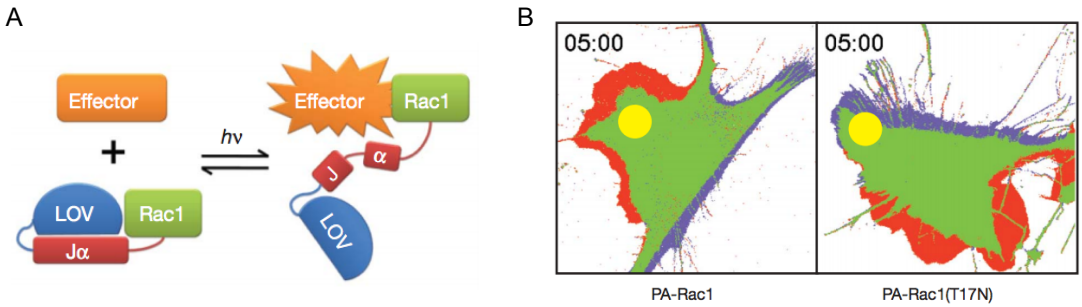


**Figure 12**: **A)** Schematic of optochemical control of Rac1 using LOV domain. **B)** Motility of mammalian cell expressing the LOV-Rac1 fusion protein. Cells were irradiation at the position indicated in yellow. Cells protrusion is indicated by red and cell retraction is indicated by purple. The first box shows the motility of a cell expressing the photoactivatable constitutively active Rac1, and the second box shows the motility of a cell expressing the photoactivatable dominant negative Rac1. Reprinted by permission from Macmillan Publishers Ltd: Nature Wu, Y. I.; Frey, D.; Lungu, O. I.; Jaehrig, A.; Schlichting, I.; Kuhlman, B.; Hahn, K. M. *Nature* 2009, *461*, 104, copyright 2009.

In 2011, Gautier and coworkers targeted the ATP binding pocket using **PCK** to control MEK1 activity.[65] **PCK** was genetically incorporated into position 97. This blocks binding of ATP until UV irradiation, decaging and restoration of the native lysine. Figure 13**A** shows that expression of constitutive active MEK1, denoted as A in lane 2, in mammalian cells phosphorylates ERK1/2. The caged MEK1, denoted as C in lanes 7-10, shows no ERK1/2 phosphorylation in the absence of UV irradiation. This is because **PCK** is encoded at position 97 and ATP cannot bind to the kinase. Upon irradiation and a short reaction time, ERK1/2 phosphorylation can be seen. The amount of ERK1/2 phosphorylation increases with increasing reaction time as expected. Furthermore, caged MEK1 can be expressed in mammalian cells and ERK1/2 localization can be observed in real time (Figure 13**B**). MEK1 phosphorylates ERK1/2 and induces translocation to the nucleus where it continues the signaling cascade through phosphorylation of transcription factors: c-myc, CREB, c-Jun, and ets. These transcription factors play a role in cell proliferation, apoptosis and cell cycle.[72-74] The translocation of ERK1/2 upon phosphorylation by MEK1 can be utilized to determine MEK1 kinase activity. In cells expressing EGFP-ERK2 and caged MEK1, EGFP fluorescence can be seen in the cytoplasm

before UV irradiation. This is due to the inactivity of MEK1 and lack of phosphorylation on ERK2. After irradiation, translocation of EGFP-ERK2 can be seen. Translocation occurs because caged MEK1 is decaged, which restores the native lysine at position 97 and the function of MEK1. MEK1 then phosphorylates EGFP-ERK2 and EGFP-ERK2 is quickly translocated to the nucleus. Epidermal growth factor (EFP) stimulates the receptor to begin the signaling cascade (Figure 13) and was shown to induce translocation within 4.5 minutes. Stimulation with EGF also results in the eventual export of ERK2 from the nucleus through the dephosphorylation of ERK2 by MAPK phosphatases (MKP in Figure 13**B**). It was hypothesized that this dephosphorylation and export from the nucleus is a negative feedback loop that inactivates the signaling pathway. Nature uses negative feedback mechanisms to terminate signaling to avoid over activation of signaling pathways.[75] Within 10 minutes of UV irradiation, the nuclear to cytoplasmic ratio of EGFP-ERK2 was found to be 4-fold higher. Light-activation of MEK1 induced translocation within 1.5 minutes, thus yielding a quicker response. This is due to the immediate activation of MEK1, unlike activation with EGF, which must be transduced from the receptor. However, in contrast to EGFP activation, photoactivation of MEK shows a steady-state of nuclear localization of EGFP-ERK2 over time. This leads to the conclusion that the negative feedback loop inactivates a kinase upstream of MEK1 in the pathway and not MEK1. This is in agreement with previous research that determined negative feedback loops using tradition genetic approaches such as siRNA knockdown and small molecule inhibitors. Mammalian cells were stimulated with platelet-derived growth factor (PDGF), which initiates signaling through the phosphoinositide 3-kinase pathway and the ERK pathway, and using various combinations of knockdown and small molecular inhibitors, the phosphorylation levels of ERK1/2 and MEK were investigated. Through this work, it was determined that ERK-dependent negative feedback

loop mediates signaling downstream of Ras. Although negative feedback loops were determined using traditional genetic approached, an immense amount of data was required to validate their signaling pathway model.[76] The kinetics of ERK2 phosphorylation had previously been investigated *in vitro* and a sigmoidal curve that was found when data were plotted was produced by the distributive, and not processive, phosphorylation of ERK2 at dual-phosphorylation sites by MEK1. This means that each phosphorylation site requires a separate kinase-substrate binding occurrence. It was hypothesized that the rate of import of ERK2 into the nucleus is determined by the MEK1 phosphorylation of ERK2. This was confirmed using photoactivatable MEK1 as the same sigmoidal kinetic graphs were observed for translocation of EGFP-ERK2 to the nucleus after irradiation and activation of MEK1. The determination of kinetics and the investigation of the negative feedback loop were possible because of the highly specific activation of MEK1. Light activation adds a precise level of control with minimal disruption compared to other techniques such as gene silencing or small molecule inhibition. Additionally, gene silencing and small molecule inhibition of kinases turn off function and have a slower reaction time in comparison to optochemical techniques, which turn on function as well as have a quicker initiation time. Being able to activate a signaling pathway at any point other than the cell membrane allows for investigation of temporal regulation of that pathway. Moreover, the approach of blocking the ATP binding site with **PCK** was proposed as a general approach to the optochemical control of kinases.

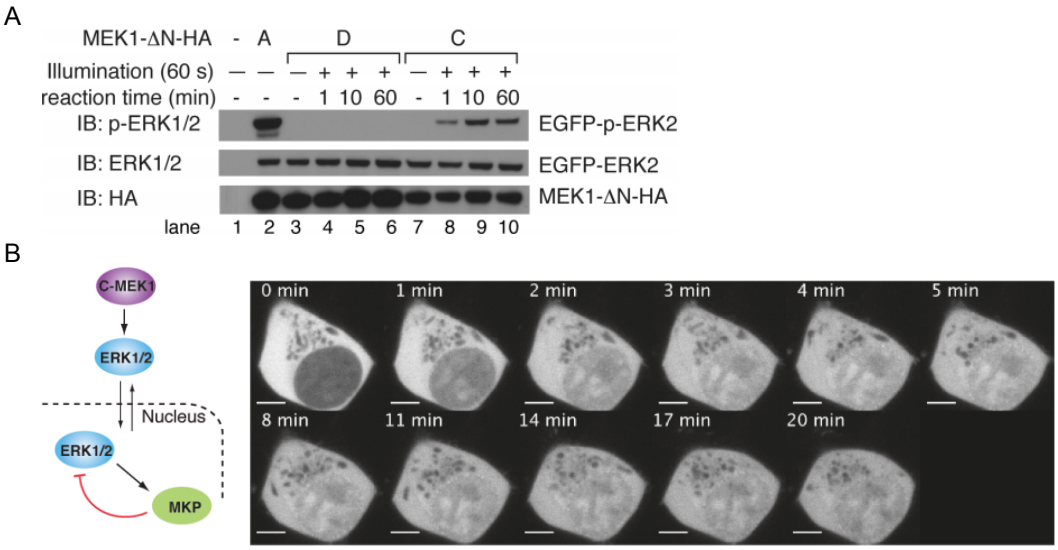


**Figure 13: A)** Phosphorylation of ERK2 by photocaged MEK1. MEK1-ΔN-A is a constitutively active variant of MEK1. Other forms used are identified as: D for dominant negative, and C for caged. IB denotes immunoblotting of specific proteins. **B)** Schematic and fluorescent images of EGFP-ERK2 nuclear import upon phosphorylation by MEK1 after UV irradiation. This is an unofficial adaptation of an article that appeared in an ACS publication. ACS has not endorsed the content of this adaptation or the context of its use. Gautier, A.; Deiters, A.; Chin, J. W. *J Am Chem Soc* 2011, *133*, 2124.

Also in 2011, two rapamycin analogs were used to control a small GTPase and a kinase, respectively.[45,46] Both of these examples are explained in Chapter 5.0 in detail. While conditional control of signal transduction proteins was successful using rapamycin analogs, they required fusion proteins, which could possibly interfere with protein function as well as a small molecule, which limits spatial control. Additional approaches for optochemically controlling kinases have been developed using the light sensitive protein domains described in Chapter 1.0 [38,77] The use of a photocaged amino acid, specifically **PCK**, in the ATP binding pocket eliminates these limits. Using this approach, the research below will describe three different potential targets within the signaling pathway for optochemical control of signal transduction.

## 2.1 OPTICAL CONTROL OF CDC42 AND RHOA ACTIVITY

### 2.1.1 Introduction

The first proteins that were targeted for optochemical control of signal transduction were cdc42 and RhoA. These are small molecular switches that cycle between GTP and GDP- bound states towards the beginning of the signaling cascade.[78] Binding of GTP induces a conformational change, that allows binding and activation of effector proteins.[79] cdc42 and RhoA have been implicated in the regulation of the cytoskeleton, transcription factors, cell-cycle progression, cell-cell contact and cell transformation.[78] Previous approaches to optochemically control cdc42 and RhoA have focused on their activation by Rac1[71] or have used a fused light-sensitive domain.[38] It was hypothesized that RhoA and cdc42 could be directly controlled through the installation of **PCK** in the GTP binding pocket and this precise spatio-temporal control could be used to further investigate the feedback loops between GTPases and Rac1.[71,80].

### 2.1.2 Caged cdc42 and RhoA

Plasmids expressing constitutively active and kinase dead RhoA (Q63L and T19N, respectively) and cdc42 (Q61L and T17N, respectively) were purchased from Addgene (plasmids #15900, #15901, #15906, and #15907). Site-directed mutagenesis was performed on the pRK5myc-GTPase plasmid to introduce a TAG mutation at K16 of cdc42 and K18 of RhoA. These lysine residues are conserved in Rho, Rac, cdc42 and Ras isoforms and are located in the phosphate-binding loop of the ATP binding pocket in each protein (Figure 14).[81] The main chain and side

chain of this conserved lysine residue participate in hydrogen bonding with the phosphate group of the GTP substrate.

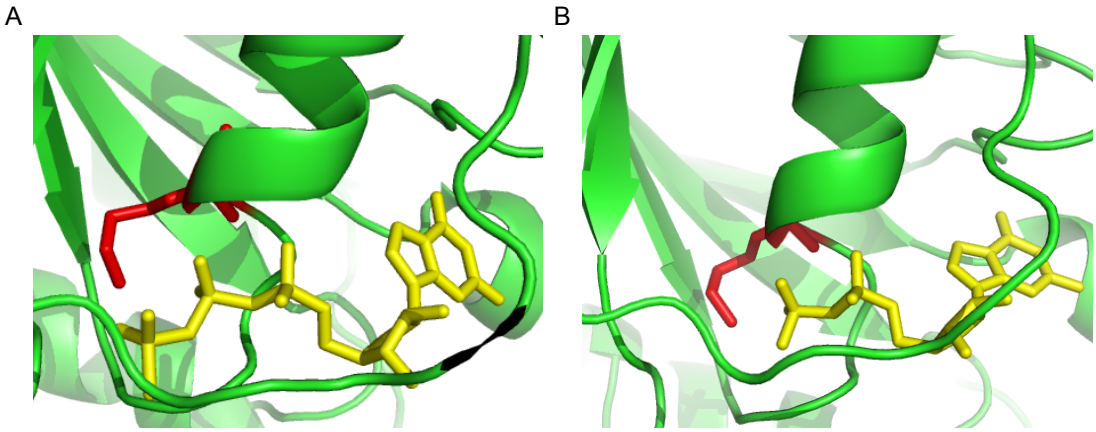


**Figure 14**: Crystal structures of **A**) RhoA and **B**) cdc42. K18 of RhoA and K16 of cdc42 are highlighted in red. An ATP analog in the RhoA structure and ADP in the cdc42 structure are highlight in yellow. PDB structures 1A2B (RhoA) and 2NGR (cdc42).

HEK293T cells were transfected with the plasmid expressing PCKRS and PylT[82] and pRK5myc-caRhoA K18TAG or pRK5myc-cacdc42 K16TAG in the presence of 1 mM of **PCK**. Twenty-four hours post-transfection, cells were lysed and analyzed for caged protein expression by Western blot using an anti-myc-tag antibody (Figure 15). Expression of the constitutively active and kinase dead mutant was detected, however no caged protein was detected for RhoA or cdc42 in the presence of **PCK**. Different parameters, such as **PCK** concentration, amount of DNA, transfection time, and lysis conditions, were explored but caged protein was not detected.

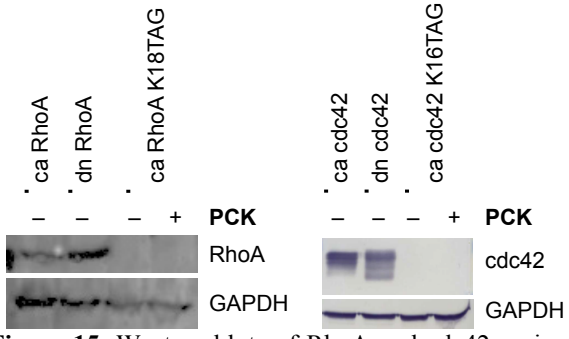


**Figure 15**: Western blots of RhoA and cdc42 variants. "ca" designates the constitutively active variants and "dn" designates the enzymatically inactive variants.

### 2.1.3 Experimental

**Site-directed Mutagenesis**. pRK5-myc-RhoA-Q63L and pRK5-myc-cdc42Q63L were mutated to contain K18TAG and K16TAG using the QuikChange Lightening protocol (Agilent). Primers were QC_RhoAK18TAG_Forw (5'-GATGGAGCCTGTGGATAGACATGCTTGCTC ATA) and QC_RhoAK18TAG_Rev (5'-TATGAGCAAGCATGTCTATCCACAGGCTCCATC) for mutation of RhoA. For mutation of cdc42, primers were QC_cdc42K16TAG_Forw (5'-GAT GGTGCTGTTGGTTAGAACTGTCTCCTGATA) and QC_cdc42K16TAG_Rev (5'-TATCAG GAGACAGTTCTAACCAACAGCACCATC) Annealing temperature was 60 ˚C and extension time was 4 minutes.

**Western Blotting of Caged GTPases**. HEK293T cells were maintained as described in Section 6.5 and split the day before transfection as described in Section 6.6. Transfection was performed with 1 μg of pRK5-myc-caGTPase TAG and 1 μg of pPCKRS-PylT or 2 μg of pRK5-myc-caGTPase or 2 μg of pRK5-myc-kdGTPase. Cells were incubated overnight at 37 ˚C/5% $CO_2$. The next day cells were washed with 1 mL of PBS and lysed with 500 μL of Mammalian Protein Extraction Buffer (GE Healthcare). Cells were shaken on ice of 10 minutes and lysates were centrifuged for 10 minutes at maximum speed (15,000 rpm/21,130 × *g*). Western blot was performed as described in Section 6.9 with mouse anti-myc and mouse anti-GAPDH antibodies (Santa Cruz) at a 1:1000 dilution. Secondary antibody was goat anti-mouse-HRP (Santa Cruz) diluted 1:1000 in TBST. Detection method used for the cdc42 Western blot was colorimetric. Colorimetric detection was performed by mixing 120 μL of 0.3% hydrogen peroxide with 4 mg of 4-chloro-1naphthol (4CN) in 20 mL of TBS. This solution was added to the membrane and allowed to develop for 15 minutes. Images were taken with a scanner. RhoA Western blots were detected with chemifluorescent ECL 2 Western Blotting Substrate (Thermo

Scientific) on a Typhoon Phosphorimager using 457 nm excitation and 520/40 nm emission settings.

**Optimization of Caged GTPase Expression**. In an effort to express caged GTPases, multiple parameters were adjusted. The amount of DNA used for transfection ranged from 2 μg to 4 μg total. Lipofectamine 2000 and branched polyethylenimine (PEI) transfection reagents were used. During transfection, DNA and Lipofectamine 2000 were incubated with the cells for 4 hours before media was changed and cells were incubated for 18-24 hours for protein expression. Branched PEI and DNA transfection mixtures were incubated on cells for 18-24 hours. The concentration of **PCK** was also varied from 1 mM to 2 mM without successful incorporation. The Mammalian Protein Extraction Buffer (GE) as well as homemade PAK1 lysis buffer was used to lyse the cells before Western blotting. Caged GTPases were not detected by Western blot with any of the above optimizations.

## 2.2 OPTICAL CONTROL OF PAK1 ACTIVITY

### 2.2.1 Introduction

The PAK (p21-activated kinases) protein family represents a group of serine/threonine kinases that are regulated by small GTPases, including CDC42 and Rac1 and are part of multiple signal pathways, including the ERK pathway (Figure 16). There are six members of the PAK family. PAK1 through 3 exhibit a higher level of homology than the recently discovered PAK4 through 6. PAK1 specifically has a complex structure consisting an N-terminal regulatory domain, five SH3-binding domains, a CDC42 and Rac interaction binding domain, a p21-binding domain, an

autoinhibitory domain, and a C-terminal catalytic domain.[83] Binding of PAKs to CDC42 or Rac1 leads to conformational changes as well as the ability for PAKs to autophosphorylate. Autophosphorylation activates the kinase function of PAKs and induces conformational changes that expose the SH3 binding domain.[84]

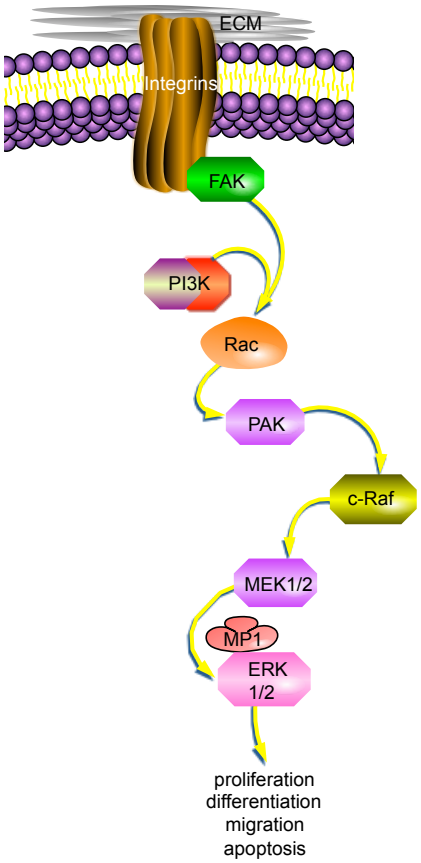


**Figure 16:** Signaling pathway including PAK1. Adapted from http://www.sabiosciences.com/pathway.php?sn=ERK_Signaling

Downstream targets of PAK1 include paxillin[85] and cofilin[86] which affect focal adhesion turnover and actin polymerization, respectively. It was further found that PAKs, PAK1 in particular, are critical for cell migration and establishing the spatiotemporal relationship between actin organization, myosin phosphorylation and focal adhesion dynamics.[85,87] PAK1 has kinase-dependent and kinase-independent functions, which have long been debated in the literature.[83] Light-activation of PAK1 allows for specific spatial and temporal activation of the signaling

pathway. This precise control of PAK1 could be used in the determination of the negative feedback loop in the ERK2 pathway that was discussed above.[65,88,89] The hypothesis that Raf-1 is the target of the negative feedback loop can be tested using the photocaged PAK1.

### 2.2.2 Caged PAK1

In order to control PAK1 activity with light, constitutively activate PAK1 was mutated to have **PCK** incorporated at K299 (Figure 17). K299 has been shown to undergo an ionic interaction with glutamate 315 that stabilizes the α- and β-phosphates of ATP and contributes to the γ-phospho-transfer.[90]

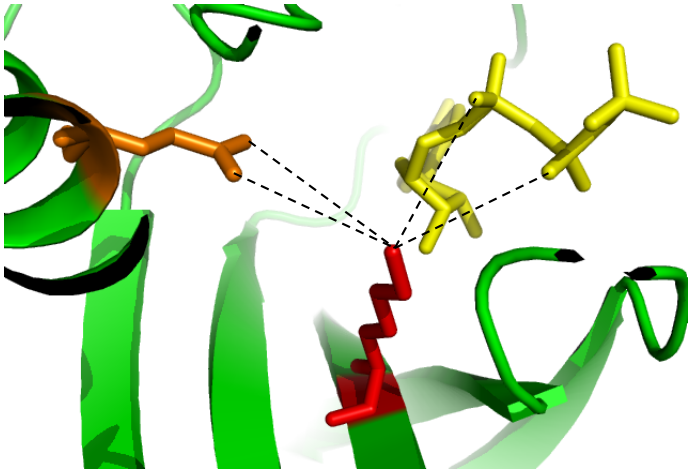

**Figure 17**: Crystal structure of PAK1 with K299 highlighted in red, E315 highlighted in orange and ATP highlighted in yellow. Interactions are shown in dashed black lines. PDB structure 3Q53.

Plasmids expressing the constitutive active, denoted as "ca," and inactive, denoted as "kd" for kinase dead, PAK1 containing myc tags were obtained from Addgene (plasmids: #12208 and #12210). In these plasmids, T423 was mutated to glutamate to induce constitutive activity and K299 was mutated to arginine to generate a catalytically inactive kinase. Mutation of K299 to TAG in the plasmid expression the caPAK1 yielded the plasmid pCMV6-myc-caPAK1 K299TAG that could be used for expression of caged caPAK1 when transfected into mammalian

cells with the plasmid expressing the PCKRS and pylT. The wildtype PAK1 was also mutated to allow for incorporation of **PCK**. Figure 18 shows that, gratifyingly, when **PCK** was added to the media, caged caPAK1 was expressed and detected by Western blotting with an anti-myc antibody (lanes 3, 5, 9, and 11). As expected, expression levels are lower than those of non-caged PAK1 (lanes 1, 2, 7, and 8).

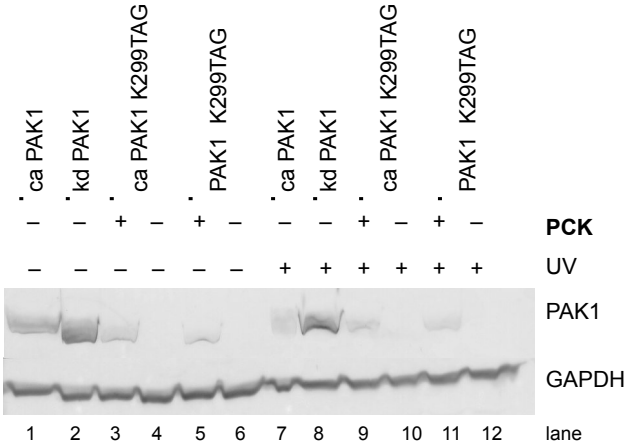


**Figure 18**: Western blot of PAK1 variants.

Once expression of caged PAK1 was confirmed an activity assay was performed using myelin basic protein (MBP) as a phosphorylation target for PAK1.[84,91] MBP is a generic target for a variety of kinases that is commonly used in kinase activity assays. Purified PAK1 variants were combined with MBP and radioactive ATP in kinase reaction buffer and phosphorylation was analyzed by SDS-PAGE. Figure 19 shows that ca PAK1 phosphorylates MBP (lanes 1 and 7) and kd PAK does not phosphorylate MBP (lanes 2 and 8) regardless of irradiation, as expected. In the absence of **PCK**, no PAK1 is expressed and therefore no phosphorylation of MBP (lanes 4, 6, 10, and 12) was observed. In the presence of **PCK** and absence of UV irradiation, MBP is not phosphorylated either, indicating inhibition of enzymatic activity due to the presence of the caging group (lane 3 and 5). After UV irradiation, a native lysine at position

K299 is restored and PAK1 becomes active, phosphorylating MBP (lane 9). When the wildtype caged variant of PAK1 is decaged (lane 11), only a minor band can be seen for MBP phosphorylation due to the reduced activity compared to the "ca" enzyme. In summary, the *in vitro* activity assay results in Figure 19 show that PAK1 activity can be optically controlled using **PCK**.

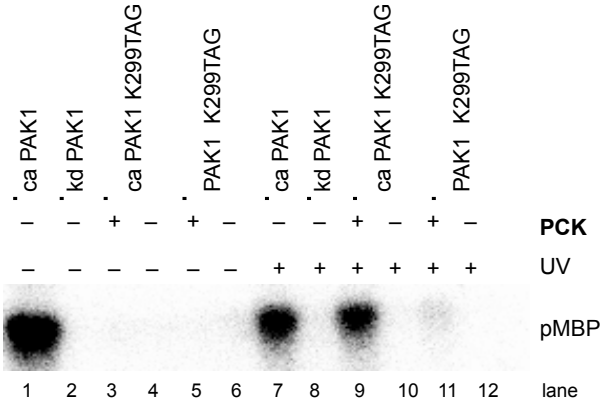


**Figure 19**: *In vitro* kinase activity assay of PAK1 variants.

A phenotype microscopy assay was also performed in collaboration with Dr. Shoeb Ahmed of the Haugh Lab at North Carolina State University. HeLa cells expressing GFP-paxillin as well as the caged ca PAK1 were imaged using TIRF microscopy. Paxillin is a phosphorylation target of PAK that has been implicated in focal adhesion turnover.[92] Activation of PAK1 through irradiation should induce a retraction of paxillin-containing focal adhesions due to phosphorylation by PAK1. This is in fact what was observed (Figure 20). GFP-paxillin can be seen slowly disappearing from the imaging frame overtime. This is only observed after irradiation and due to the activation of PAK1 and subsequent phosphorylation. This is a promising result that shows that PAK1 activity can be optically controlled in mammalian cells.

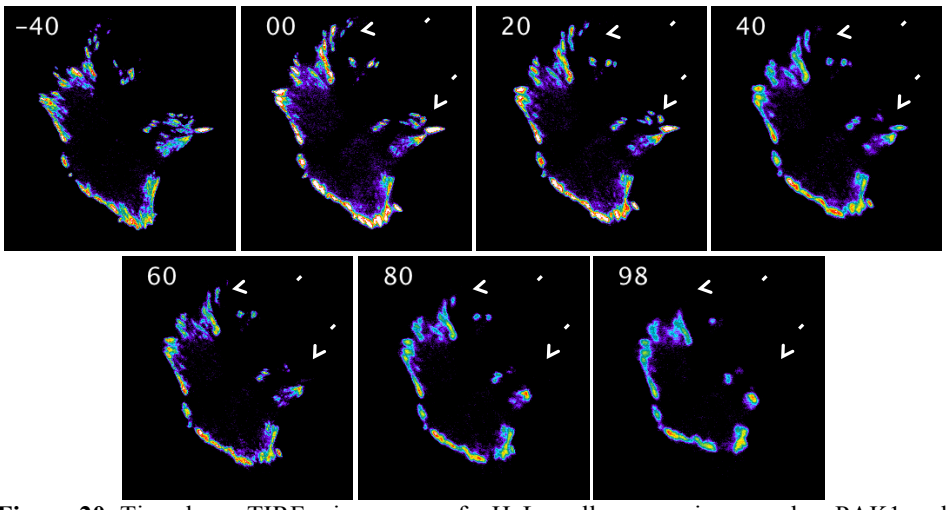


**Figure 20**: Time-lapse TIRF microscopy of a HeLa cells expressing caged ca PAK1 and GFP-Paxillin. The cell was irradiated with a DAPI filter at time 00. Arrows indicate focal adhesions that retract upon UV irradiation and activation of PAK1. Data was generated by Shoeb Ahmed of the Haugh Lab (North Carolina State University).

### 2.2.3 Experimental

All expression constructs were previously generated by Hank Chou in the Deiters lab.

**Western Blotting of Caged PAK1**. HEK293T cells were maintained as described in Section 6.5 and split the day before transfection as described in Section 6.6. Transfection was performed with 1 µg of pCMV6-myc-caPAK1 K299TAG and 1 µg of pPCKRS-PylT or 2 µg of pCMV6-myc-caPAK or 2 µg of pCMV6-myc-kdPAK1 using the LPEI transfection protocol found in Section 00. Cells were incubated overnight at 37 ˚C/5% $CO_2$. The next day cells were washed with 1 mL of PBS and lysed with 250 µL of PAK1 lysis buffer (2.5 mL 10% Triton X-100, 1.25 mL 1 M Tris-HCl pH 7.4, and 1.67 mL 3 M sodium chloride filled to 50 mL with MilliQ water). Cells were shook on ice of 20 minutes and lysates were centrifuged to 20 minutes at 15,000 rpm. Western blot was performed as described in Section 6.9 with mouse anti-myc and mouse anti-GAPDH antibodies (Santa Cruz) at a 1:1000 dilution. Secondary antibody was goat anti-mouse-HRP (Santa Cruz) diluted 1:1000 in TBST. Colorimetric detection was performed by

mixing 120 µL of 0.3% hydrogen peroxide with 4 mg of 4-chloro-1naphthol (4CN) in 20 mL of TBS. This solution was added to the membrane and allowed to develop for 15 minutes. Images were taken with a scanner.

**Immunoprecipitation of PAK1**. Lysate (200 µL) was mixed in a tube with 2 µg of anti-myc antibody (Santa Cruz) and 30 µL of Protein A-Sepharose beads (Sigma). These were incubated overnight at 4 ˚C with shaking. The next day beads were centrifuged for 30 seconds at 500 rpm/23 × *g*, the supernatant was decanted, beads were washed with 400 mL of wash solution A (20 mM Tris-HCl, pH 7.4 and 500 mM sodium chloride), and centrifuged again. This process was repeated twice with wash solution A and twice with was solution B (20 mM Tris-HCl, pH 8.0 and 10 mM magnesium chloride). Beads were resuspended in 30 µL of kinase buffer (5X kinase buffer: 100 mM Tris-HCl, pH 7.4, 5 mM DTT, 50 mM magnesium chloride, 5 mM EDTA, 20 mM manganese chloride).

**Kinase assay**. Each 20 µL kinase reaction contained 5 µL of the indicated PAK1-bead solution, 10 µg of myelin basic protein (Sigma Aldrich), 50 µM ATP, 10 µCi $\gamma$-$^{32}$P-ATP in 1X kinase buffer. Reactions were incubated at 30 ˚C for 30 minutes, 5 µL of 4X SDS-PAGE loading dye was added to each sample and they were boiled for 5 minutes. Samples were separated on a 15% SDS-PAGE gel. The gel was exposed to a phosphor storage screen overnight and scanned using a Typhoon Phosphorimager (GE Healthcare).

## 2.3 OPTICAL CONTROL OF MAPK KINASE ACTIVITY

### 2.3.1 Introduction

Multiple stimuli initiate ERK2, p38α, and JNK1 signaling cascades, however, the MAPKs are towards the end of the signaling cascade and typical translocate to the nucleus for terminal function.[73,89] MAPK kinases have been implicated in a wide range of cellular processes including proliferation, migration, apoptosis, motility, structural support and differentiation. Furthermore, MAPK kinases have been associated with diseases such as Alzheimer's disease, Parkinson's disease, Lou Gehrig's disease and cancer.[73] It has been shown that crosstalk between the pathways of ERK2, p38α, and JNK1 is significant, however there are some upstream effectors that have been shown to be MAPK specific.[89] The use of **PCK** to optically control MAPK kinase activity was hypothesized to allow for elucidation of co-regulatory signals and determination of crosstalk between MAPK signaling pathways. The ability to test this hypothesis is facilitated by specific activation of the kinase in question. Global activation through receptor stimulation causes reaction by all members of the pathway, which can create data that is difficult to interpret.

### 2.3.2 Caged ERK2, p38α, and JNK1

In order to optochemically control MAPK kinase activity, plasmids expressing wildtype ERK2, p38α, and MKK7-JNK1 were purchased from Addgene (plasmids #8974, #20351 and #19726). Three mutations are necessary to generate the constitutively active ERK2: L73P, S151D, and D319N.[93] A constitutively active p38α variant requires two mutations, D176A and F372S, in combination with an MKK6 fusion (Addgene plasmid #13518), its upstream MAPKK.[94] Site

directed mutagenesis was used to introduce a TAG mutation a K52, K53 and K55 of ERK2, p38α, and JNK1, respectively. This conserved lysine is located in the ATP binding pocket of all three MAPK kinases and plays a crucial role in positioning the triphosphate in the binding pocket for catalysis (Figure 21).[95]

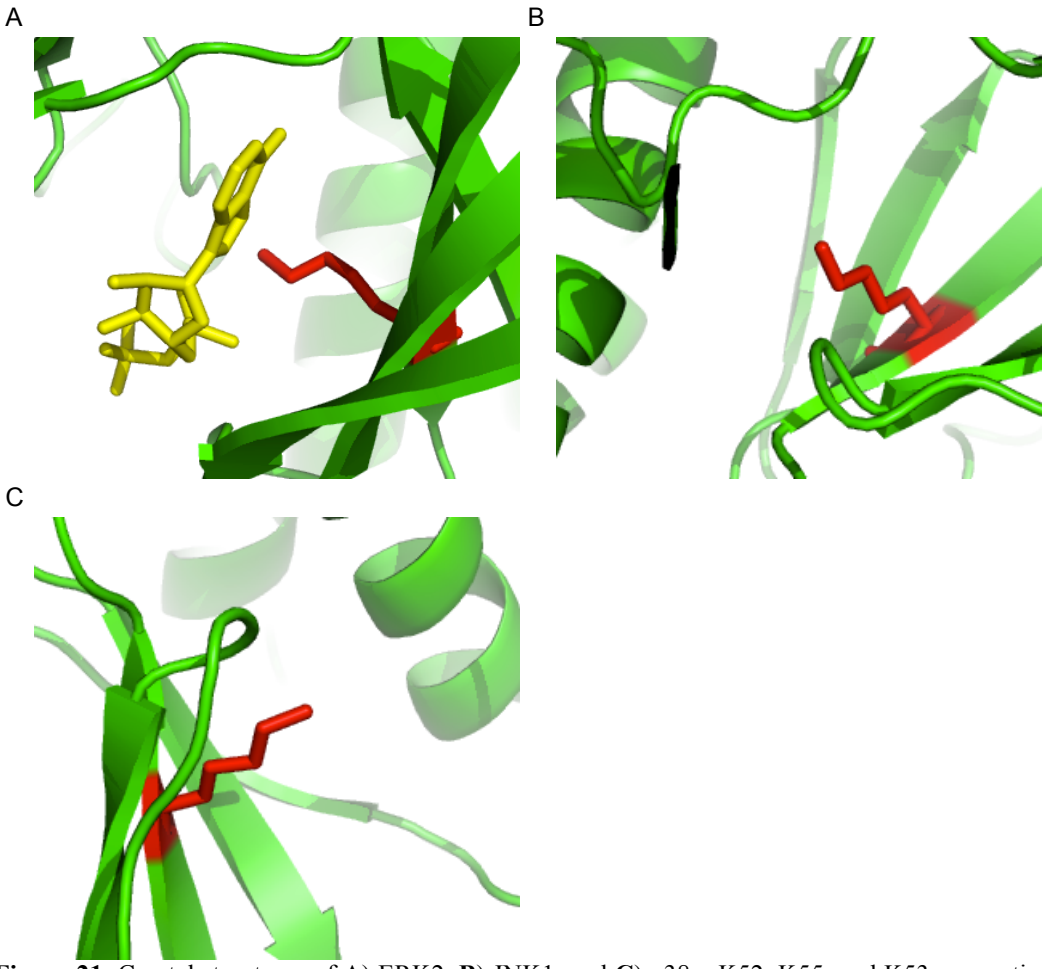


**Figure 21**: Crystal structures of **A**) ERK2, **B**) JNK1, and **C**) p38α. K52, K55, and K53, respectively are highlighted in red and point in to the ATP binding site. ADP is highlighted in yellow in the ERK2 structure. PDB structures 4GVA (ERK2), 3O17 (JNK1), and 1R39 (p38α).

Unfortunately, L74 was mutated to TAG instead of L73 in ERK2 and the incorrect lysine was mutated within JNK1 and p38α for incorporation of **PCK**. In JNK1, K55 should have been mutated to TAG, K56 was mutated to TAG and in p38α, K53 should have been mutated to TAG,

but K54 was mutated to TAG due to incorrect primer design. Wildtype ERK2, MKK6-p38α, and MKK7-JNK1 expressed in sufficient yields (Figure 22).

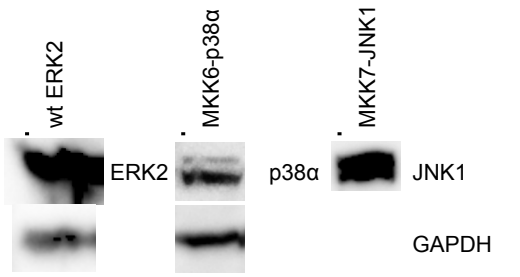


**Figure 22**: Western blots of ERK2, p38α and JNK1 variants.

In conclusion, the optochemical control of kinase function has been challenging to achieve. **PCK** incorporation in PAK1 was successful, however, caged cdc42 and RhoA were not expressed. The kinase activity of PAK1 was photochemically controlled *in vitro*, but transitioning the assay to mammalian cells has not yielded robust results. A retraction of paxillin-containing focal adhesions has been observed, but more data needs to be collected to further examine the role of PAK1 with Rac1 activation and in the MEK1/ERK2 pathways. Ongoing work in the optochemical control of MAPKs will hopefully yield three caged kinases that can be used to photochemically dissect the regulation signals and feedback loops that are involved in those pathways that could not be elucidated without the use of photocaging methodology.

### 2.3.3 Experimental

**Generation of pCMV6-FLAG-MKK6-p38α**. Phusion PCR was performed on pCMV6-FLAG-p38α using primers NheI-p38a and p38alpha_HpaI-PCR_Rev and on pCMV6-FLAG-MKK6 using primers HindIII-FLAG-MKK6 and MKK6-NheI according to the protocol in Section 6.1. PCR products were purified using the protocol from Omega PCR Purificatin Kit (Omega).

Inserts were then double digested according to Section 6.2 using NheI and HpaI for p38α and HindIII and NheI for FLAG-MKK6. After digestion, insert were PCR purified again and then ligated together as described in Section 6.2. pCMV6-FLAG-MKK6 was double digested with HindIII and HpaI according to Section 6.2, AP treated, and gel purified with a Gel Purificatin kit (Omega). The ligated insert, FLAG-MKK6-p38α, was then ligated into pCMV6 according to Section 6.2 to generate pCMV6-FLAG-MKK6-p38α.

**Site-directed Mutagenesis of MAPKs.** Constitutively active mutations were introduced using the following DNA and primers:

**Table 2**: Primer sequences of site-directed mutagenesis of MAPKs.

| **Mutation** | **DNA** | **Primer A** | **Primer B** |
|---|---|---|---|
| ERK2 L74P* | pCMV6-HA-wtERK2 | ERK2 L73P Forw (5'-AAAATCCTACCCCGCTTCAGACATGAGAACATCATCGGCATCAATGACATCATC) | ERK2 L73P Rev (5'-TCTGAAGCGGGGTAGGATTTTTATCTCTCTCAGGGTTCTCTGACAGTAGGT) |
| ERK2 S151D | pCMV6-HA-ERK2 L73P | ERK2 S151D Forw (5'-CTCAAGCCTGACAACCTCCTGCTGAACACCACTTGTGATCTCAAGATCTGTGACTTT) | ERK2 S151D Rev (5'-CAGGAGGTTGTCAGGCTTGAGGTCACGGTGCAGAACATTAGCTGAATGTATATACTTTAATCC) |
| ERK2 D319N | pCMV6-HA-ERK2 L73P S151D | ERK2 D319N Forw (5'-GACCCAAGTAACGAGCCCATTGCTGAAGCACCATTCAAGTTTGACATGGAGC) | ERK2 D319N Rev (5'-AATGGGCTCGTTACTTGGGTCATAATACTGCTCCAGGTACGGGTGGGC) |
| p38α D176A | pCMV6-FLAG-MKK6-p38α | p38alpha D176A Forw (5'-CACACTGATGCCGAGATGACAGGCTACGTGGCTACCAGGTGGTAC) | p38alpha D176A Rev (5'-TGTCATCTCGGCATCAGTGTGCCGAGCCAGCCCAAAATCCAGAATCTT) |
| p38α F372S | pCMV6-FLAG-MKK6-p38α D176A | p38alpha F327S Forw (5'GACCAGTCCTCCGAAAGCAGGGACCTTCTCATAGATGAGTGGAAGAGCCTGACCTATGATGAAGTC) | p38alpha D327S Rev (5'-CCTGCTTTCGGAGGACTGGTCATAAGGGTCAGCAACAGGCTCATCATCAGGGTC) |
| ERK2 K52TAG | pCMV6-HA-caERK2 | ERK2 K52TAG Forw (5'-GCTATCAAGTAGATCAGTTTT | ERK2 K52TAG Rev (5'-AGGACTGATCTACTTGATAGCAACTCGAACTTTGTTGA |

| | | | |
|---|---|---|---|
| | | GAGCACCAGACCTACTGT) | GATTATCATAAGC) |
| JNK1 K56TAG* | pCMV6-FLAG-MKK7-JNK1 | Jnk1a1 K55TAG Forw (5'-GCAATCAAGTAGCTAAGCCGACCATTTCAGAATCAGACTCATGCC) | Jnk1a1 K55TAG Rev (5'-TCGGCTTAGCTACTTGATTGCAACATTTCTTTCAAGAATGGCATCATAAGC) |
| p38α K54TAG* | pCMV6-FLAG-MKK6-cap38α | p38alpha K53TAG Forw (5'-GCAGTTAAGTAGCTGTCGAGACCGTTTCAGTCCATCATTCACG) | p38alpha K53TAG Rev (5'-TCTCGACAGCTACTTAACTGCCACACGATGCCC) |

Mutations that were incorrect due to primer design are indicated with an asterisk (*).

**Western Blotting of MAPKs**. HEK293T cells were maintained as described in Section 6.5 and split the day before transfection as described in Section 6.6. Transfection was performed with 2 μg of pCMV6-HA-wtERK2, pCMV6-FLAG-MKK6-p38α, or pCMV6-FLAG-MKK7-JNK1 using the LPEI transfection protocol found in Section 6.6. Cells were incubated overnight at 37 ˚C/5% $CO_2$. The next day cells were washed with 1 mL of PBS and lysed with 250 μL of kinase lysis buffer (Appendix A). Cells were shook on ice of 20 minutes and lysates were centrifuged to 20 minutes at 15,000 rpm/21,130 × *g*. Western blot was performed as described in Section 00 with rabbit anti-HA (Cell Signaling) and a rabbit anti-GAPDH (Santa Cruz) or mouse anti-FLAG (Sigma) and mouse anti-GAPDH antibodies (Santa Cruz) depending on the tag indicated above at a 1:1000 dilution. Secondary antibody was goat anti-rabbit-HRP and goat anti-mouse-HRP (Santa Cruz) diluted 1:30,000 in TBST. Protein bands were detected by chemiluminescence as described in Section 6.9.

# 3.0 OPTOCHEMICAL CONTROL OF MEMBRANE LOCALIZATION

Localization of proteins within mammalian cells is important for proper function. For example, transcription factors must be transported into the nucleus and many signaling molecules need to be transported to the cell membrane in order to perform their respective functions properly.[96,97] The plasma membrane is one specific location within the cell that is home to multiple types of proteins, including transport proteins such as ion channels, receptors such as G protein-coupled receptors, and signaling proteins such as Ras.[98-100] Each cell type requires a different set of proteins to be localized to specific domains within the membrane at specific times in order for the cell to function properly.[101] The differences in the localization of proteins contribute to the diversity of cells and also allows one protein to function in multiple aspects.[102] The mislocalization of proteins has been determined to be a cause of diseases such as cystic fibrosis, kidney disease, and cancer.[102-105] While there are multiple reasons why a protein is translocated to the membrane, such as extracellular stimuli or cellular feedback loops, protein are located at the membrane through transmembrane domains, signaling peptides, fatty acid anchors, and lipid anchors.[101,106] Post-translational modifications of these signaling sequences with fatty acid residues are one mechanism for protein localization to the membrane (Table 3).

**Table 3:** List of fatty acid modifications. Adapted by permission from Macmillan Publishers Ltd: Nature Chemical Biology. Resh, M. D. Trafficking and signaling by fatty-acylated and prenylated proteins. 2, 584-590, copyright 2006.

| Modifying group | Chemical structure | Enzyme | Linkage | Sequence |
|---|---|---|---|---|
| Myristate | 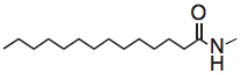 | NMT | Amide to *N*-Gly | MGXXXS/T |
| *S*-Palmitate | 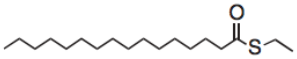 | PATs | Thioester to Cys | See text |
| *N*-Palmitate | 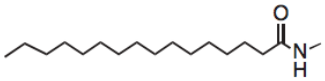 | Rasp | Amide to *N*-Cys | CGPGR |
| Farnesyl | 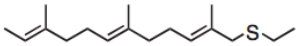 | FTase | Thioether to Cys | CAAX |
| Geranylgeranyl | 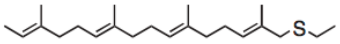 | GGTase I | Thioether to Cys | CAAL |
| | | GGTase II | Thioether to Cys | CC, CXC or $CC(X)_{n=1-3}$ |

## 3.1 OPTICAL CONTROL OF MEMBRANE LOCALIZATION THROUGH CAAX DOMAIN CAGING

### 3.1.1 Introduction to Protein Farnesylation

One signaling sequence that is post-translationally modified to direct proteins to the cellular membrane is the CaaX domain. The CaaX domain consists of a cysteine (C) that is alkylated, two aliphatic amino acids (xx), and a C-terminal amino acid (X) that determines the type of modification, either farnesylation or gernylgernylation.[97] CaaX domain processing proceeds as shown in Figure 23.[107,108] Prenylation (farnesylation or geranylgeranylation) occurs in the cytosol by farnesyl transferase (FTase). Farnesylated proteins are transported to the

endoplasmic reticulum where the aaX sequence is cleaved by Ras converting enzyme 1 (Rce-1) and carboxylmethylated by Isoprenylcysteine carboxyl methyltransferase (Icmt). At this point the pathways diverge depending on a second signaling sequence upstream of the CaaX domain: 1) proteins with a poly-basic region are transported directly to the membrane via an unknown pathway, due to their polylysine-rich second signaling sequence.[109] 2) proteins with a second signal of palmitoylation are transported to the Golgi where a palmitoyl-transferase attaches a palmitoyl group the cysteines up-stream of the farnesylated cysteine.[110] From the Golgi, the farnesylated and palmitoylated proteins are transported to the membrane through the exocytic pathway.[111] Membrane localization of these proteins is reversible due to the labile thioester linkage between the cysteine and palmitoyl group.[108]

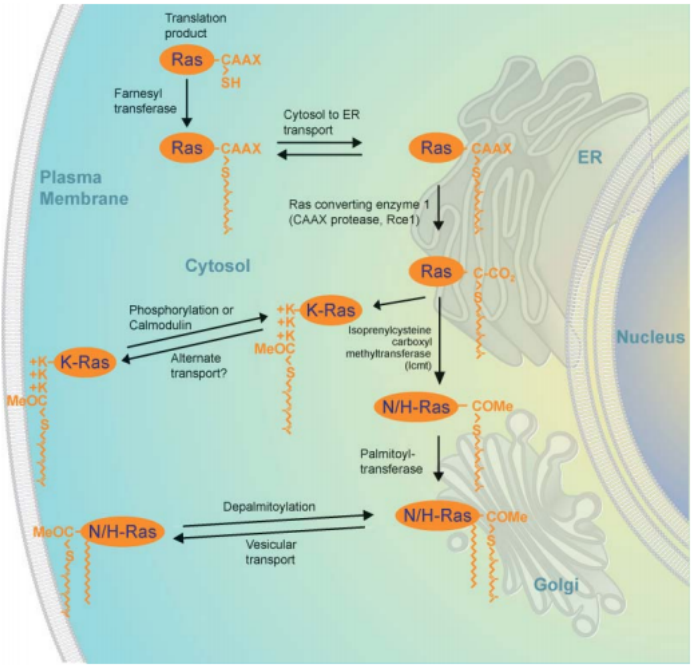


**Figure 23:** Processing of Ras proteins due to CaaX domains. Adapted with permission from Journal of Lipid Research. Wright, L. P.; Philips, M. R. *J Lipid Res* 2006, *47*, 883.

H-Ras and K-Ras are two important signal transduction proteins with CaaX domains. They are members of the Ras superfamily of GTPases. This superfamily can be further broken down into six subfamilies: Ras, Rho, Rab, Ran, Rad and Arf, that collectively contain over 50

GTPases.[112] Ras GTPases are involved in signal transduction as a response to extracellular stimuli such as growth factors, cytokines, hormones and neurotransmitters that results in synthesis and translocation of proteins, vesicular trafficking, cell proliferation, differentiation, apoptosis, cell cycling and nuclear import.[113-115] All members of the Ras superfamily cycle between active-GTP bound and inactive-GDP bound conformations.[116] GTP-bound Ras interact with GTPase-activating proteins (GAPs) to increase the rate of GTP hydrolysis and convert Ras to its inactive form. Guanine nucleotide exchange factor proteins (GEFs) then aid in the release of GDP and re-activation of the GTPase with the addition of GTP. Each cycle of GTP hydrolysis acts as a signaling event from stimuli to downstream effectors.[117] All members of the Ras superfamily are posttranslationally modified to be directed to the cell membrane,[118] because membrane localization is necessary for proper fuction.[119]

The Ras subgroup of proteins is comprised of four isoforms: H-Ras, N-Ras, K-Ras4A and K-Ras4B that are 90% homologous except for the 25 C-terminal amino acids, known as the hypervariable region. The section is only 10-15% homologous and is likely to determine the biological differences, such as effector preference, between the isoforms, Figure 24.[109,118] Within the hypervariable region, there is the CaaX box, and the linker region upstream of the CaaX domain direct H-Ras and K-Ras to the plasma membrane.[110] The X position is a serine in H-Ras[120] and a methionine in K-Ras a methionine[110] leading to farnesylation of the terminal cysteine of both proteins. K-Ras has a poly-basic second signaling sequence, which allows for translocation of K-Ras to the membrane through the first scenario described above. H-Ras has a second signaling sequence that requires palmitoylation. The two upsteam cysteines from the farnesylated cysteine are palmitoylated at the Golgi and H-Ras is transported to the membrane through the exocytic pathway.[109]

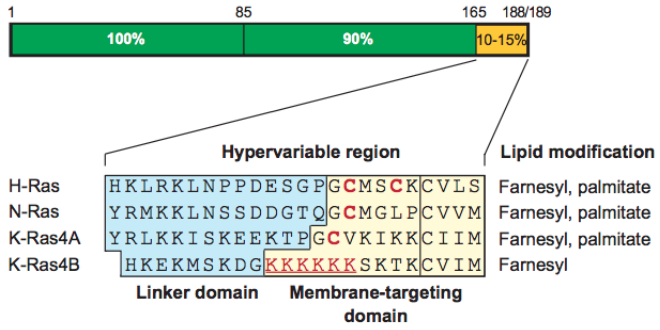


**Figure 24**: Sequence homology of Ras GTPases. The hypervariable region is shown in detail. The red cysteines are palmitoylated. The red and underlined lysine residues are the second signal for K-Ras4B. The last cysteine residue in each sequence is farnesylated. Adapted with permission from Journal of Cell Science. Prior, I. A.; Hancock, J. F. *J Cell Sci* **2001**, *114*, 1603.

Once H-Ras and K-Ras are translocated to the plasma membrane, they localize to different areas.[109] It was first seen that H-Ras signaling, but not K-Ras signaling, is interrupted when the concentration of cholesterol in the membrane is perturbed.[121] Prior *et al.* went on to investigate the sites of membrane localization and found that K-Ras exclusively operates in the disordered regions of the cell membrane. While for H-Ras, it was determined that the GTP/GDP binding state dictates the microdomain of the plasma membrane that it resides in.[122] Upon farnesylation and palmitoylation, H-Ras is targeted to cholesterol-rich lipid rafts and caveolae. However, H-Ras is being reallocated to disordered regions upon activation through binding of GTP. The equilibrium shift from lipid rafts to disordered regions contributes to the increased efficiency of Ras effector activation. The lateral movement within the membrane and increased activation could be due to the conformational change of H-Ras when it is bound to GTP, which exposes specific residues within the hypervariable region that favor interactions with the disordered regions of the membrane and also allow for more favorable interactions with effector proteins.[118,123] Early on it was speculated that Ras effectors were localized in the disordered region lending to the equilibrium shift for Ras-GTP.[122] However, recent studies has not been able

to prove this as the major reason for reallocation, but only that the hypervariable region is necessary for movement.[118,122]

H-Ras and K-Ras contain a lysine residue directly upstream of the farnesylated cysteine, leading to the hypothesis that membrane localization could be optochemical controlled through the replacement of this lysine residue with **PCK**. The photochemical control of H-Ras and K-Ras membrane localization will allow for the elucidation of the kinetics of these processes because a starting point can be generated through light exposure. Furthermore, the caged CaaX domain could be used with any protein of interest to temporal control its membrane localization. This could be useful for investigation of protein function based upon localization.

### 3.1.2 Previous Approaches to Optically Control Membrane Localization and the Farnesylation Pathway

Membrane localization has been previously optochemically controlled through the use of caged small molecule protein dimerizers, such as rapamycin.[45,124] Chapter 5.0 describes examples of this approach. Phytochromes and crytochromes have also been used to control membrane localization with light.[38, 125] These approaches are described in Chapter 1.0

An example of using photocaging to control FTase function was reported in 2012 using a caged FTase inhibitor.[126] A FTase inhibitor, FTI, was chemically modified with a bromohydroxycoumarin-caging group at an essential thiol, Figure 25**A**. Its activity was measured through the detection of H-Ras and ERK (a target of H-Ras) phosphorylation (Figure 25**B**). H-Ras is only phosphorylated (and activated) when properly translocated to the membrane, a process that it is inhibited by FTI. As seen in Figure 25**B**, the caged Bhc-FTI is completely inactive allowing H-Ras and ERK phosphorylation. However, after Bhc-FTI exposure to UV

light and decaging, FTase and thereby H-Ras translocation is inhibited, leading to the inhibition of H-Ras and ERK phosphorylation.

To further confirm that Bhc-FTI was acting as expected, membrane localization of a GFP-H-Ras fusion was used as a readout (Figure 25**C-H**). In agreement with the Western blot results, Bhc-FTI is inactive, leading to GFP-H-Ras farnesylation and exclusive membrane localization (Figure 25**E**). However, light-induced FTI decaging inhibits FTase and leads to the retention of some GFP-H-Ras in the cytoplasm (Figure 25**F**). Inhibition of membrane translocation is more pronounced in the treatment with non-caged FTI.

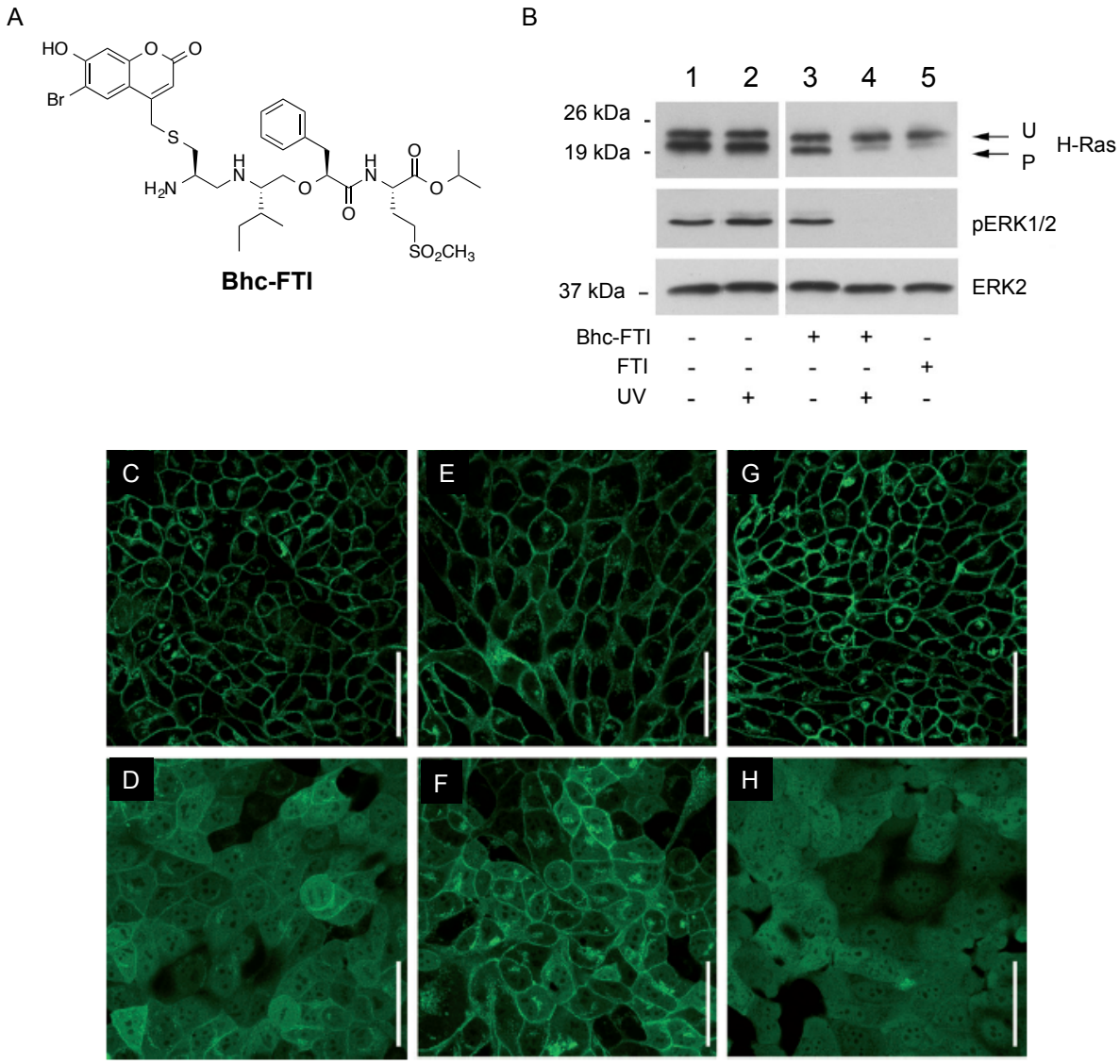


**Figure 25:** Photocaged FTase inhibitor and functional assays. **A)** Structure of caged FTase inhibitor, Bhc-FTI. **B)** Western blot assay of ERK phosphorylation by H-Ras in conjunction with Bhc-FTI. GFP-Ras localization **C)** in the presence of 0.2% DMSO. **D)** in the presence of 1 µM FTI (non-caged FTase inhibitor). **E)** in the presence of 5 µM Bhc-FTI. **F**) in the presence of 5 µM Bhc-FTI with UV irradiation. **G)** with UV irradiation. **H)** 5 µM FTI.

While the examples presented above are good examples of using caging groups on small molecule effectors of enzymes and using light sensitive protein fusions, the caging of proteins and protein substrates of the CaaX processing pathway represents a more direct way of controlling its function with light.

### 3.1.3 Incorporation of PCK into CaaX domains for the Optical Control of Membrane Localization

To facilitate the visualization of CaaX box-tagged proteins, an EGFP fusion was chosen.[127, 128, 129, 130, 131] DNA encoding the ten C-terminal amino acids (GCMSCK**CVLS**) of H-Ras were cloned onto the C-terminus of EGFP.[131] Total internal reflection fluorescence (TIRF) microscopy was used to image only the membrane-localized protein.[132] This technique is widely used to study processes that are occurring at the cell membrane. As expected, membrane localization of EGFP was observed when the plasmid encoding EGFPc10HRas was transfected into cells (Figure 26**A**). Upon introduction of a TAG mutation at the K6 codon and expression in the presence of **PCK**, membrane localization was no longer observed (Figure 27**A**), in agreement with a negative control expression in the absence of **PCK** (Figure 26**C**). By not supplying the cells with caged lysine, translation will halt at the TAG mutation, leading to EGFP expression without a functional CaaX domain and localization in the cytosol. As expected, irradiation of the positive and negative control (365 nm, 20 sec) did not induce significant changes in fluorescence intensity (Figure 26**B** and **D)**. Thus, the UV light did not have non-specific effects of EGFP localization.

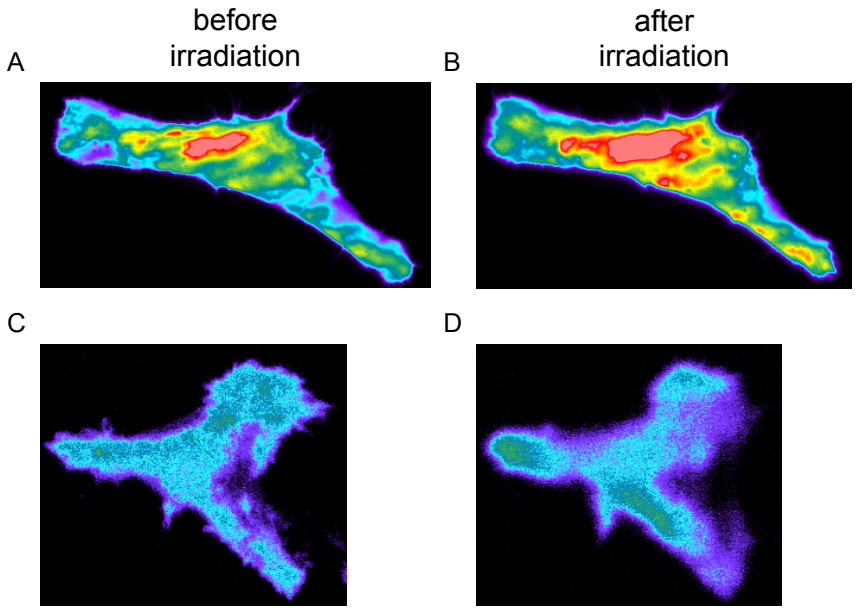


**Figure 26:** TIRF images of EGFPc10HRas. pEGFPc10HRas expressed in HeLa cells **A)** before and **B)** after irradiation. pEGFPc10HRas K6TAG without **PCK** expressed in HeLa cells **C)** before and **D)** after irradiaiton. Images were taken with a prism-based TIRF microscope that was built around a Zeiss Axioskop 2 FS by the Haugh Lab (NCSU). A 40X (0.8 NA Achroplan; Zeiss) objective was used and GFP was excited at 488 nm. Images were collected using MetaMorph software. Yellow/red pseudo color represents high membrane fluorescence, while blue/purple pseudo-color represents low membrane fluorescence.

HeLa cells were transfected with a plasmid encoding EGFPc10HRas K6TAG and the PCKRS and a plasmid encoding the PylT in the presence of **PCK** (1 mM). Cells were imaged for 20 min before irradiation and after irradiation (365 nm, 20 sec) for 60 min (Figure 27**A**). The increase in fluorescence before irradiation may be due to the fluctuation in the cells during temperature equilibration at the beginning of imaging experiments. Imaging experiments began 10-15 minutes after cells were placed on the incubated stage. Membrane fluorescence dramatically increases after irradiation, as seen when plotting fluorescence intensity versus times (Figure 27**B**). The resulting graph was fitted to a first-order exponential reaction equation, revealing a rate constant of 0.0492 $s^{1-}$ and a lag time of ~3 minutes after irradiation. Fluorescence intensity reaches a plateau after 50-60 minutes. The reaction kinetics of CaaX domain-mediated membrane localization have not been investigated before the presented work, as it was impossible to define the start point of the translocation process. The kinetics of FTase and

palmitoyltransferase have been determined,[133,134] however, the kinetics of membrane localization in its entire process have not been elucidated. The obtained results demonstrate that translocation of CaaX box-tagged EGFP containing a K6→**PCK** mutation can be controlled by light. Thus, before irradiation the presence of the caging group either prevents the addition of the farnesyl group or restricts the processing of the CaaX box at later stages of the pathway shown in Figure 23. Based on the crystal structure of FTase, it is possible that caging K6 interrupts the exit mechanism of the farnesylated protein.[135] The lysine-6 residue seemingly points away from the reaction pocket. For these reasons, it is difficult to predict with certainty that farnesylation is the process that is being controlled with the substitution of the lysine-6 position with **PCK**.

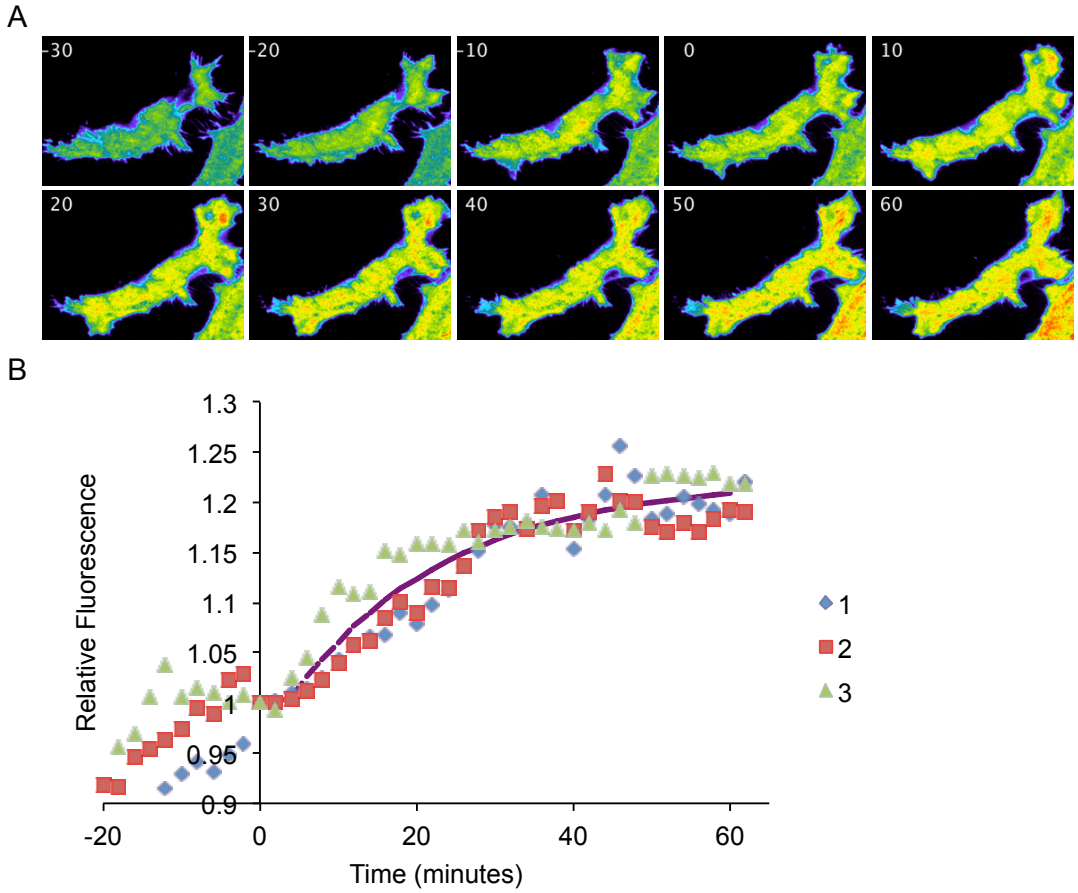


**Figure 27**: Optical control of membrane localization using a caged CaaX domain, CVLS. **A)** Representative TIRF microscopy images of EGFPc10HRas K6TAG in the presence of **PCK** (1 mM). Images were taken with a prism-

based TIRF microscope that was built around a Zeiss Axioskop 2 FS by the Haugh Lab (NCSU). A 40X (0.8 NA Achroplan; Zeiss) objective was used and GFP was excited at 488 nm. Cells were irradiated at time point 0 for 20 seconds using a DAPI filter (excitation 365/50 nm). Images were collected using MetaMorph software. **B)** Relative fluorescence vs. time plot of TIRF microscopy observation of EGFPc10HRas K6TAG. t=0 is the point of irradiation. Three independent cells were observed The purple plot is an exponential fit.

After successfully controlling protein membrane translocation using a caged H-Ras CaaX sequence, additional positions were investigated for optical control using **PCK**. Hougland *et al*. had studied a variety of CaaX box sequence as substrates for FTase.[136] Two CaaX boxes, one with lysine in the $a_1$ position (CKIS) and one with the lysine in the $a_2$ position (CTKF), were found to be functional in translocating to the membrane. Thus, the previously used EGFPc10H-Ras constructs were mutated to CKIS and CTKF CaaX domains. When transfected into HeLa cells, EGFPc10HRas CKIS produced a membrane bound EGFP phenotype, while CTKF did not (Figure 28).

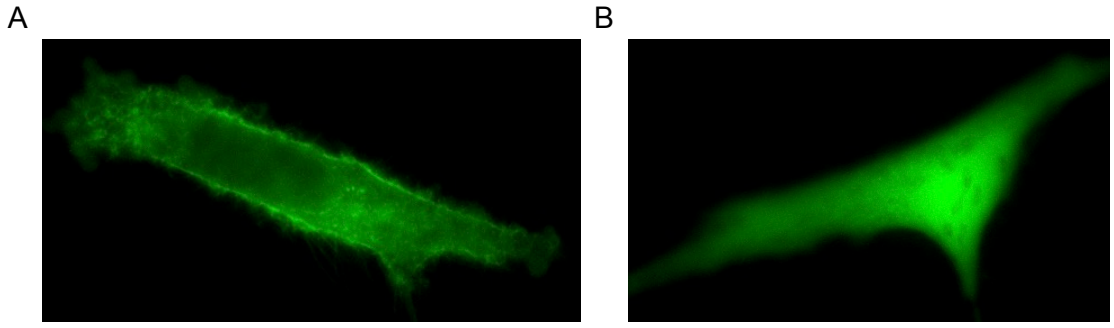


**Figure 28:** HeLa cells transfected with plasmids encoding CaaX domain variants. **A)** EGFPc10HRas CKIS **B)** EGFPc10HRas CTKF. Cells were imaged 24 hours after transfection using a Zeiss Observer Z1 microscope using the 40X objective with the GFP (38 HE) filter (ex: BP470/40; em: BP525/50).

A K8TAG mutation was introduced into EGFPc10HRas CKIS and positive and negative control experiments were performed with EGFPc10HRas CKIS and EGFPc10HRas C-K8TAG-IS in the absence of caged lysine. As expected, EGFPc10HRas CKIS was targeted to the membrane and strong fluorescence was seen before and after a 20 second irradiation at 365 nm, (Figure 29**A** and **B)**, while the K8TAG mutant did not lead to any membrane fluorescence (Figure 29**C** and **D)**. Irradiation had no effect on EGFP localization.

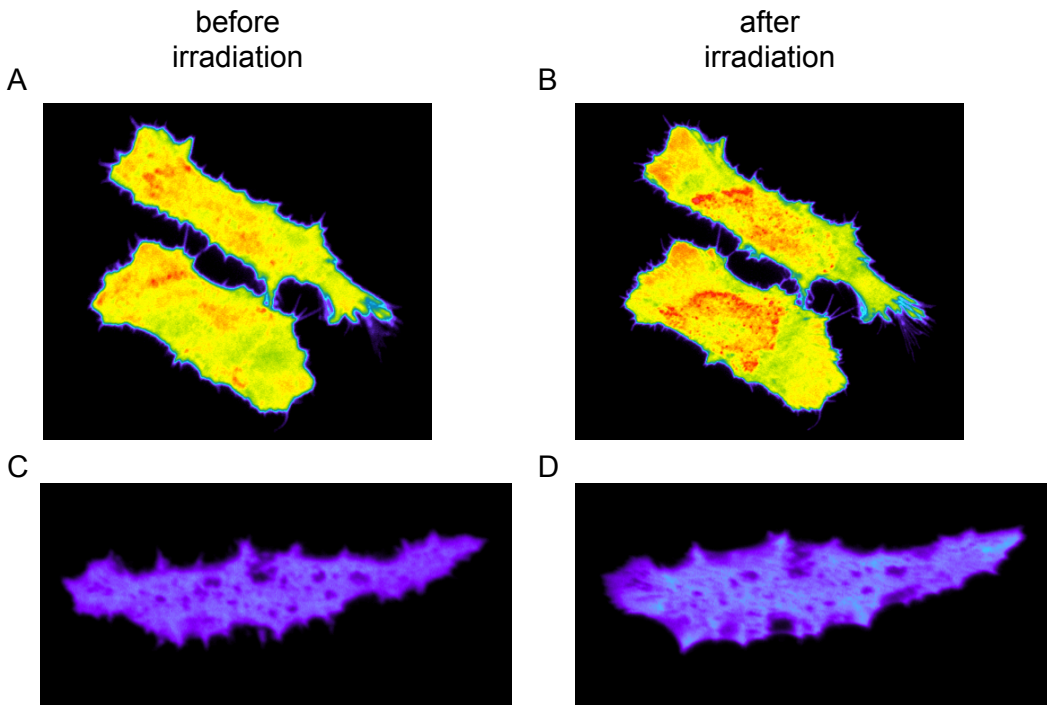


**Figure 29:** TIRF images of EGFPc10HRas CKIS. pEGFPc10HRas CKIS expressed in HeLa cells **A)** before and **B)** after a 20 second UV irradiation using a DAPI excitation filter (365/50 nm). pEGFPc10HRas C-K8TAG-IS without **PCK** expressed in HeLa cells **C)** before and **D)** after irradiaiton. Images were taken with a prism-based TIRF microscope that was built around a Zeiss Axioskop 2 FS by the Haugh Lab (NCSU). A 40X (0.8 NA Achroplan; Zeiss) objective was used and GFP was excited at 488 nm. Images were collected using MetaMorph software.

The EGFPc10HRas CK8TAGIS system was then employed in light-activation experiments identical to the EGFPc10HRas K6TAG system (Figure 30). A rate constant of 0.0178 $s^{1-}$ and a lag time of ~13 minutes after irradiation was obtained first-order exponential kinetics. The increased lag time is most likely a result of the CaaX box mutation. Hougland *et. al*. reported that this substrate has a $k_{cat}/K_m$ value an order of magnitude lower than other substrates in their experiments. However, they did not exam the translocation rate of the wild-type H-Ras CaaX sequence.[136]

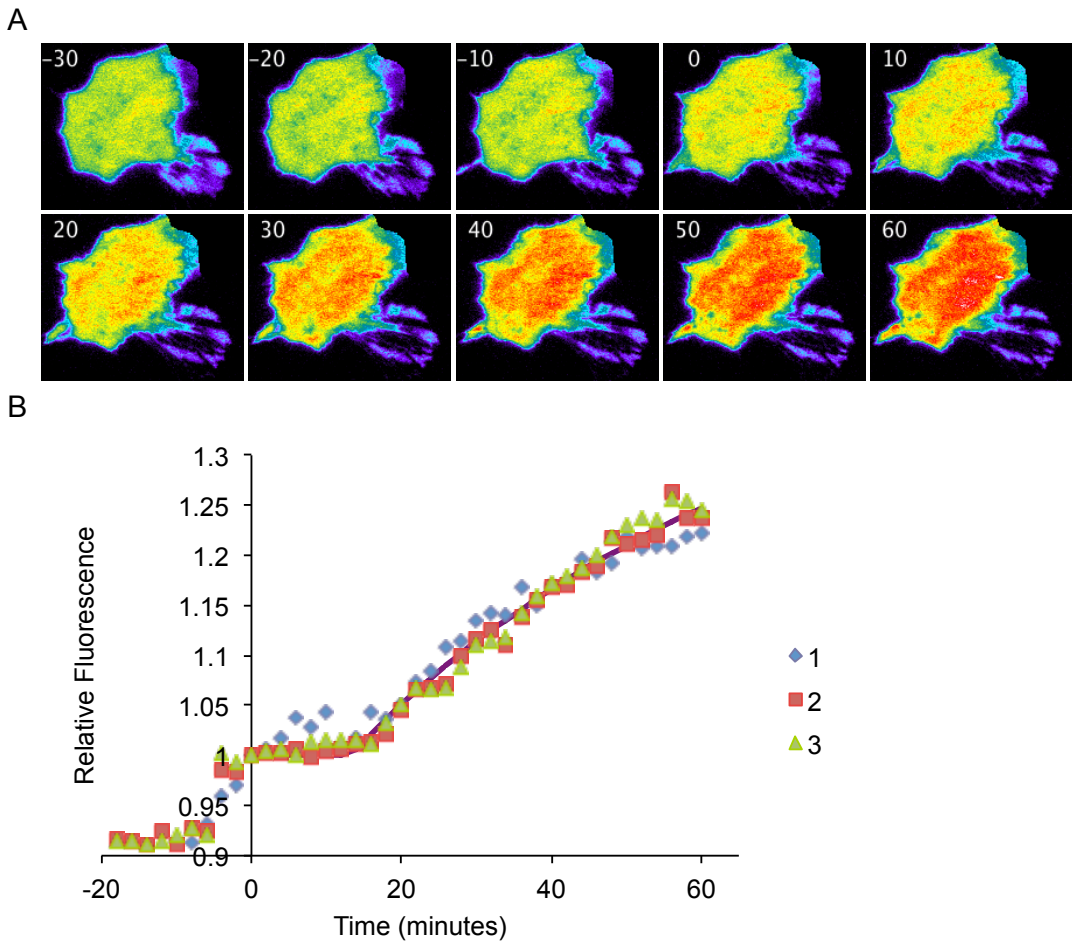


**Figure 30:** Optical control of membrane localization using a caged CaaX domain, CKIS. **A)** TIRF microscopy micrographs of HeLa cells expressing EGFPc10HRas C-K8TAG-IS in the presence of **PCK** (1 mM). Images were taken with a prism-based TIRF microscope that was built around a Zeiss Axioskop 2 FS by the Haugh Lab (NCSU). A 40X (0.8 NA Achroplan; Zeiss) objective was used and GFP was excited at 488 nm. Irradiation was performed at time point 0 for 20 seconds using a DAPI excitation filter (365/50 nm) Images were collected using MetaMorph software. **B)** Relative fluorescence vs. time plot of TIRF microscopy observation of EGFPc10HRas C-K8TAG-IS t=0 is the point of irradiation. Three independent cells were observed and the data was plotted. The purple plot is an exponential fit.

These studies were then extended to the K-Ras CaaX box and its second signal consisting of a polybasic region. DNA encoding the 14 C-terminal amino acids (KKKKKKSKTK**CVIM**) of KRas was hybridized[131] and inserted downstream of EGFP, generating EGFPc14KRas. Transfection of the construct into HeLa cells produced membrane-targeted EGFP expression (Figure 31**A)**. Mutation of K10 to TAG and expression of EGFPc14KRas K10TAG in the presence of **PCK**, lead to substantial variation between experiments, (Figure 31**C)**. Relative

fluorescence was determined by dividing fluorescence intensity at each time point by the fluorescence intensity at the point of irradiation, thus allowing change to be compared. However, no clear trend was observed and caging of K10 in the K-Ras CaaX domain did not allow for robust photocontrol of protein translocation.

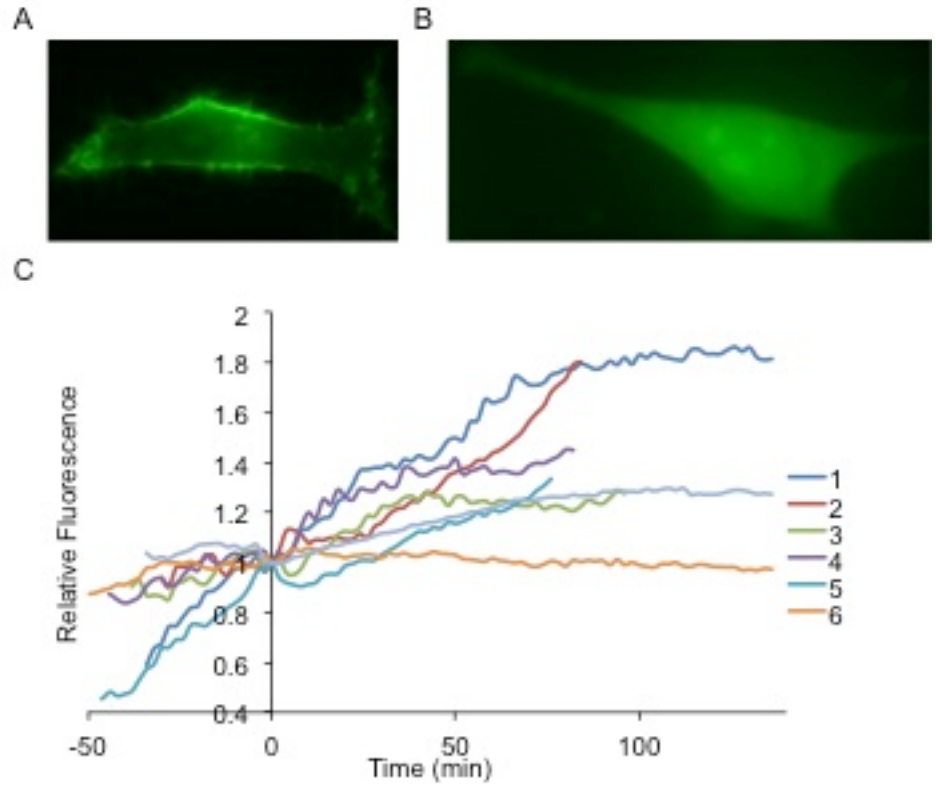


**Figure 31**: HeLa cells transfected with a plasmids encoding K-Ras CaaX domain. **A)** EGFPc14KRas **B)** EGFPc14KRas K10TAG in the presence of **PCK** (1 mM). Cells were imaged 24 hours after transfection using a Zeiss Observer Z1 microscope using the 40X objective with the GFP (38 HE) filter (ex: BP470/40; em: BP525/50). Cells were irradiated for 20 seconds at time point 0 using a DAPI excitation filter (365/50 nm).

It was next sought to determine what CaaX-modifying enzyme was inhibited by the presence of **PCK**. It was hypothesized that FTase was being blocked from adding the farnesyl group.[137] In order to test this hypothesis, an alkyne modified farnesol group was used, **C15AlkOH** (Figure 32).[138] If FTase is functional, **C15AlkOH** will be attached in place of a wild-type farnesyl group on the cysteine of the protein of interest. Cell lysates can be reacted with an azide-conjugated dye labeling modified proteins.

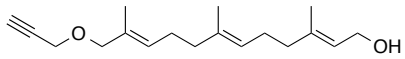


**C15AlkOH**

**Figure 32:** Structure of alkyne modified farnesol group, C15AlkOH.

HEK293T cells were transfected with pPCKRS-EGFPc10HRas or pPCKRS-EGFPc10HRas K6TAG and pPylT, and were incubated in the presence of **PCK** (2 mM). All samples were exposed to 50 μM of lovastatin and 25 μM of **C15AlkOH**. Cells were lysed after 24 h and a click reaction was performed with an azide-rhodamine dye. SDS-PAGE analysis revealed that EGFP was present in the EGFP-CaaX and caged EGFP-CaaX samples (Figure 33); however, no selective rhodamine labeling of EGFPc10HRas was observed and bands occurred in all samples, precluding further studies of the farnesylation status of H-Ras.

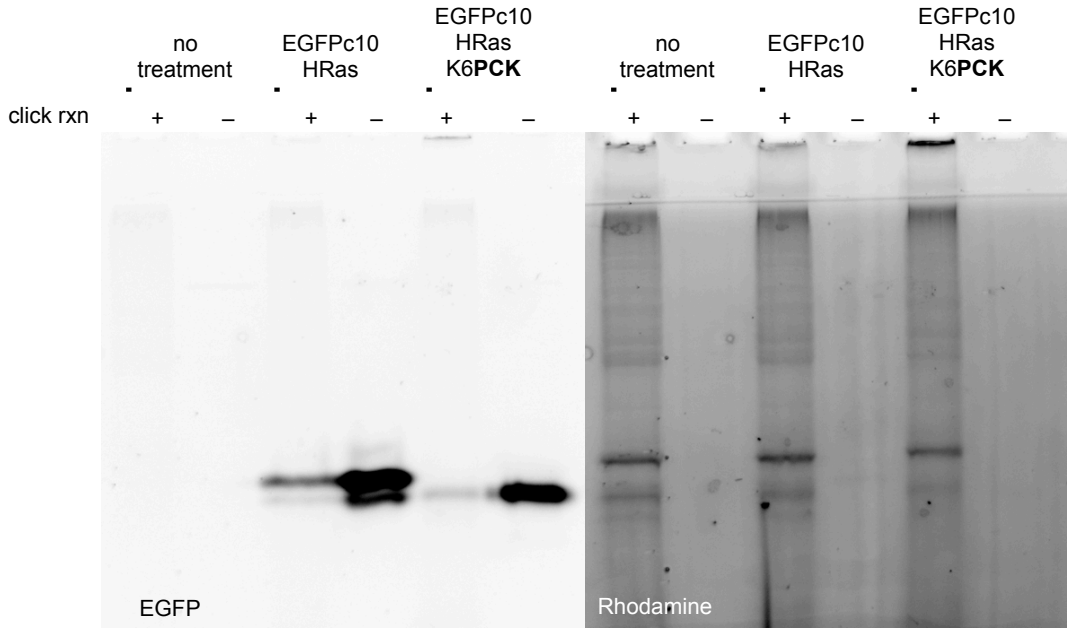


**Figure 33**: EGFP and rhodamine fluorescence from lysates of HEK293T cells treated with 50 μM lovastatin and 25 μM **C15AlkOH** during transfection with linear PEI. Click reaction with rhodamine-azide was performed after cell lysis.

In conclusion, optical control of membrane localization was achieved through the incorporation of **PCK** at position K6 in the CaaX domain of H-Ras, and at position K8 of the

CaaX domain of Rab. Optical control of membrane localization through the caging of the K-Ras CaaX domain was not successful. This is the first time that the kinetics of the CaaX domain-processing pathway have been determined as a whole. Previously, individual enzymes have been investigated, but there was no technology available to explore the pathway in a cellular setting. Optical control through unnatural amino acid mutagenesis has made this possible as it allows for temporal control and a defined starting point for kinetic measurements. The precise mode of action of inhibition of translocation through strategically placed **PCK** into the CaaX domain still remains elusive.

### 3.1.4 Experimental

**Cloning of pPCKRS-EGFPc10HRas**. The 10 C-terminal amino acids of HRas were added to EGFP by Phusion PCR (Section 6.1). The reverse primer had the following nucleotide sequence: 5'- GCATCAATTGTCAGGAGAGCACACACTTGCAGCTCATGCAGCCCTTGTACAGCTC GTCCATG. The underlined sequence is that of H-Ras. pPCKRS and the EGFPc10HRas insert were double digested with NheI and MfeI and gel purification or PCR purification, respectively, were performed. The single stranded DNA fragments were then ligated together and transformed. Colonies were grown in LB Broth overnight, the pPCKRS-EGFPc10HRas plasmid was isolated and confirmed by sequencing.

**Site-directed Mutagenesis to Generate pPCKRS-EGFPc10HRas K6TAG**. The K6TAG mutation (primers: forward 5'-CTGCATGAGCTGCTAGTGTGTGCTCTC; reverse 5'-GAGAGCACACACTAGCAGCTCATGCAG) was introduced into pPCKRS-EGFPc10HRas using the QuikChange Lightening kit (Agilent Technologies, Inc).

**Live Cell TIRF Imaging**. HeLa cells were cultured as indicated in Section 6.5 and seeded in a 6 cm plate the day before transfection using 1.5 mL of cells (~1 × $10^6$ cells) and 3.5 mL of fresh DMEM. Cells were transfected with 5 μg of pPCKRS-EGFPc10HRas K10TAG (or the wild type CaaX domain) and 5 μg of pPylT (if necessary) using 37.5 μL of LPEI and the protocol in Section 6.6. Twenty-four hours post-transfection, media was removed and the cell were trypsinized using 1 mL of TrypLE (Gibco). Cells were centrifuged for 10 minutes at 1000 rpm and resuspended in 1 mL of phenol red free DMEM. Cells were counted and 50,000 cells were plated onto a poly-lysine coated cover slip with a PVC ring attached with grease. Cells were incubated for 3 hours at 37 ˚C/5% $CO_2$, and TIRF imaging was conducted by the Haugh Lab. Imaging parameters can be found in the captions of specific images. Fluorescence intensities were determined by Shoeb Ahmed in the Haugh Lab in regions of interest inside the cells (ImageJ, NIH).

**Metabolic Labeling Using C15AlkOH**. HEK293T cells were maintained as indicated in Section 6.5. Cells were seeded in a 6-well plate as indicated in Section 6.6. HEK293T cells were transfected with 1 μg of pPCKRS-EGFPc10HRas or pPCKRS-EGFPc10K10HRas and 1 μg of pPylT using the LPEI protocol in Section 6.6. All samples had 25 μM **C15AlkOH** present and and 25 μM lovastatin. Cells were incubated for 24 hours and then lysed with 200 μL of lysis buffer (PBS with 0.1% SDS, 0.2% Triton X-100, 2.4 μM PMSF and protease cocktail inhibitor). An aliquot of the lysates (25 μL) were combined with 100 μM rhodamine-azide (synthesized by Meryl Thomas in the Deiters Lab, **Figure 34**), 1 mM TCEP, 100 μM TBTA, and 1 mM $CuSO_4$ and incubated for 2 hours at room temperature while shaking. Protein loading dye was added and samples were loaded on a 10% SDS-PAGE gel. The gel was imaged for GFP and rhodamine fluorescence

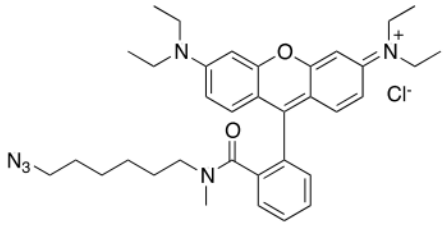


**Figure 34:** Structure of rhodamine-azide for metabolic labeling.
rhodamine-azide

## 3.2 OPTICAL CONTROL OF MEMBRANE LOCALIZATION USING SH4 DOMAINS

### 3.2.1 Introduction

Protein tyrosine kinases are an integral part of signaling pathways and are typically associated with transmembranre receptors.[139] Src family kinases (SFKs) are a group of nonreceptor protein tyrosine kinases with nine members, Src, Lck, Hck, Fyn, Blk, Lyn, Fgr, Yes, and Yrk.[140] SFKs have been implicated in multiple cellular functions including cell poliferation, cytoskeletal alterations, differentiation, survival, adhesion, and migration.[141] The structure of SFKs is composed of six regions: the Src homology (SH) 4 domain, the unique region, the SH3 domain, the SH2 domain, the kinase domain, and a regulatory C-terminal domain (Figure 35).[140]

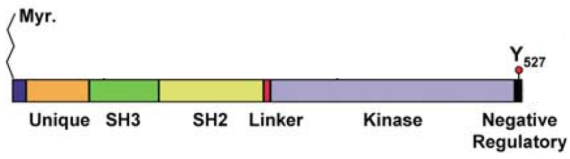

**Figure 35**: Structure of SFKs. The dark blue domain is the SH4 domain and controls membrane localization of SFKs.

The unique region of SFKs is the only distinct region within SFKs and is implicated in determining the specific binding partners of each of the kinases within the family. The SH3 domain is responsible for interactions with substrates by recognition of proline-rich sequences and is an integral part of SFKs' regulation. The SH2 domain recognizes phosphotyrosine and the amino acids C-terminal to the tyrosine to distinguish binding partners. The kinase domain of SFKs is comprised of two lobes: the N-terminal lobe is the smaller of the two and plays a part in the regulation of SFKs, and the larger C-terminal lobe aids in tyrosine phosphorylation. The ATP binding and phosphorylation takes place in the cleft between the lobes. The final region, the C-terminal regulatory domain, contains a tyrosine (Y527 in Figure 35) that can be phosphorylated. When phosphotyrosine is present, the SH3 and SH2 adopt a conformation that secures the kinase domain in an inactive state. Activation of SFKs occurs through binding of SH2 and/or SH3 domains to their binding partners, interrupting the intramolecular interactions and phosphorylation of Tyr416.

The presented research will focus on the SH4 domain of Fyn and Src. The SH4 domain is a 14 to 16-amino acid sequence on the N-terminal of SFKs that is modified for plasma membrane targeting.[141] All SFKs have a myristate group added to the N-terminus after removal of the methionine in position one. A glycine in position two is necessary for addition of the myristate and *N*-myristyltransferase prefers a serine or threonine in position six.[142] As in case of the Ras proteins, a second signal is required for translocation to the plasma membrane. The second signal is palmitoylation at C3 for Fyn and a polybasic region for Src. Myristoylation occurs co-translationally via formation of a stable amide bond, while palmitoylation is a reversible post-translational modification via a thioester bond.[143] Fyn and Src have lysine

residues in the 7 and 9 position, and Src has an additional lysine in the 5 position. It was found that mutations of K7 and K9 in Fyn reduce membrane association due to inefficient myristoylation,[144] and mutation of K7 in Src also reduces membrane targeting.[145] It was later discovered that K7 and K9 of Fyn are trimethylated after myristoylation and palmitoylation.[146] Using this information, we hypothesized that membrane translocation could be controlled with light by incorporating the caged lysine **PCK** at positions 7 and 9 in Fyn. It also sought to control translocation and determine the role of K5 and K9 in Src. Src family kinases are a part of multiple signaling pathways that have yet to be completely elucidating.[141] Using photocaged SH4 domains, Fyn and Src can be activated with precise spatial and temporal control allowing for defined cellular responses to be observed and pathway connections to be clarified.

### 3.2.2 Incorporation of PCK into the SH4 domains of Fyn and Src for Optical Control of Membrane localization

DNA oligos encoding the sixteen N-terminal amino acids of Fyn (MGCVQCKDKEATKLTE)[146] and of Src (MGSSKSKPKDPSQRRR)[143] were annealed and ligated to the N-terminus of the EGFP gene and the remaining internal ATG start codon (M22) of EGFP was silenced through mutation to GGG to encode for the incorporation of glycine. Expression of these mutants showed defined membrane localization of EGFP before introduction of a TAG mutant (Figure 36**)**.

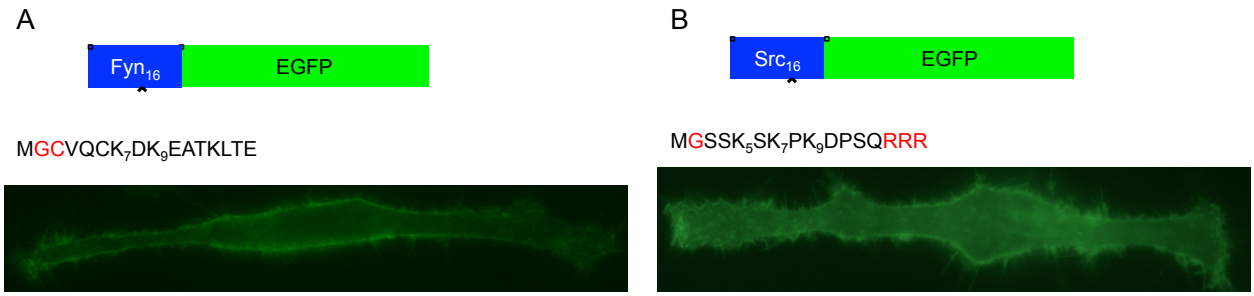


**Figure 36:** Schematic of SH4 domain tagged EGFP and expression in HeLa cells. **A**) $Fyn_{16}$EGFP. **B)** $Src_{16}$EGFP. Images were taken using a Zeiss Observer Z1 microscope with a 63X objective (NA 1.40 oil/plan-apochromat; Zeiss) and a GFP (38 HE) filter (ex: BP470/40; em: BP525/50).

Photochemical control was then attempted with these constructs. First, a TAG mutation was introduced at K7 of Fyn, and K5 and K9 of Src. Plasmids encoding these mutants as well as PylRS and PylT were transfected into HeLa cells in the presence and absence of **PCK** under multiple conditions (Figure 37). As expected, no fluorescence was observed in the absence of **PCK** for all constructs (Figure 37**F-J**). Increasing the amount of pPylT from 100 ng to 200 ng resulted in promising expression of $Fyn_{16}$EGFP K7TAG (Figure 37**B**). However, membrane localization before irradiation is seen in both samples. This likely indicates that mutation of one lysine residue within the Fyn SH4 domain does not disrupt the membrane localization. Previously literature has shown that mutation of one residue does reduce the membrane localization some, but mutation of both K7 and K9 together displays maximal suppression.[144] The expression of Src SH4 domain tagged EGFP was optimal for K5TAG **PCK** (Figure 37**C**).

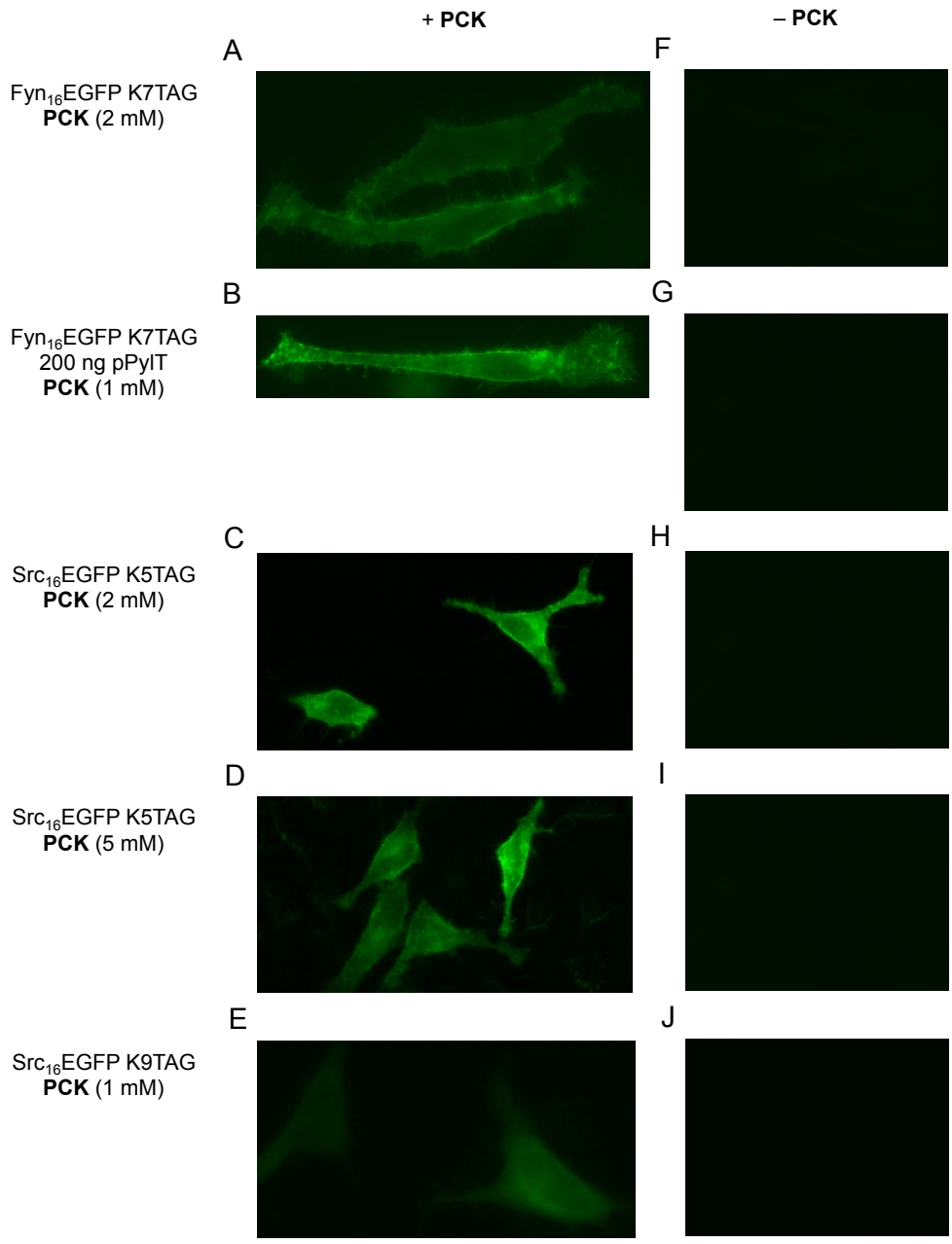


**Figure 37:** Expression of EGFP fused with caged SH4 domains. **A**) and **F**) $Fyn_{16}$EGFP K7TAG with **PCK** (2 mM) and **B**) and **G**) 200 ng of the PylT plasmid and **PCK** (1 mM), **C**) and **H**) $Src_{16}$EGFP K5TAG with **PCK** (2 mM) and **D**) and **I**) with **PCK** (5 mM) and **E**) and **J**) $Src_{16}$EGFP K9TAG with **PCK** (1 mM) in HeLa cells. All samples were transfected with 100 ng of pPylT unless otherwise indicated. Images were taken using a Zeiss Observer Z1 microscope with (**A** and **B**) 40X objective (NA 0.75 /EC plan-apochromat; Zeiss) (**C**-**E**) 20X (NA 0.8 / plan-apochromat) and a GFP (38 HE) filter (ex: BP470/40; em: BP525/50).

The first attempt to photochemically control membrane localization with a caged SH4 domain used the $Fyn_{16}$EGFP K7TAG construct and the optimal conditions (Figure 37**B)**. HeLa cells were transfected with a plasmid encoding $Fyn_{16}$EGFP K7TAG and the PCKRS and a

plasmid encoding the PylT (200 ng) in the presence of **PCK** (1 mM). Twenty-four hours post-transfection, cells were imaged for expression and then irradiated for 30 seconds using a DAPI filter and imaging was continued for 40 minutes (Figure 38). No translocation was seen during this time. Before irradiation, cytosolic EGFP was observed, allowing for the assumption that $Fyn_{16}$EGFP K7TAG was not processed properly and one or more of the myristoylation, palmitoylation, or methylation events did not occur. This is different from the results seen in Figure 37. Previously, some membrane localization was seen when the plasmid was used, however during this experiment ubiquitous EGFP fluorescence was seen. After irradiation and decaging, membrane-targeting activity was not restored and EGFP was not localized to the membrane. This experiment was tried multiple times in two different cells types, KNRK and HeLa cells, with different irradiation durations, 15 seconds, 30 seconds, 1 minute, and 2 minutes, and no translocation was observed using this imaging setup. It is possible that using confocal microscopy or TIRF microscopy would show membrane localization after irradiation.

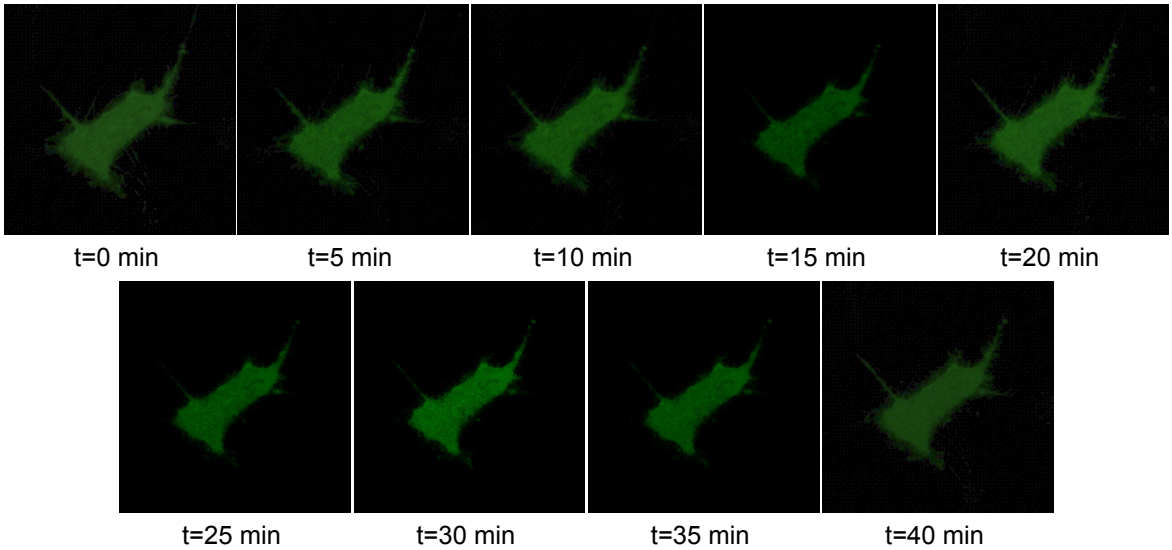


**Figure 38:** Photochemical control of $Fyn_{16}$EGFP K7TAG in the presence **of PCK** (1 mM). Cells were irradiated at t=0 for 30 seconds at 365 nm using a DAPI filter. Images were taken using a Zeiss Observer Z1 microscope with a 40X objective (NA 0.75/ EC plan-apochromat; Zeiss) and a GFP (38 HE) filter (ex: BP470/40; em: BP525/50).

$Src_{16}$EGFP K5TAG was then investigated by transfecting HeLa cells with a plasmid encoding $Src_{16}$EGFP K5TAG and PCKRS and pPylT in the presence of **PCK** (2 mM) (Figure 39). After the media was replace to remove **PCK**, cells were irradiated for 15-120 sec at 365 nm (DAPI filter) through a 20X objective using the microscope Xe/Hg lamp and then incubated for 24 h. Cells were then imaged for translocation of EGFP to the membrane (Figure 39**E-H**). Slight membrane localization can be seen in the cells that have been irradiation for 30 and 60 seconds (Figure 39**F and G)**. Unfortunately, this translocation is not as pronounced as hoped. More noticeable membrane localization could potentially be seen if microscopy techniques such as confocal microscopy or TIRF were used. Translocation kinetics of SH4 domains are not easily determined because modification are done co-translationally.[97] For this reason, it is difficult to know how long it will take a caged SH4 domain to translocate to the nucleus. There is some literature evidence that newly synthesized SH4 domain-tagged proteins are trafficking to the membrane within an hour.[147]

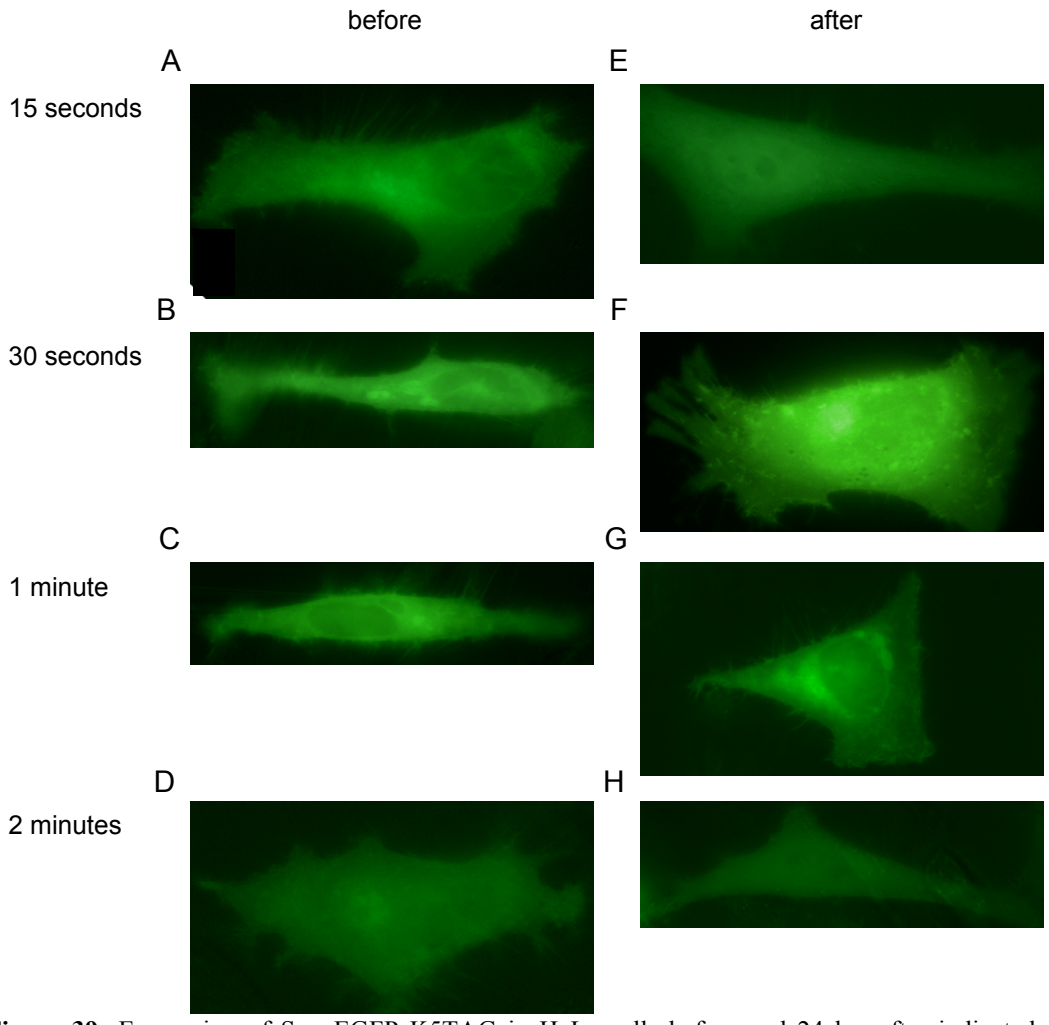


**Figure 39:** Expression of $Src_{16}$EGFP K5TAG in HeLa cells before and 24 hrs after indicated irradiation times. Irradiation was performed using a DAPI filter (365/50 nm). Images were taken using a Zeiss Observer Z1 microscope with a 63X objective (NA 1.40 oil/plan-apochromat; Zeiss) and a GFP (38 HE) filter (ex: BP470/40; em: BP525/50).

$Src_{16}$EGFP K7TAG and $Src_{16}$EGFP K9TAG were also investigated for photochemical control of translocation (Figure 40). Cells were irradiated for 15 seconds and again, no translocation of EGFP was seen for K7TAG or K9TAG after 24 hours.

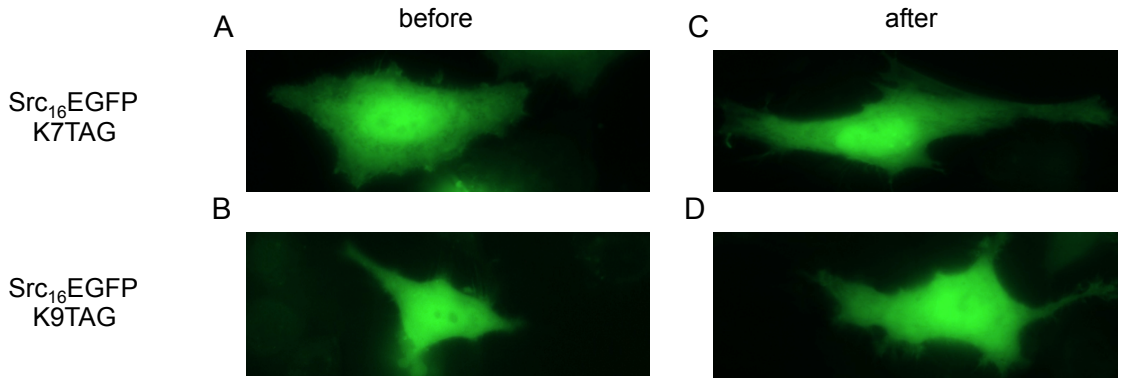


**Figure 40:** Expression and irradiation of $Src_{16}$EGFP K7TAG and $Src_{16}$EGFP K9TAG. Cells were transfected with the Src and PCKRS expression plasmid as well a pPylT with **PCK** (2 mM). Cells were irradiated with a DAPI filter (365/50 nm) Images were taken using a Zeiss Observer Z1 microscope with a 63X objective (NA 1.40 oil/plan-apochromat; Zeiss) and a GFP (38 HE) filter (ex: BP470/40; em: BP525/50).

Disruption of membrane localization through the caging of lysine residues within the Fyn and Src SH4 domain was not surprising as it is reported previously that mutation of K7 of Src and K7 and K9 of Fyn causes reduced membrane localization.[146] However, it is not clear why after decaging localization to the membrane was not restored. If only small amounts of protein are decaged and translocate to the membrane, epi-fluorescent imaging will not be sufficient to detect this and TIRF microscopy could be used as it is more sensitive to activity at the membrane.[132] Another explanation could be the fact that N-myristolyation occurs during protein synthesis,[97] and not-postranslationally. However, light-induced **PCK** decaging can only be conducted after protein synthesis is complete.

### 3.2.3 Experimental

**Cloning of pPCKRS-EGFP plasmids with N-terminal SH4 domains**. pEGFP-N1 was double digested with NheI and AgeI, treated with Antarctic Phosphatase, and gel purified. Purchased inserts for $Fyn_{16}$ and $Src_{16}$ were ligated into double digested pEGFP-N1. $Fyn_{16}$EGFP (Primers: forward 5'-CTAGCATGGGCTGTGTGCAATGTAAGGATAAAGAAGCAACAAAACTGAC

GGAGGGA; reverse 5'- CCGGTCCCTCCGTCAGTTTTGTTGCTTCTTTATCCTT ACATTGCACACAGCCCATG) and $Src_{16}$EGFP (Primers: forward 5'- CTAGCATGGGTAGCAACAAGAGCAAGCCCAAGGATGCCAGCCAGCGGCGCCGCGG A; reverse 5'- CCGGT**CC** GCGGCGCCGCTGGCTGGCATCCTTGGGCTTGCTCTTGTTGC TACCCATG) inserts were generated by Phusion PCR with NheI and MfeI digestion sites. pPCKRS and SH4-domain inserts were double digested and gel purified or PCR purified, respectively. Each SH4-EGFP insert was ligated into pPCKRS. Plasmids were confirmed by sequencing.

**Live-cell Imaging**. HeLa cells were maintained as described in Section 6.5. The day before transfection cells were seeded in an 8-well chamber slide as described in Section 6.6 and incubated overnight at 37 ˚C/5% $CO_2$. Cells were transfected with 200 ng total of DNA (200 ng of the wild type SH4 domain plasmids or 100 ng of pPCKRS-$Fyn_{16}$($Src_{16}$)EGFP TAG mutants + 100 ng of pPylT using the LPEI protocol in Section 00. Cells were incubated overnight at 37 ˚C/5% $CO_2$. The next day media was replaced with 200 μL of phenol red free DMEM for imaging. Imaging parameters can be found in the captions for specific images.

# 4.0 OPTICAL CONTROL OF PROTEASE ACTIVATED RECEPTOR 2

## 4.1.1 Introduction to PAR2

Protease-activated receptor 2 (PAR2) (also known in the literature as proteinase-activated receptor 2) is a member of a family of four G-protein coupled receptors that are embedded in the cell membrane.[148] PARs are expressed at the plasma membrane and upon cleavage of their extracellular N-terminus by serine proteases are irreversibly activated. PAR2 is cleaved by trypsin, tryptase, gingipains-R, elastase, cathepsin G and proteinase-3. These serine proteases are secreted from the pancreas, microbes and immune cells.[149,150, 151] PAR2 is the only PAR that is not activated by thrombin. This cleavage exposes a "tethered" ligand sequence that will interact with an extracellular loop to induce a confirmation change and further signal transduction (Figure 41**A**). Activation of PARs can also be achieved through use of an activating peptide (AP), (Figure 41**B**). In the absence of proteases, a synthetic peptide with the identical sequence of the tethered ligand can be used to activate PARs.[152]

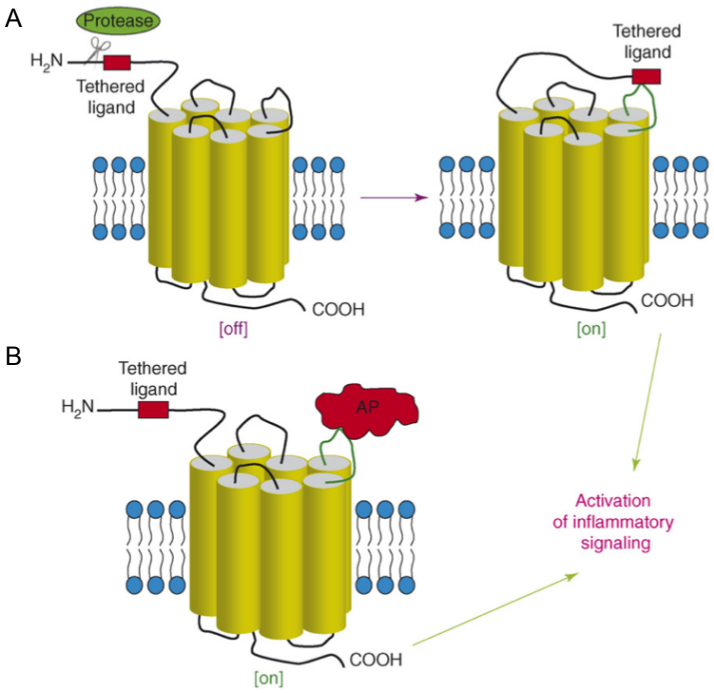


**Figure 41**: Schematic of PAR2 activation. **A**) Activation of PAR2 through cleavage of the tethered ligand peptide by a protease. **B**) Activation of PAR2 through binding of an activating peptide.

In addition to downstream signaling, activation of PAR2 induces an increase in cellular $Ca^{2+}$ concentration.[153] After repeated exposure to trypsin the cellular concentration of $Ca^{2+}$ no longer was affected due to the uncoupling of the G-protein from PAR2 by protein kinase C, and internalization of PAR2 into early endosomes. It was later determined that $Ca^{2+}$ is necessary for PAR2 trafficking as it is required for protein kinase C function and β-arrestins are involved in the desensitization of PAR2.[150] PAR2 is eventually targeted to lysosomes where is it degraded. In order to facilitate further signaling, PAR2 is transported from Golgi storage to the membrane or newly synthesized.[153]

PARs have been implicated in tissue-damage repair, hemostatsis, cell survival, inflammation and pain response.[148] PAR2, specifically, is found in the gastrointestinal tract and pancreas and regulates the secretion of signaling molecules responsible for inflammatory and

anaphylactic reaction response and ion channel activity.[150] The tethered ligand sequence of PAR2 contains a lysine residue.[151]

### 4.1.2 Incorporation of PCK into PAR2 to Photochemically Control Activation

It was hypothesized that the PAR2 interaction with the tethered ligand sequence and thus activation, translocation, and signaling could be controled with light by replacing the lysine with the **PCK** (Figure 42). Photochemical control of PAR2 activation and translocation will allow the investigation of new pathways involving PAR2. Downstream signals can be observed and the timing of PAR2 interactions can be determined due to the precise temporal control of PAR2 activation that is made possible by using light as trigger.

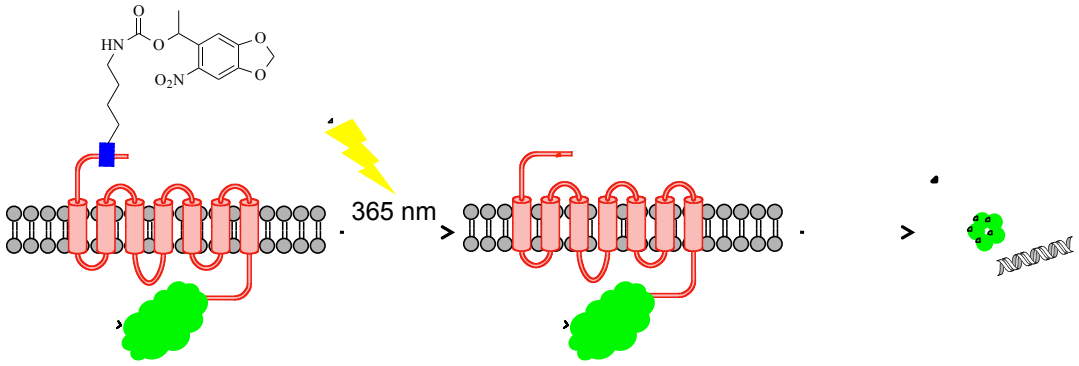


**Figure 42**: Schematic of optical control of PAR2 activation and localization.

It has been shown that activation and cellular translocation of PAR2 can be followed by imaging of a PAR2-EGFP fusion protein.[150] Using a PAR2-EGFP construct from the Bunnett Lab (UCSF), a full length PAR2-EGFP gene and a truncated-tethered ligand exposed PAR2-EGFP gene were cloned into a vector containing the PCKRS. Expression of full length PAR2-EGFP in Kirsten murine sarcoma virus transformed Normal Rat Kidney (KNRK) cells yielded membrane localization of PAR2-EGFP as expected when imaged 24-hours post-transfection

(Figure 43**A**). Transfection of a plasmid encoding the tethered-ligand exposed PAR2-EGFP (ptPAR2-EGFP) into KNRK cells and imaging 24 hours later showed localization of PAR2-EGFP in perinuclear vesicles (Figure 43**B**).[150] This is because the tethered ligand sequence is exposed in the truncated protein and it is constitutively active.

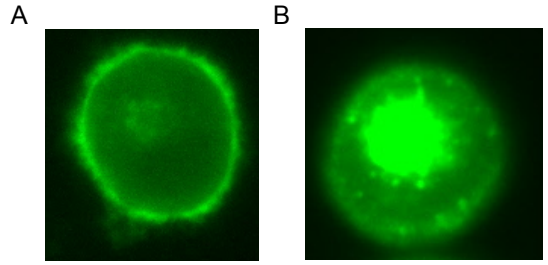


**Figure 43**: Phenotype of PAR2 variants in KNRK cells. **A**) KNRK cell expressing PAR2-EGFP. Full length PAR2 is localized to the membrane. **B**) KNRK cell expressing tPAR2-EGFP. Truncated PAR2-EGFP has the tethered-ligand sequence exposed and therefore is localized to perinuclear vesicles.

Introduction of a TAG mutation at K5 in truncated PAR2-EGFP (tPAR2-EGFP) should mask the tethered ligand, sending tPAR2-EGFP to the membrane. Upon irradiation, the tethered ligand should become exposed and translocation to perinuclear vesicles should be observed (Figure 42).

When KNRK cells were transfected with pPCKRS-tPAR2-EGFP-K5TAG in the absence of **PCK**, expression was still observed (Figure 44**A**). However, there is less PAR2-EGFP localization either at the membrane or perinuclear vesicles compared to that in the cell in Figure 43**A**. When tPAR2-EGFP is expressed (Figure 43**B)** fluorescence is seen in perinuclear vesicles with very little background in other regions of the cells. KNRK cells transfected with pPCKRS-tPAR2-EGFP-K5TAG and pPylT in the presence of **PCK** show expression at the membrane, in perinuclear vesicles and a higher background in the cytosol (Figure 44**B**). Unfortunately, translocation of membrane localized PAR2-EGFP to perinuclear vesicles after 10 seconds of irradiation at 365 nm was never observed. This is likely due to the fact that K5 was found to not

be essential in the tethered linker signaling.[154] It was hoped that **PCK** would be large enough that it would sterically block any signaling before irradiation.

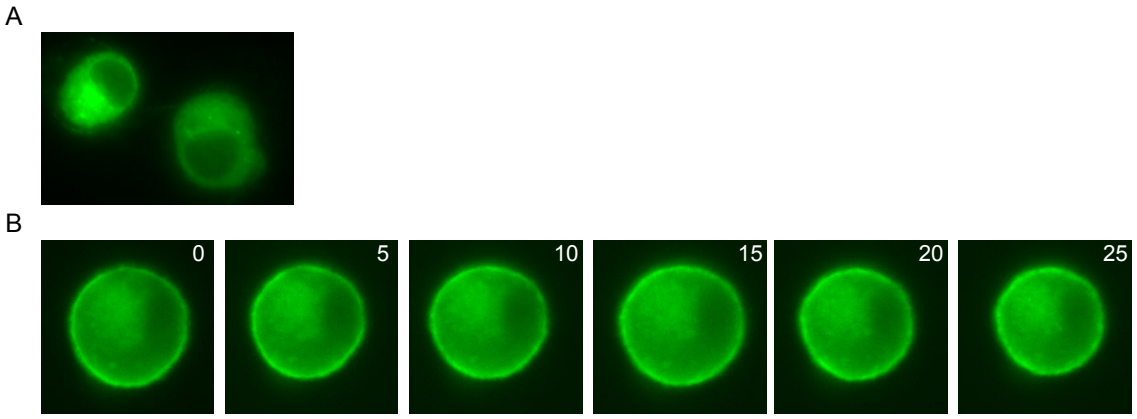


**Figure 44**: Expression of pPCKRS-tPAR2-EGFP-K5TAG with pPylT **A**) in the absence of **PCK** and **B**) in the presence of **PCK.**

In conclusion, substitution of K5 with **PCK** in the tethered ligand sequence of truncated PAR2 did not allow for photochemical control of PAR2 activation and translocation. Localization of tPAR2-EGFP K5TAG in the presence of **PCK** was not exclusively found at the membrane as expected, due to incomplete suppression of the TAG mutation or the inability for **PCK** to block the activation of PAR2 as mutation of K5 is reported to reduce PAR2 activation by 60%,[154] and upon irradiation, translocation of membrane bound tPAR2-EGFP K5TAG to perinuclear vesicles was not seen. This is unexpected, as the decaging should allow for restoration of the lysine residue and activation comparable to cleavage with trypsin. Based on these experiments, a different approach to photochemical control of PAR2 was explored.

### 4.1.3 Caged peptide control of PAR2

As discussed earlier, PAR2 can be activated by an external peptide with the same sequence as that of the tethered ligand. The addition of the activating peptide (AP) induces the translocation of PAR2 from the membrane to perinuclear vesicles, just as cleavage of full-length PAR2 by proteases. In hopes to elucidate the role of K5 in PAR2 activation, efforts were turned to a caged activating peptide. A peptide with the sequence S L I G **PCK** V was synthesized by Rajendra Uprety.

First, the activating peptide (Sigma) was added to KNRK cells expressing PAR2-EGFP at a concentration of 100 μM (Figure 45). The AP was added immediately after time point zero and ruffling of the membrane was observed between 5 and 15 minutes. Translocation of PAR2-EGFP into perinuclear vesicles was the seen starting at 20 minutes. The response of PAR2-EGFP was comparable to that reported in the literature.[153]

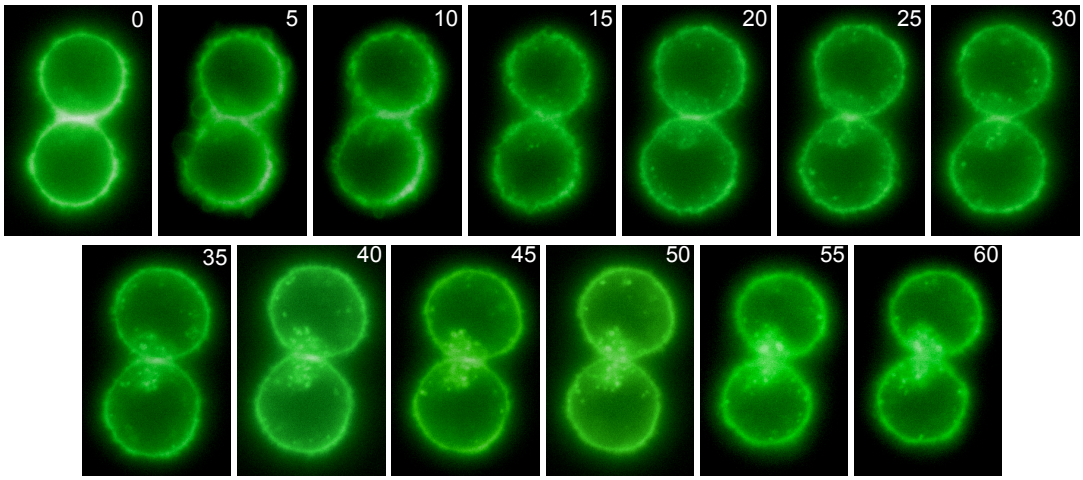


**Figure 45**: Translocation of PAR2-EGFP from the membrane to perinuclear vesicle due to treatment with the activating peptide (AP). Time is indicated in minutes in the top right corner.

The caged AP (cAP) was added to cells that had been transfected with PAR2-EGFP 24-hours prior to the experiment and cells were observed for 35 minutes (Figure 46). The cells were

then irradiated for 10 seconds at 365 nm and watched for another 35 minutes. Unfortunately, the cAP induced translocation of PAR2-EGFP before irradiation. This can be seen by the ruffling of the membrane fluorescence, formation of a double ring and increase in perinuclear vesicle fluorescence 25-30 minutes after the addition of the cAP. This response is not the exact respons seen when the AP was added to cells expressing PAR2-EGFP, but comparable in the increase of fluorescence at perinuclear vesicles. Cells were irradiated in hopes that the rate of translocation from the membrane to perinuclear vesicles would increase. However, cells did not show a substantial reaction after irradiation. From these results, photochemical control of PAR2 activation and translocation through the use of a caged lysine in the AP sequence was not achieved.

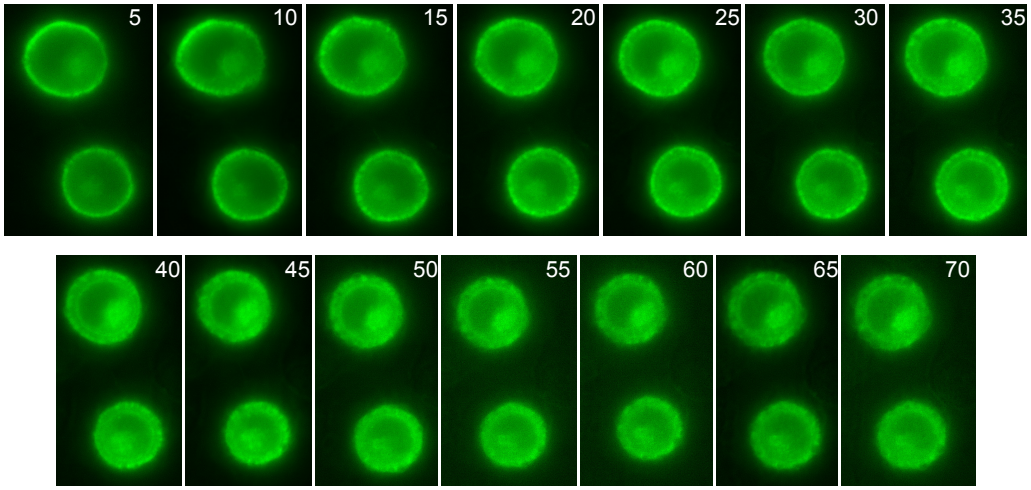


**Figure 46**: Translocation of PAR2-EGFP from the membrane to perinuclear vesicle due to treatment with the caged activating peptide (cAP). cAP was added at time point zero. Cells were irradiated at time point 35. Time is indicated in minutes in the top right corner.

In conclusion, photochemical control of PAR2 has not been achieved. Expression of full length and truncated PAR2-EGFP did show membrane-bound and perinuclear located protein, respectively.[150] However, substitution of K5 with **PCK** in the tethered ligand sequence and expression in KNRK cells presented a mixed phenotype. Fluorescence could be seen at the membrane, as expected, but also in perinuclear vesicles and in the cytosol, before irradiation.

This could be because K5 is not a key residue in the interaction for activation and allows for some protein to be directed to the membrane, but not exclusively, or that the caging group is not large enough to block the activity of the peptide.[154] Previous work has been published that investigated the key residues within the tethered ligand sequence. This work demonstrated that the first two residues of the sequence, serine and leucine, are the most important in determining the activation of PAR2.[154] Mutation of each residue to alanine was performed and only mutation of Ser1 and Leu2 disrupted activation of PAR2 significantly. The work presented here agrees with lysine not being the most important residue in PAR2 activation.

### 4.1.4 Experimental

**Generation of pPCKRS-tPAR2**. pPAR2-GFP was a gift from Dr. Nigel Bunnett (UCLA).[150] Phusion PCR (Section 6.1) was performed to generate the following inserts: wtPAR2-GFP, tPAR2-GFP, and tPAR2-GFP K41TAG with NheI and EcoRI (compatible with MfeI on pPCKRS) restriction sites. Primers are listed below.

PAR2_PCR_tWT+NheI: 5'- ACTGGCTAGCACCATGCGGAGCCCCAGCGCGGC

PAR2_PCR_tWT+NheI: 5'- ACTGGCTAGCACCATGAGCCTTATTGGTAAGGTTG

PAR2_PCR_tTAG+NheI: 5'- ACTGGCTAGCACCATGAGCCTTATTGGTTAGGTTG

EGFP_PCR_WT+EcoRI: 5'- TTACGAATTCCTTACTTGTACAGCTCGTCCATGCC

The single stranded DNA inserts were double digested as described in Section 6.2 and ligated into pPCKRS.

**Live-cell Imaging**. KNRK cells were maintained as described in Section 6.5 and split into an 8-well chamber slide the day before transfection. The day of transfection DMEM was replaced with OptiMEM. Transfection mixtures contained 100 ng of pPCKRS-PAR2-GFP

variants, 100 ng of pPylT, and 0.5 μL of Lipofectamine 2000 (Life Technologies) in 50 μL of OptiMEM the mixture was incubated for 20 minutes at room temperature and then added to the cells. Cells were incubated for 4 hours at 37 ˚C/5% $CO_2$ and then the OptiMEM was replaced with fresh DMEM contained 1 mM **PCK** if required. Cell were incubated overnight at 37 ˚C/5% $CO_2$. The day of imaging DMEM was replaced with phenol red-free DMEM. Images were taken using a Zeiss Observer Z1 microscope with a 40X objective (NA 0.75 /EC plan-apochromat; **Zeiss**) and a GFP (38 HE) filter (ex: BP470/40; em: BP525/50).

# 5.0 OPTICAL CONTROL OF PROTEIN DIMERIZATION

## 5.1.1 Introduction

Chemical inducers of dimerization (CIDs) are small molecules that are used to bring two proteins of interest together. CIDs typically have two binding faces that can bind the same (homodimerizer) or two different (heterodimerizer) proteins of interest. Multiple CIDs have been developed (Figure 47) and been used in the study protein-protein interactions, signal transduction, gene expression and protein secretion.[155]

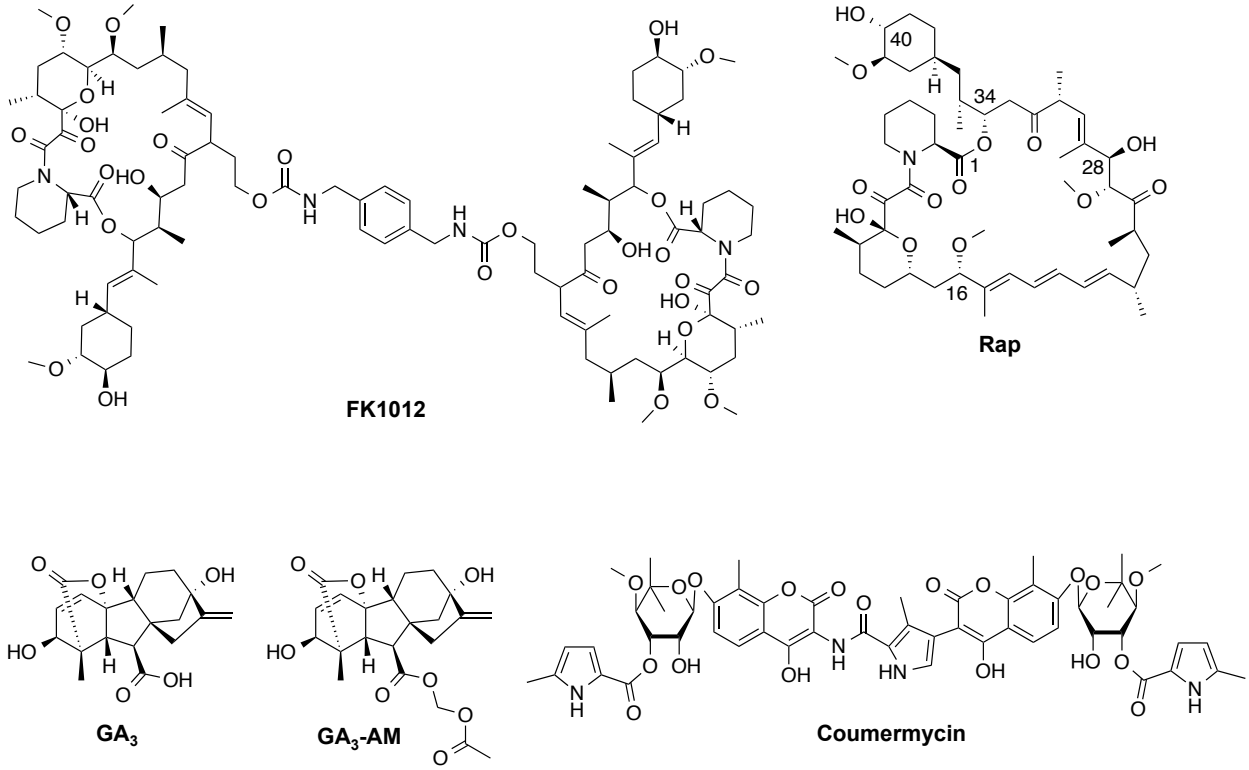


**Figure 47:** Structures of chemical inducers of dimerization.

One of the first homodimerizers developed was **FK1012** (Figure 47). This is a dimer of FK506, which is an immunosuppressant and binds FK506 binding protein (FKBP) and calcineurin to impair T-cell signaling. The homodimerization of FKBP12 has been used in the investigation of cell proliferation,[156] receptor function,[157] apoptosis,[158] and expansion of a specific subset of genetically modified cells.[159] **FK1012** is a FKBP homodimerizer unlike rapamycin, **Rap,** which induces formation of the ternary complex FKBP and FKBP-rapamycin binding (FRB) domain of the mammalian target of rapamycin (mTOR) heterodimerizer.

A heterodimerizer that was developed from a plant hormone, gibberellin, is **$GA_3$**.[160] This small molecule dimerizes gibberellin insensitive dwarf 1 (GID1) and gibberellin insensitive (GAI) through a conformational change of GID1 when a gibberellin metabolite, such as **$GA_3$**, is bound. Miyamoto and coworkers optimized GID1 and GAI to develop a CID system that is completely orthogonal to rapamycin. In order to increase the membrane permeability, an acetoxymethyl group was added to **$GA_3$** to yield the small molecule **$GA_3$-AM**. This modification allows for the **$GA_3$-AM** to cross the cellular membrane and then cellular esterases cleave the acetoxymethyl group to reveal the active **$GA_3$**. **$GA_3$-AM** was used with **Rap** to demonstrate the orthogonality of the two compounds as well as the ability to build logic gates using the two dimerizers. An OR gate and an AND gate were constructed using various combination of GID1, GAI, FKBP, and FRB. $GA_3$-AM has since been used as rapidly control the localization of proteins within cells[161] and to determine the diffusion barrier of cilia.[162] The biggest advantage of this system is that it is completely orthogonal to the FKBP-rapamycin-FRB system. This allows for conditional control of two different proteins of interest, simultaneously. $GA_3$-AM is also a

much smaller molecule than rapamycin, however, due to the negative charge that it carried at physiological pH, it must be modified into cross the cellular membrane.

Another homodimerizer is coumermycin, which has two identical substituted coumarin rings linked together.[163] This small molecule biologically inhibits the *E. coli* DNA gyrase and prevents bacterial growth, however, the binding ability has been further exploited as a chemical biology tool. Coumermycin specifically binds with the N-terminal domain of the DNA gyrase, GyrB, and does not have a eukaryotic target. This makes is especially attractive as a tool in eukaryotic system as it will not interfere with endogenous proteins. This homodimerizer has been using to investigate the signaling pathways of G-protein coupled receptors,[164] Raf-1 kinase[165] and the transcription factor, Stat3.[166]

One of the most extensively used heterodimerizers is rapamycin. The macrocyclic natural product rapamycin, **Rap (**Figure 47) was isolated in the 1970s and has received substantial attention from the scientific community due to its immunosuppressant activity.[167] Naturally rapamycin binds to FKBP12 with a $K_d$ between 0.2 and 0.4 nM.[168] The FKBP12-rapamycin complex then binds to the FRB domain (amino acids 2025-2114) of mTOR, forming a ternary complex consisting of the two proteins and the small molecule.[167,168] This rapamycin-induced protein dimerization has been exploited as a research tool to control a wide range of cellular processes.[169-171,172,173,174,175,176] FKBP12 and FRB are modular proteins that have been fused to a variety of protein targets to conditionally regulate them, including transcription factor domains,[169] kinases,[46] split enzyme systems such as Tobacco Etch Virus Protease (TEVp)[170] and Cre recombinase,[171] as well as cellular localization domains[177] in order to allow for temporal control over protein function with the addition of rapamycin.

Rapamycin naturally interacts with mTOR can be inhibit cell growth. To prevent the resulting cellular toxicity, so called "rapalogs" and FRB mutants have been developed,[178] including **MaRap**, **BSRap**, **iRap**, and **AiRap** (Figure 48). These are analogs of rapamycin with modifications at either the C16 or C20 position. The first rapalog was developed based on the observation that modification of C16 abolished FRB binding.[179] Specific residues within FRB were mutated to create libraries that were then screened for specific binding to the rapalog. In addition to being less toxic than rapamycin, the rapalogs also offer the orthogonal triggering of two different FKBP/FRB-mutant dimerizations.

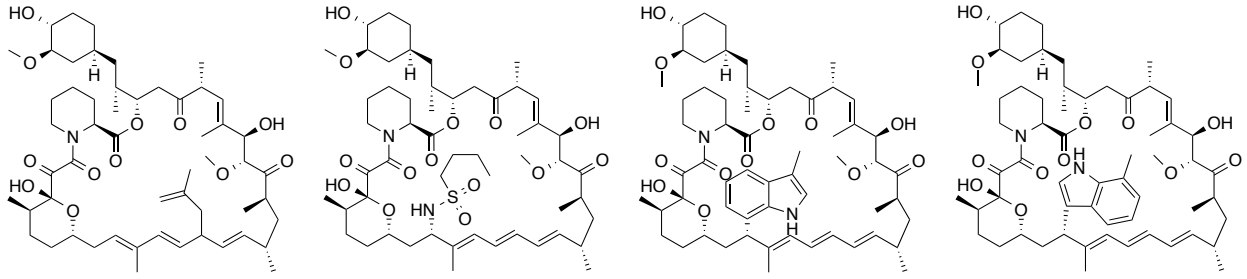


**Figure 48:** Structures of MaRap, BSRap, iRap and AiRap.

Within FRB, there are three amino acids in close proximity ot C16 that have been found to be important in rapamycin binding: K2095, T2098, and W2101. Using a secreted alkaline phosphatase (SeAP) assay, the $EC_{50}$ of each rapalogs was determined for multiple FRB mutants (Table 4**)**. As shown, rapamycin binds with the lowest $EC_{50}$ to the wild type FRB. It was found that a W2101F mutant allows for increased binding affinity of **MaRap**. However, this mutation greatly decreases the binding affinity of the rapalogs with modifications at C16. More specifically **MaRap** and **BSRap** can be used to specifically induce complex formation of their specific FRB mutants and FKBP because they are orthogonal to each other.

**Table 4:** $EC_{50}$ values of rapalogs with FRB mutants. Reprinted from Chemistry & Biology, Bayle, J. H. *et al.* Rapamycin Analogs with Differential Binding Specificity Permit Orthogonal Control of Protein Activity. *Chem Biol* 13, 99-107. Copyright 2006, with permission from Elsevier.

| Mutant Frb | Rapamycin | C20-Marap | C16-BSrap | C16-iRap | AP21967 (C16-AiRap) |
|---|---|---|---|---|---|
| KTW | 0.45 | —[a] | 2.7 | 2.3 | —[a] |
| PLF | 0.80 | 4.5 | —[a] | 6.1 | —[a] |
| KLW | 3.2 | 52 | 16 | 1.2 | 37 |
| PLW | 5.0 | 30 | 26 | 13 | 26 |
| TLW | 2.1 | 34 | 7.4 | 4.6 | 19 |
| ALW | 1.7 | 34 | 7.5 | 4.3 | 19 |
| PTF | 3.3 | 4.5 | —[a] | —[a] | ND |
| ATF | 2.7 | 15 | —[a] | —[a] | ND |
| TTF | 3.0 | 13 | —[a] | —[a] | ND |
| KLF | 0.93 | 4.5 | —[a] | 6.1 | —[a] |
| PLF | 0.8 | 4.5 | —[a] | 6.4 | —[a] |
| TLF | 1.6 | 8.5 | —[a] | 4.3 | —[a] |
| ALF | 1.6 | 1.0 | —[a] | 12 | —[a] |
| KTF | 1.8 | 9.3 | —[a] | —[a] | —[a] |
| KHF | 1.5 | 6.5 | —[a] | 14 | ND |
| KFF | 2.2 | 15 | —[a] | —[a] | ND |
| KLF | 0.93 | 4.5 | —[a] | 12 | —[a] |

Values are measured in the rapalog-dependent transcriptional switch and restandardized for transfection efficiency between experiments according to the $EC_{50}$ of rapamycin against KTW or PLF. ND, not determined.
[a] A half-maximal concentration greater than 150 nM that cannot be determined accurately.

Nuclear protein import and export was used to show the orthogonality of **BSRap** and **MaRap** (Figure 49**)**. An FKBP12-GSK3β-GFP fusion was designed to be used with $FRB^{TLW}$-nuclear export signal (NES) and $FRB^{KTF}$-nuclear localization signal (NLS). GSK3β is a kinase that is typically localized in both the nucleus and the cytoplasm. By fusing it with FKBP12, the localization of GSK3β could be determined based on which rapalog was added to the system. When the proteins are coexpressed in the absence of any rapalogs, GFP fluorescence can be seen throughout the cells (Figure 49**A)**. Cells that have been treated with **BSRap** have GFP excluded from the nucleus (Figure 49**B)**. This is because **BSRap** interacts with $FRB^{TLW}$ over $FRB^{KTF}$ and causes heterodimerization of the FKBP12-GSK3β-GFP to the nuclear export signal. When **MaRap** is used, the an FKBP12-GSK3β-GFP/$FRB^{KTF}$-NLS dimer is formed (Figure 49**C**). This shows that protein dimerization (and thereby protein localization) can be conditionally controlled based on which rapalog is added to cells and which FRB mutant is expressed.

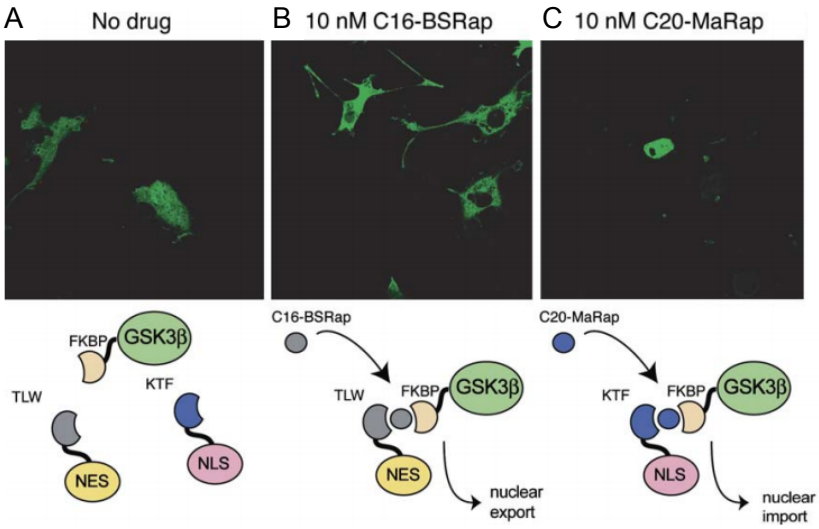


**Figure 49**: Control of cellular localization using orthogonal rapamycin analogs. **A)** Localization through out the cell before addition of rapalog. **B)** Cytoplasmic localization due to binding of the nuclear export signal with the addition of **BSRap**. **C)** Nuclear localization after the addition of **MaRap** due to the binding of the nuclear import signal. Reprinted from Chemistry & Biology, Bayle, J. H. *et al.* Rapamycin Analogs with Differential Binding Specificity Permit Orthogonal Control of Protein Activity. *Chem Biol* 13, 99-107. Copyright 2006, with permission from Elsevier.

Woolley and co-workers developed a caged rapamycin, **C7pRap** (Figure 50**A**) to optically control the function of the mammalian target of rapamycin complex 1, mTORC1.[180] mTORC1 is a complex of 5 proteins, one being the mammalian target of rapamycin (mTOR) that activates protein synthesis through a signaling cascade that ends in the phosphorylation of S6 ribosomal protein.[181] To investigate the role of mTORC1 in protein synthesis, rapamycin can be used due to its ability to bind and inhibit mTOR activity. Analysis of the FKBP-rapamycin-mTOR x-ray crystal structure showed that C-16 is positioned facing towards mTOR, thus a dimethoxynitrobenzyl caged group was synthetically added to rapamycin to generate **C7pRap**.[168] HeLa cells were then used to determine the activity of mTORC1 by probing Western blots for phosphorylation of S6 (Figure 50**B**). Cells treated with 50 or 20 nM rapamycin (Figure 50**B**, lanes C and D) show a decrease in S6 phosphorylation due to the inhibition of mTORC1 by rapamycin and FKBP binding. When cells were treated with 50 or 20 nM **C7pRap**, (Figure 50**B**, lanes E and F) the levels of phosphorylated S6 are equivalent to those in the control

or vehicle samples (lanes A and B). After a 1 minute irradiation at 365 nm, **C7pRap** decages to generate 7-hydroxy rapamycin which has been reported to have similar activity to native rapamycin.[182] This rapamycin derivative was also shown to be active in this assay as the levels of phosphorylated S6 are reduced (Figure 50**B**, lanes G and H). This reduction in phosphorylation is due to the binding of 7-hydroxy rapamycin-FKBP to mTORC1 and inhibition of mTORC1 function. This caged rapamycin was shown to optically control mTORC1 activity and subsequent phosphorylation of S6.

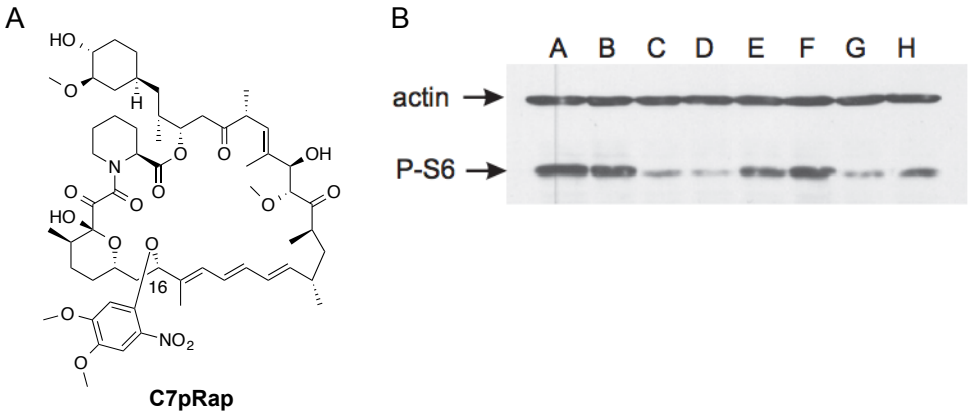


**Figure 50**: Optical control of protein phosphorylation. **A**) Chemical structure of **C7pRap**. **B**) Phosphorylation analysis of S6 by Western blot. Actin was used as a load control Lanes: A: control, B: vehicle, C: 50 nM rapamycin, D: 20 nM rapamycin, E: 50 nM **C7pRap**, F: 20 nM **C7pRap**, G: 50 nM **C7-DMNB-caged rapamycin** + UV, H: 20 nM **C7pRap** + UV. Reprinted from Bioorganic & Medicinal Chemistry, 18, Sadovski, O., Jaikaran, A.S.I., Samanta, S., Fabian, M.R., Dowling, R.J.O., Sonenberg, N., and Woolley, G.A., A Collection of Caged Compounds for Probing Roles of Local Translation in Neurobiology, 7746-7752, 2010, with permission from Elsevier.

In 2011, the photocleavable rapamycin-biotin conjugate **cRb-A** was developed.[45] This worked off the principle that attaching **HERapa** to a macromolecule, such as avidin, would prevent **HERapa** from crossing the cell membrane and interacting with FRB and FKBP12, until fragmentation of a photocleavable linker releases **HERapa** from avidin, (Figure 51**A**). Cell expressing a membrane bound FRB along with a YFP-FKBP12 fusion protein exhibited YFP

fluorescence throughout the cell before irradiation. After irradiation and release of **HERapa**, heterodimerization and membrane localization of YFP occurred (Figure 51**B)**.

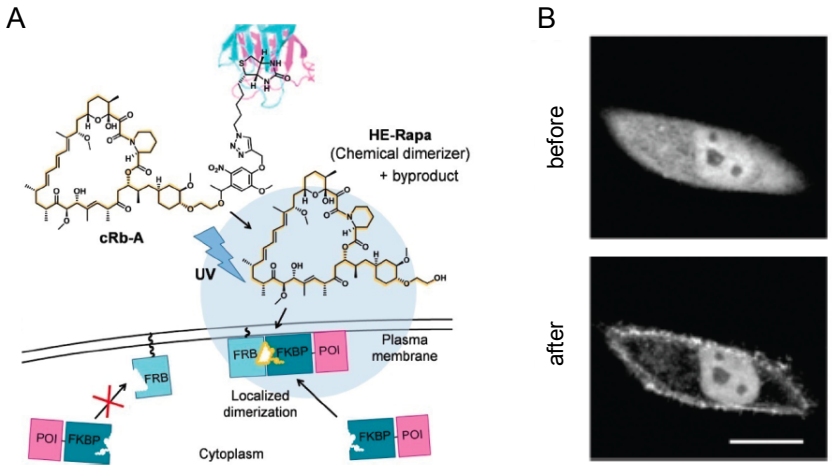


**Figure 51**: Photochemical control of protein dimerization using **HERapa**-avidin (**cRb-A**) conjugate. **A)** Structure of **cRb-A** and schematic of optical control. **B)** Membrane localization in the presence of **cRb-A** before and after UV irradiation. Adapted with permission from Umeda, N., Ueno, T., Pohlmeyer, C., Nagano, T. & Inoue, T. A Photocleavable Rapamycin Conjugate for Spatiotemporal Control of Small GTPase Activity. *J Am Chem Soc* 133, 12-14, doi:10.1021/ja108258d|10.1021/ja108258d (2011). Copyright 2011 American Chemical Society.

To demonstrate the applicability of this caged rapamycin, the activity of Rac GTPase was optically controlled using localization of Tiam1. When Tiam1 is recruited to the membrane, Rac is activated and membrane ruffling can be seen. The membrane localized FRB was used along with a YFP-FKBP12-Tiam1 in NIH3T3 cells. The addition of **cRb-A** to the media did not induce membrane ruffling until a small area near the membrane was irradiated (Figure 52**A)**. Importantly, Rac activation outside of the irradiated area due to diffusion of **HERapa** was not observed (Figure 52**B)**.

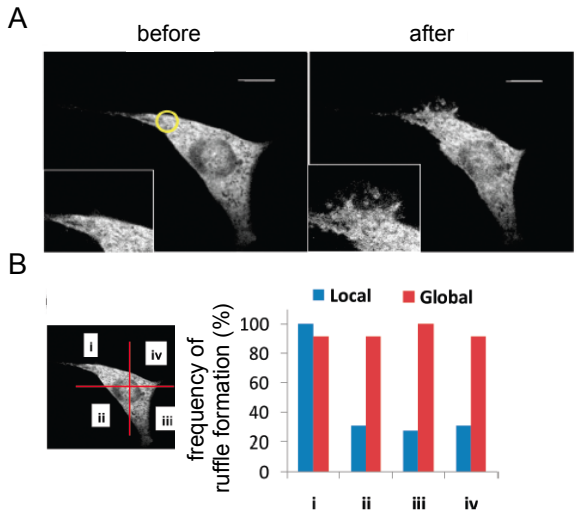


**Figure 52**: Photochemical control of Rac GTPase activity using **cRb-A**. **A)** Spatial irradiation of cellular membrane in the presence of **cRb-A**. Before UV irradiation Tiam1 is not localized to the membrane, thus Rac is inactive. After UV irradiation and release of **HERapa,** Tiam1 is localized to the membrane through heterodimerization and membrane ruffling can be seen as a result of Rac activation. **B)** Spatial irradiation of **cRb-A** in quadrant I caused membrane ruffling only in that quadrant. Adapted with permission from Umeda, N., Ueno, T., Pohlmeyer, C., Nagano, T. & Inoue, T. A Photocleavable Rapamycin Conjugate for Spatiotemporal Control of Small GTPase Activity. *J Am Chem Soc* 133, 12-14, doi:10.1021/ja108258d|10.1021/ja108258d (2011). Copyright 2011 American Chemical Society.

The Deiters lab reported the caged rapamycin **pRap** (Figure 53) in conjunction with an engineered FKBP domain in 2011.[46] It was demonstrated that **pRap** had a similar activity as wild type rapamycin in mediating the dimerization of natural FKBP and FRB. Thus, a truncated mutant of FKBP12 was employed in order to improve the sensitivity of the interaction between **pRap** and FKBP. The truncation of FKBP12, termed iFKBP,[183] is thought to lead to increased mobility of the K52–E54 loop, based on molecular dynamic simulations.[46] This loop is in close proximity to the binding location of the caging group at C40.

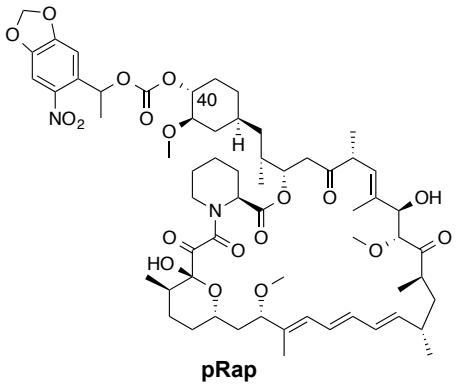


**Figure 53:** Structure of photocaged-rapamycin, **pRap**.

The caging group effectively blocked the **pRap**-mediated dimerization of iFKBP-FRB until the caging group was removed through irradiation (Figure 54**A)**.[46,183] This was used to optochemically control the previously designed iFKBP-FAK.[183] Focal adhesion kinase (FAK) was inactivated by inserting a small portion of FKBP near the catalytic domain. Upon addition of rapamycin and heterodimerization of FRB and iFKBP, a conformational change activated FAK kinase. This system was used to show that **pRap** could be used to optochemically control FAK activity. Immunoprecipitation and kinase assays (Figure 54**B**) were also performed to show optochemical control of FAK activity. After UV irradiation, the heterodimization of iFKBP-FAK and GFP-FRB can be detected as well as the restored kinase activity of FAK through the phosphorylation of paxillin, a target of FAK.

FAK activity was also photochemically control in live cells by expressing iFKBP-FAK and Cherry-FRB in HeLa cells (Figure 54**C**). When treated with **pRap** and before UV irradiation, the cell showed a normal phenotype, however, upon UV irradiation and activation of FAK, membrane ruffling can be seen, which is an indication that FAK has been activated due to the heterodimerization of iFKBP and FRB.

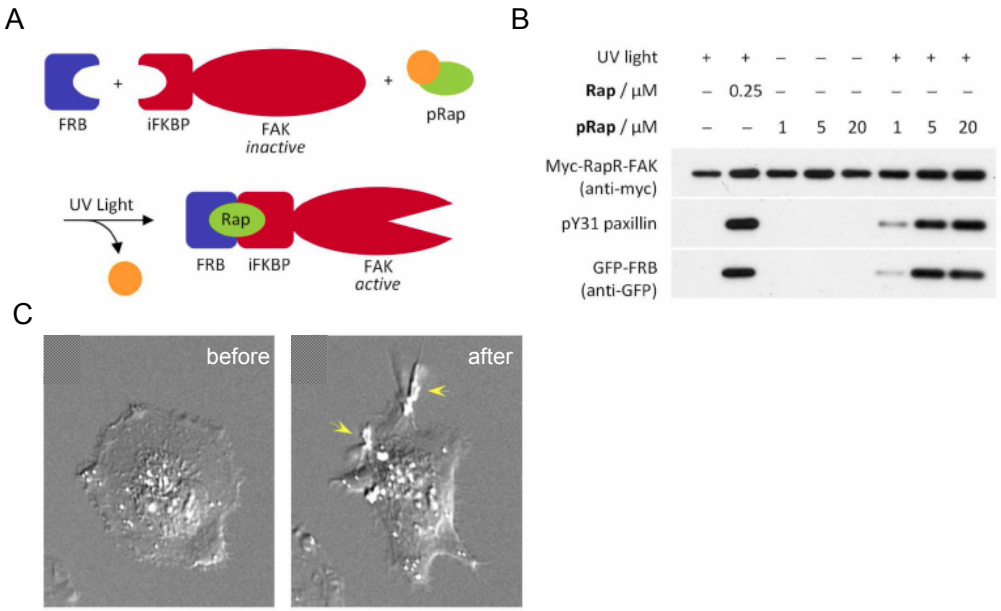


**Figure 54**: Application of **pRap** for controlling FAK. **A)** Schematic of photochemical control of FAK activity. **B)** Immunoprecipitation and kinase assay in the presence and absence of **Rap** and **pRap**. **C)** Photochemical control of FAK activity in live cells determined by membrane ruffling of a HeLa cell. Adapted with permission from Karginov, A. V. *et al.* Light Regulation of Protein Dimerization and Kinase Activity in Living Cells Using Photocaged Rapamycin and Engineered FKBP. *J Am Chem Soc* 133, 420-423, doi:10.1021/ja109630v (2011). Copyright 2011 American Chemical Society.

### 5.1.2 Optical Control of Protein Dimerization Using a Rapamycin Dimer

Since **pRap** is found to be still active in mediating the heterodimerization of FKBP12 and FRB, it was hypothesized that a larger caging group was required in order to fully abrogate its function. Furthermore, we speculated that an efficient way to substantially increase the size of the caging group is by using a second rapamycin molecule as a sterically demanding structure that is able to recruit an even more sterically demanding second FKBP molecule.[184] Thus, the light-cleavable rapamycin dimer **dRap** was designed, in order to allow for optical control of wild-type FKBP12-FRB interactions, obviating the need for protein engineering of the many established rapamycin-controlled processes.[169-176]

The light-cleavable rapamycin dimer **dRap**, (Figure 55) was synthesized from rapamycin in just two steps by Yan Zou (Deiters Lab). After UV irradiation, two native rapamycin molecules are released to participate in the binding of FRB and FKBP12.

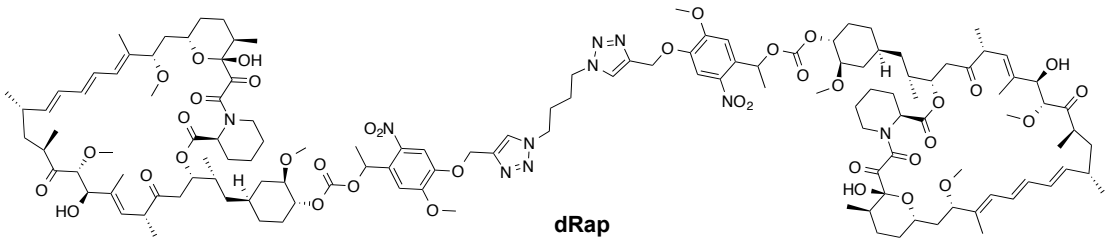


**Figure 55:** The structure the light-cleavable rapamycin dimer (**dRap**).

Based on the crystal structure information of FRB-**Rap**-FKBP12 binding, it was hypothesized that **dRap** homodimerizes FKBP12 before UV irradiation. Fluorescence polarization was used to investigate this capability using a fluorescein isothiocyanate (FITC) labeled FKBP12 (Figure 56**)**. Indeed, the addition **dRap** to a solution of FKBP12-FITC led to an increase in fluorescent polarization, indicating homodimerization of FKBP12-FITC. Moreover, further addition of a 10-fold excess of **dRap** led to a decrease in fluorescence polarization due to the saturation of FKBP12 binding sites with **dRap** molecules, effectively preventing protein dimer formation. Thus, it was speculate that the FKBP12-**dRap**-FKBP12 complex effectively prevents binding of FRB, until it is fragmented through photochemical cleavage of **dRap**. This hypothesis is supported by the comparison of complex formation energies calculated in molecular dynamics simulations.[185]

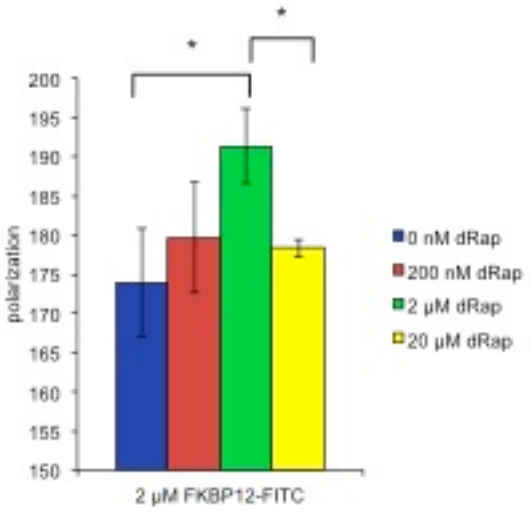


**Figure 56:** Fluorescence polarization of FITC labeled FKBP12 in the presence of dRap. Asterisks represent statistically significant differences in fluorescence polarization; P value < 0.05. Reproduced from Brown, K. A. et al. Light-cleavable rapamycin dimer as an optical trigger for protein dimerization. Chemical communications 51, 5702-5705, doi:10.1039/c4cc09442e (2015) with permission from The Royal Society of Chemistry.

In order to further validate **dRap** as an effective light-activation tool, a K-LISA mTOR Activity assay (Calbiochem) was performed (Figure 57**A)**. mTOR phosphorylates the target protein p70S6K. However, when mTOR forms a ternary complex with FKBP12 and rapamycin, it cannot maintain kinase activity. Through an α–phosphorylation–HRP conjugated antibody, the presence of phosphorylation was monitored. As seen in Figure 57**B**, phosphorylation is indicated by high levels of luminescence in the absence of rapamycin as well as in the presence of **dRap** before UV irradation. This is due to the inability of **dRap** to dimerize FKBP12 and mTOR, allowing mTOR to retain kinase activity. Phosphorylation is reduced by nearly 80% in the presence of rapamycin as a result of the mTOR–**Rap**–FKBP12 complex formation. The decaging of **dRap** after exposure to UV light of 365 nm releases two native rapamycin molecules and FKBP12–mTOR heterodimerization is observed by a decrease in luminescence to the same level as in case of rapamycin. This shows that only upon irradiation and photolysis, but not before, **dRap** successfully dimerizes FKBP12–mTOR *in vitro*.

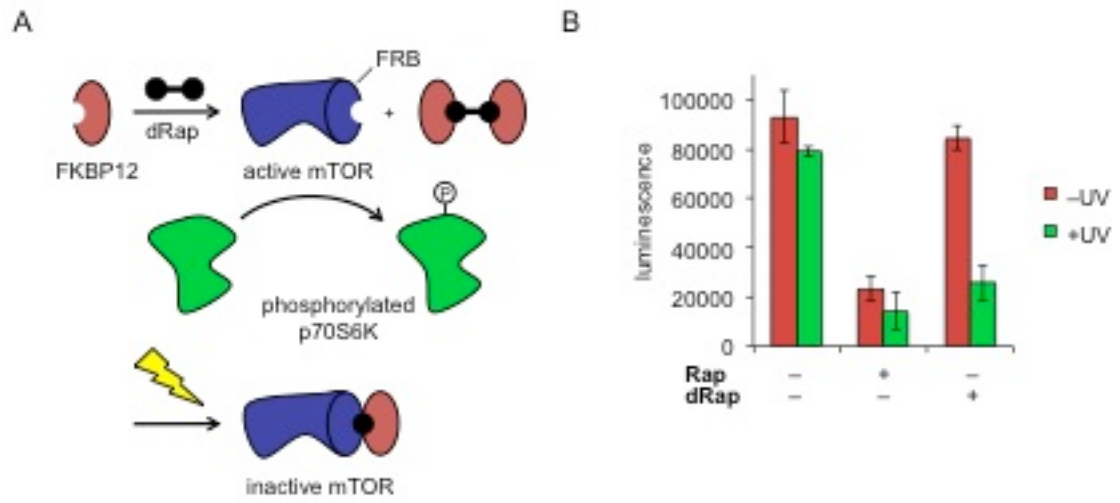


**Figure 57:** K-LISA mTOR assay of **Rap** and **dRap**. **A)** mTOR incubated with FKBP12 and **dRap** will be able to phosphorylate the target protein, p70S6K, due to the homodimerization of FKBP12 by **dRap**. UV exposure generates two native **Rap** molecules that lead to formation of the FKBP12-**Rap**-mTOR complex and eliminate the kinase activity of mTOR. **B)** In the absence of **Rap** or **dRap**, mTOR is functional, leading to high luminescence. dRap (50 nM) is blocked from inducing the heterodimerization of FKBP12 and mTOR, as shown by the high levels of luminescence before irradiation. Irradiation with UV light at 365 nm for 3 minutes converts **dRap** into **Rap** which leads to formation of the FKBP12-**Rap**-mTOR complex and to the same low levels of phosphorylation and thus luminescence as observed in the case of **Rap**. Reproduced from Brown, K. A. et al. Light-cleavable rapamycin dimer as an optical trigger for protein dimerization. Chemical communications 51, 5702-5705, doi:10.1039/c4cc09442e (2015) with permission from The Royal Society of Chemistry.

In order to understand why **dRap** does not engage in formation of a ternary complex with FKBP12 and FRB, a series of atomistic molecular dynamics simulations were conducted by David Shirvanyants from the Dokholyan lab at the University of North Carolina. Several different scenarios were computationally explored to explain the experimentally seen FKBP12 homodimers instead of FKBP12-FRB heterodimers. First, it was excluded that steric hindrance imposed by the second rapamycin molecule may block complex formation, since it appears that FRB binding would be allowed in an outstretched linker conformation. Next, the binding poses of rapamycin and dRap to FKBP12 were examined to determine if it is possible that dRap is found in a position that in unfavorable for FRB binding. However, it was found that dRap frequently assumes FRB favorable binding positions. The final set of simulations determined the energies necessary for formation of the dRap mediated FKBP12 homodimer and the dRap mediated FKBP12-FRB heterodimer. These showed that the formation of dRap mediated

FKBP12 homodimers is more favorable than FKBP12-FRB heterodimers. Thus, the inability of dRap to heterodimerize FRB and FKBP12 is likely caused by the dominating engagement of dRap in the formation of FKBP12 homodimers.

The large free energy of **dRap** mediated homodimerization produces highly stable FKBP12-**dRap**-FKBP12 complexes that are virtually inert to FRB, until activated by **dRap** photolysis. This tightly controlled **dRap** complex formation makes it well suited for light-regulation of biological functions in live cells, as demonstrated by two important biological processes – protein cleavage and DNA recombination – that were investigated in tissue culture. Tobacco etch virus NIa protease (TEVp) is a widely used protease that recognizes a specific seven amino acid sequence, ENLYFQG. Cleavage occurs between the glutamine and glycine residues, and this recognition sequence has been genetically engineered into various proteins to either activate or deactivate their function.[170] TEVp has been used to intracellularly cleave proteins from purification tags,[186] to cleave stabilization proteins from bioactive glycopeptides,[187] to aid in the discovery of protein-protein interactions,[188] and in the inactivation of proteins *in vivo*.[189] Conditional control of TEVp activity was achieved through the application of an inducible TEV expression system[186] and the development of a split TEVp system.[170] In latter case, TEVp was divided into N- (amino acids 1-118) and C- (amino acids 119-241) terminal fragments and each fragment was fused to FRB and FKBP12, respectively. Co-expression of both fusion proteins did not display any protease activity until the addition of rapamycin, which induces dimerization and restores activity of TEVp.

To investigate the photochemical control of protease activity (Figure 58**A**), **dRap** was tested in HEK293T cells expressing the FKBP12-TEV C-terminus and the FRB-TEV N-terminus,[170] as well as a circularly permuted luciferase reporter containing a TEVp cleavage site

(GloSensor, Promega).[190] Active TEVp will cleave the GloSensor protein, causing a conformational change that leads to an activation of the luciferase reporter and luminescence. As seen in (Figure 58**B**) addition of wild-type rapamycin to the transfected cells led to the generation of a luminescence signal, while in the absence of rapamycin only a very low background level of luminescence was detected. Importantly, only background luminescence was observed when the light-cleavable rapamycin dimer **dRap** was added to the media in the absence of UV irradiation. This demonstrates the inability of **dRap** to heterodimerize FRB and FKBP12. Upon a 5-minute irradiation with UV light of 365 nm, the luminescence signal is restored to the same level as rapamycin induction. Thus, irradiation efficiently cleaves the light-sensitive linker, releasing two active rapamycin molecules from one **dRap** molecule. The released rapamycin stimulates dimerization of FBKP12 and FRB, leading to TEVp activity. Importantly, in addition to being fully inactive *in vitro*, the rapamycin dimer is also fully inactive in tissue culture and a brief UV irradiation restores TEVp activity to the same level as the addition of rapamycin itself.

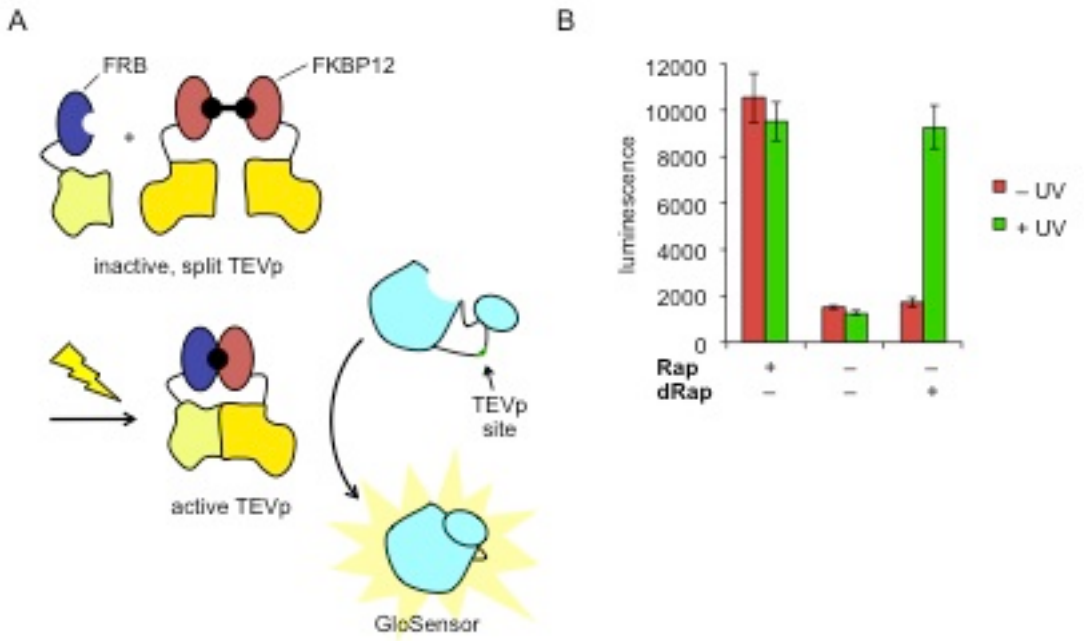


**Figure 58: A)** Representative schematic of the photochemical activation of split TEV using **dRap**. FKBP12-TEV C-terminus (blue) and FRB-TEV N-terminus (red) dimerize only after irradiation of **dRap** and release of two native rapamycin molecules. Active TEVp then cleaves the TEVp recognition site of a circularly permutated luciferase protein, inducing catalytic activity and thus luminescence. **B)** Luminescence data from the split TEVp/GloSensor assay using **dRap**. HEK293T cells expressing FKBP12-TEV C-terminus, FRB-TEV N-terminus, and the GloSensor reporter were treated with rapamycin (100 nM) or **dRap** (50 nM) and irradiated for 5 minutes at 365 nm. Luminescence readings were taken 24 hours after irradiation. Reproduced from Brown, K. A. et al. Light-cleavable rapamycin dimer as an optical trigger for protein dimerization. Chemical communications 51, 5702-5705, doi:10.1039/c4cc09442e (2015) with permission from The Royal Society of Chemistry.

Light-activation of **dRap**, and thus photochemical control of TEVp, allows for non-invasive activation of site-specific protein cleavage in live cells. In addition to protein manipulation, the application of the light-activated rapamycin dimer was also investigated in the manipulation of DNA, specifically DNA recombination by Jie Zhang of the Deiters Lab. In this context, Cre recombinase is an important tool in cell and developmental biology, as it recognizes two palindromic sequences of DNA, known as *loxP* sites, and is able to delete, insert, or invert any DNA sequence that is located between those sites, depending on their orientation.[171] Cre-catalyzed DNA recombination has been extensively used for a wide range of applications starting from simple DNA recombination in *E.* coli,[191] to genetic engineering in yeast,[192] plants[193] and mice.[194] Genetic engineering in mice is widely applied and has allowed for the

conditional control of genes by a *loxP* flanked stop region[195] as well as specific chromosomal rearrangements to mimic human diseases.[196] One of the limitations of Cre is the inability to tightly control the recombination process with external regulatory elements. Methodologies have been developed for the spatiotemporal control of Cre recombinase, including the regulation of Cre catalysis with a photocaged tamoxifen,[197] by caging the catalytic tyrosine residue within the active site,[198] and by fusing each fragment of a split Cre enzyme to a blue light-absorbing photoreceptor and its binding partner.[39] However, there are limitations to each of the current methodologies. When using photocaged tamoxifen there is need for multiple irradiations and limited restoration of Cre activity is seen.[197] There is a requirement of continuous pulses of light for 24 hours when using the split-Cre fused to a natural photoreceptor,[39] and in case of the active-site caged Cre recombinase genetic encoding in mammalian cells has not been achieved.[198]

Here, we are reporting a solution to these problems by utilizing a split Cre system composed of amino acids 19-59 (N-terminus) and amino acids 60-343 (C-terminus) that was fused to FKBP12 and FRB,[171] respectively, enabling the photochemical control of Cre-catalyzed DNA recombination by **dRap** (Figure 59).

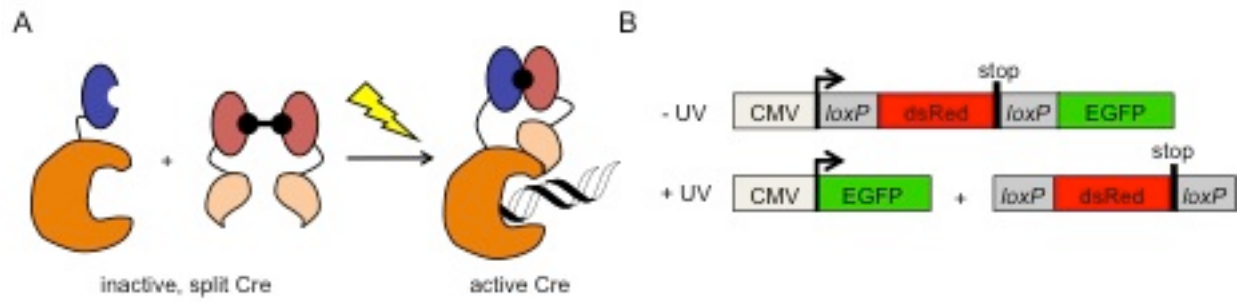


**Figure 59:** Representative schematic of the split Cre system using **dRap**. **A)** FRB-Cre C-terminus (red) and FKBP12-Cre N-terminus (blue) are dimerized after irradiation of **dRap**. **B)** The Cre stoplight reporter expresses dsRed before irradiation, but in the presence of reconstituted, active Cre, the dsRed gene is excised and EGFP is expressed. Reproduced from Brown, K. A. et al. Light-cleavable rapamycin dimer as an optical trigger for protein dimerization. Chemical communications 51, 5702-5705, doi:10.1039/c4cc09442e (2015) with permission from The Royal Society of Chemistry.

To examine the ability of **dRap** to photochemically control Cre catalyzed DNA recombination, HEK293T cells expressing a split Cre system and the Cre Stoplight reporter were used, Figure 60. The Cre Stoplight plasmid expresses DsRed when Cre recombinase is absent or non-functional. In the presence of active Cre, the gene coding for dsRed is excised from the plasmid due to flanking *loxP* sites and CMV-driven EGFP expression is activated.[199] In the presence of **dRap** but the absence of UV irradiation, only dsRed is expressed, an indicator that **dRap** is not capable of heterodimerizing FKBP12 and FRB leading to an inactive Cre recombinase (as seen by red fluorescence present in Figure 60**A**). This is in perfect agreement with the results obtained from cells that are not treated with rapamycin. DNA recombinase is active through the decaging of **dRap** with a brief 5-minute irradiation at 365 nm producing two native rapamycin molecules to participate in the FKBP12-**00**-FRB ternary complex and thus complementation of Cre fragments. The reconstituted Cre enzyme excises the dsRed gene and induces EGFP expression (Figure 59). Quantification of the micrographs using the Zen 2009 software further confirms these results (Figure 60**B**).

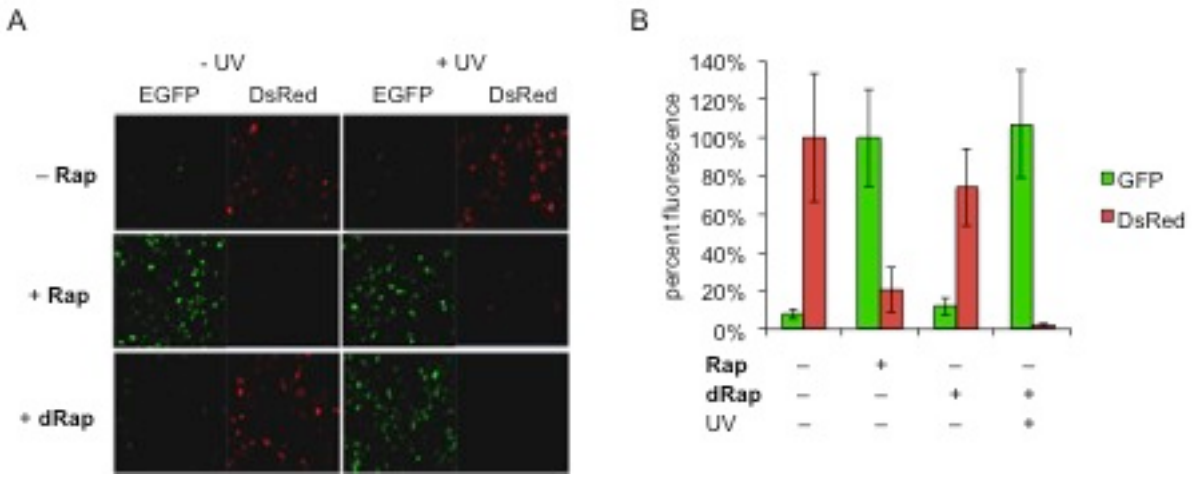


**Figure 60:** Light-activated Cre DNA recombination. Plasmids encoding each fragment of the split Cre enzyme and the Cre stoplight reporter were transfected into HEK293T cells. **A)** Cells were treated with rapamycin (5 nM) or **dRap** (10 nM) and imaged for fluorescence. **B)** Micrographs were quantified by integrating randomly selected areas using Zen imaging software. Error bars are standard deviations generated from three independent integrations. Reproduced from Brown, K. A. et al. Light-cleavable rapamycin dimer as an optical trigger for protein dimerization. Chemical communications 51, 5702-5705, doi:10.1039/c4cc09442e (2015) with permission from The Royal Society of Chemistry.

The synthetic strategy developed above was also applied to generate other **dRap** analogs, containing shorter, more rigid, and photoswitchable linkers (Figure 61**)**. The **dRap-II** and **dRap-III** analogs were thought to further reduce background due to their rigidity. The photoswitchable **dRap-IV** may provide reversible control of FKB/FRBP12 dimerization, an important goal, since no good method exists to break the FRB-**Rap**-FKBP12 complex once it has formed.

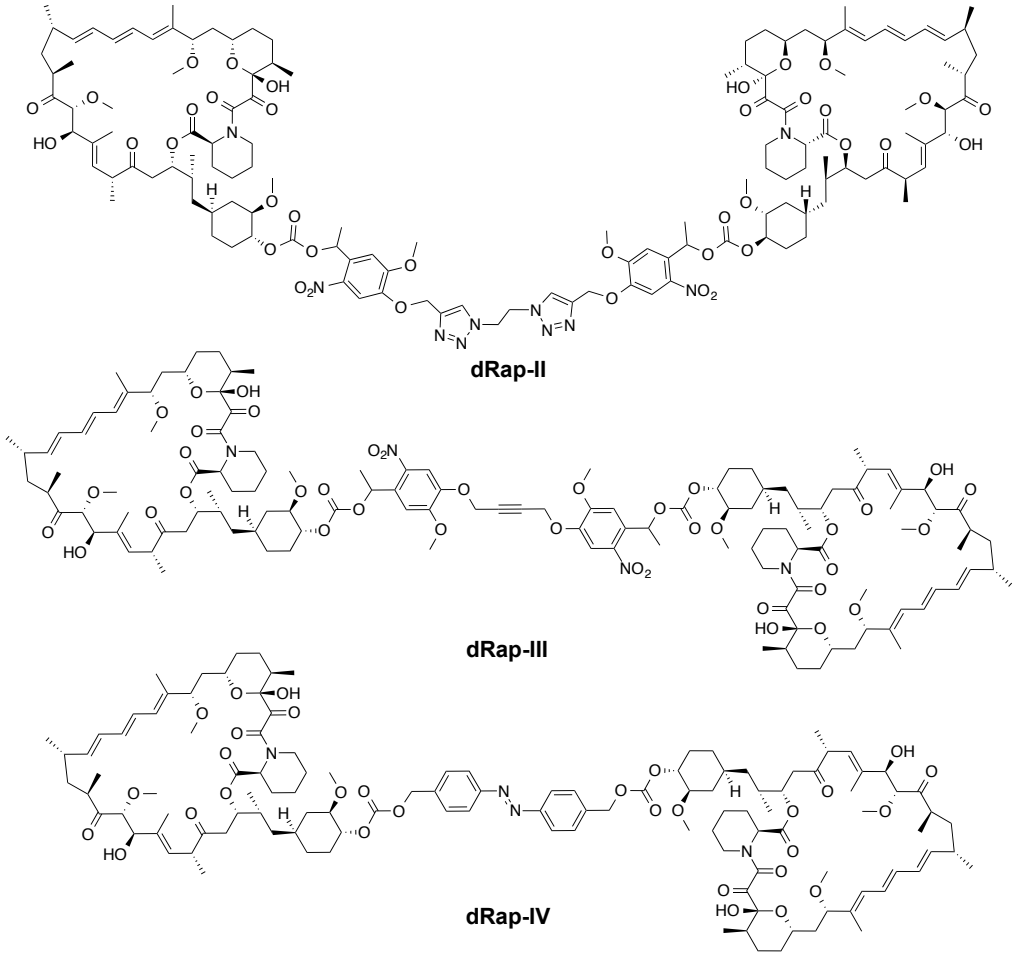


**Figure 61**: Structure of **dRap** analogs

In order to quickly and efficiently investigate the dimerizer functions of the new **dRap** analogs, a fluorescence protein membrane localization system was used (Figure 62**A)**.[124] Cells are transfected with two plasmids: pLyn-FKBP12x2-CFP and pFRB-YFP. The first plasmid expresses a CFP reporter fused to two FKBP12 proteins and anchored in the cell membrane through an N-terminal Lyn domain. The second plasmid expresses a cytosolic YFP-$FRB^{KLW}$ fusion protein. The $FRB^{KLW}$ mutant undergoes dimerization with FKBP in the presence of **iRap** or **Rap** that leads to translocation of YFP to the cell membrane (Figure 62**B)**.

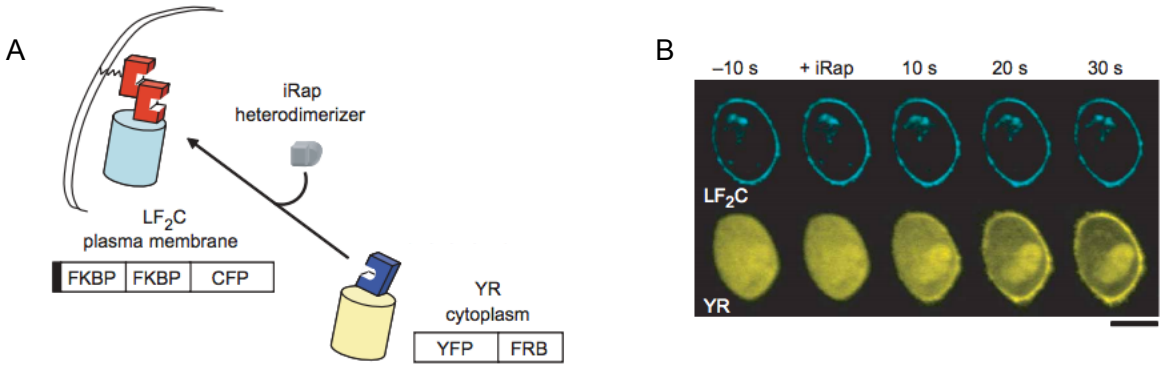


**Figure 62**: Membrane localization system for determination of heterodimerization properties of **dRap** analogs. **A)** Schematic of proteins in membrane localization system. **B)** Localization of YFP to the membrane upon addition of **iRap**. Reprinted by permission from Macmillan Publishers Ltd: Nature Methods. Inoue, T., Heo, W. D., Grimley, J. S., Wandless, T. J. & Meyer, T. An inducible translocation strategy to rapidly activate and inhibit small GTPase signaling pathways. *Nat Methods* 2, 415-418, doi:10.1038/nmeth763 (2005)., copyright 2005.

It was first determined if the **dRap** analogs induced translocation before irradiation. Cells expressing Lyn-FKBP12x2-CFP and FRB-YFP were imaged overnight in the presence of the analogs (Figure 63**)**. Importantly, **dRap-II** and **dRap-IV** did not induce translocation (Figure 63**A** and **C**). Unfortunately, **dRap-III** heterodimerized FKBP12 and FRB at a rate similar to **Rap** causing YFP translocation to the membrane (Figure 63**B)**. It is unknown as to why this analog functions as a CID before UV irradiation, since the photocleavable linker is approximately the same length as the other linkers.

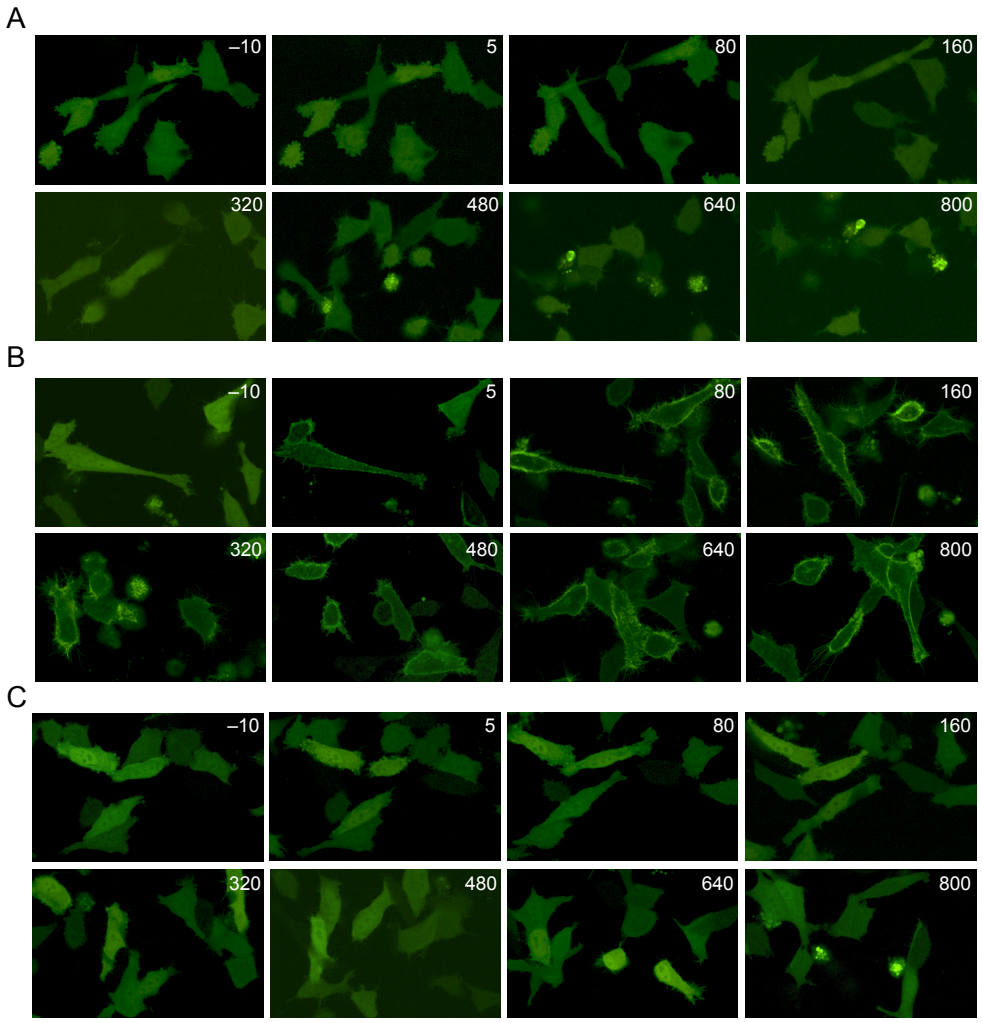


**Figure 63**: Membrane localization of YFP using **dRap** analogs. HeLa cells were expressing Lyn-FKBP12x2-CFP and FRB-YFP. Time is indicated in minutes in the upper right corner. **A)** HeLa cells treated with 100 nM **dRap-II** overnight. Membrane localization was not seen. **B)** HeLa cells treated with 100 nM **dRap-III** overnight. Membrane localization was seen slightly after 5 minutes and significantly after 80 minutes. **C)** HeLa cells treated with 100 nM **dRap-IV** overnight. Membrane localization was not seen. Images were taken on a Nikon A1 confocal microscope with a 20X objective using a 488 nm laser and detectors were set to collect emission from 505 nm to 585 nm.

TIRF microscopy was then used to quantitatively trace the YFP membrane fluorescence before and after irradiation. As seen in Figure 64, addition of rapamycin caused an exponential increase in membrane fluorescence over a short period of time, followed by a plateau. The same pattern was observed when **dRap-III** was added to cells. When **dRap** or **dRap-II** was added to cells, a small increase in fluorescence was seen. Unfortunately, after UV irradiation, a steep drop off in fluorescence was seen. **dRap-IV** induced some translocation without irradiation, which

was not seen in the confocal images. The steep drop in fluorescence after UV irradiation is hypothesized to be due to photobleaching of YFP during the irradiation. This problem has not been solved.

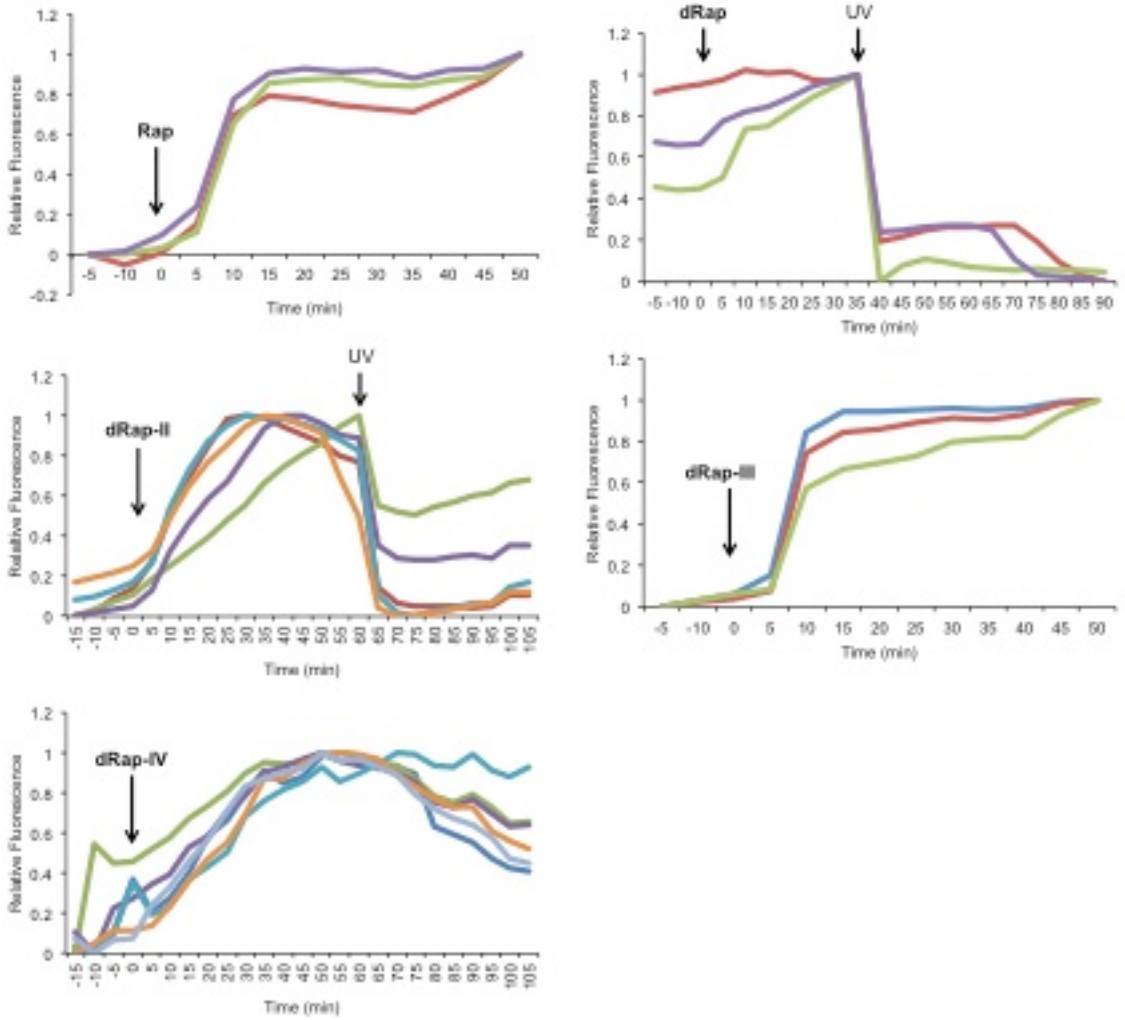


**Figure 64:** Increase in membrane fluorescence measured through TIRF microscopy. **Rap, dRap-III** or **dRap** was added to HeLa cells expressing Lyn-FKBP12x2-CFP and FRB-YFP at the indicated time and the membrane fluorescence was imaged over time. Cells with **dRap** were irradiated at the indicated time.

In conclusion, a light-cleavable rapamycin dimer (**dRap**) was developed that does not induce FKBP12 and FRB heterodimerization until it is activated through UV exposure. Light irradiation cleaves the dimer and delivers two native rapamycin molecules that mediate formation of the FKBP12-rapamycin-FRB ternary complex. Previously reported, caged

rapamycin analogs have been applied to photochemically control protein phosphorylation;[45,46, 180] however, these methodologies have substantial limitations. They require protein engineering of the FKBP domain or mislocalization of the rapamycin molecule outside of the cell, since the presence of the synthetic caging groups alone did not prevent rapamycin-induced FKBP12-FRB dimerization. Thus, the caged rapamycin analogs could not be directly interfaced with the wide range of biological processes that have been placed under conditional control through the construction of FKBP12-rapamycin-FRB based biological switches in cells and multicellular organisms. The rapamycin dimer (**dRap**) was envisioned as an optochemical approach that utilizes recruitment of an entire protein[184] in order to dramatically increase the steric hindrance imposed by the caging group installed at position C-40 of rapamycin. Moreover, the design was kept as simple as possible and utilized a naturally occurring, endogenous protein for this purpose. Thus, the light-cleavable rapamycin dimer **dRap** was synthesized and evaluated for its ability to form the ternary FKBP12-**dRap**-FRB complex before and after light irradiation. Most importantly, it was found that **dRap** was completely inactive as a heterodimerizer. In order to investigate the molecular mechanism behind this inactivity, molecular dynamics simulations were performed and it was discovered, by eliminating all other possibilities, that indeed recruitment of a second FKBP12 protein to FKBP12-**dRap** efficiently prevents interaction with FRB. Fluorescence polarization measurements support the molecular dynamics simulations. This represents the first example of intracellular formation of a highly sterically demanding caging group through the recruitment of an endogenous protein and can be used to photochemically control processes that require more steric bulk than offered by traditional caging groups to block small molecule function. UV exposure switches the FKBP12-**dRap**-FKBP12 complex to the FKBP12-**Rap**-FRB complex, and it was demonstrated that TEV protease activity and Cre DNA

recombinase activity can be optochemically controlled in living cells using this methodology. Because of the modularity of FRB and FKBP12, **dRap** has implications in the light-regulation of protein dimerization and protein activity in a wide range of biological processes that have already been rendered responsive to rapamycin, but could not be readily placed under optochemical control until now.[46,172-176]

Furthermore, the same synthetic approach that was used for **dRap** was used to develop three more analogs: two photocleavable analogs and a photoswitchable analog. **dRap-II** and **dRap-IV** did not induce translocation of YFP to the membrane before UV irradiation. Addition of **dRap-III** to the media triggers translocation of YFP to the membrane without UV irradiation. This is undesirable and **dRap-III** cannot be used of optical control of FKBP12 and FRB heterodimerization. Currently, work is progressing towards the ability to image membrane fluorescence after UV irradiation.

### 5.1.3 Experimental

**Fluorescence Polarization Assay.** FKBP12 (R&D Systems) was stirred with fluorescein isothiocyanate (FITC) at a 1:5 ratio for 3 hours in carbonate-bicarbonate buffer (pH 9.0). FKBP12-FITC was separated from free FITC by overnight dialysis (MWCO 3,500 Da; Spectrum Laboratories, Inc.) into phosphate buffered saline (PBS; pH 7.4). Protein was recovered and the concentration was determined by measuring absorbance on a NanoDrop ND-1000 spectrophotometer using the literature value for the molar extinction coefficient of FITC.[200] FKBP12-FITC was diluted to 2 μM and **dRap** was dissolved at a 100X the final concentration in PBS. FKBP12-FITC was aliquoted into a 384-well plate and **dRap** 100X stocks were added resulting in the required final concentrations of 200 nM, 2 μM, or 20 μM. After 20 minutes of

incubation at room temperature, fluorescence polarization was measured on a Biotek Synergy 4 microplate reader.

**K-LISA mTOR Activity Assay.** GST-p70S6K (Calbiochem) was incubated in glutathione coated plates for 1 hour. mTOR (Sigma-Aldrich) was mixed with FKBP12 (R&D Systems) and either rapamycin (100 nM) or **dRap** (50 nM). Samples were placed in the dark or irradiated with UV light for 3 minutes on a transillumintor (365 nm, 25 W) and then kept on ice for 20 minutes. The samples were added to GST-p70S6K containing wells and incubated at 30 ˚C for 30 minutes. p70S6K phosphorylation was detected with an α-p70S6K-T389 phosphorylation antibody and Luminata Forte ELISA HRP Substrate (Millipore) on a Biotek Synergy 4 microplate reader.

**TEVp Complementation Assay**. HEK-293T cells were maintained at 37 °C and 5% $CO_2$ in Dulbecco's modified Eagle's medium (Hyclone) supplemented with 10% fetal bovine serum (Hyclone) and 10% streptomycin/penicillin (MP Biomedicals). Cells were passaged into a 96-well plate and when 80-90% confluent, were transfected with pFRB-TEVnt, pFKBP12-TEVct, and pTriExGloSensor (100 ng/each) using Lipofectamine 2000 (0.5 μL) (Invitrogen) according to manufacturer's protocol. Twenty-four hours after transfection rapamycin (100 nM) or **dRap** (50 nM) were added and cells were incubated for 3 hours at 37 °C and 5% $CO_2$. Luciferase activity was determined using a Bright Glo-Luciferase Reporter Assay kit (Promega) and a Biotek Synergy 4 microplate reader.

**Cre Recombinase Complementation Assay.** HEK-293T cells were passaged into two 4-well chamber slides, and grown to 80% confluency. The cells were then transfected with the Cre Stoplight (600 ng, 1 well per slide), pcDNA-FKBP-Cre59 (60 ng, 1 well per slide) and pcDNA-FRB-Cre60 (60 ng, 1 well per slide) using X-tremeGENE HP DNA transfection reagent (2:1 X-

tremeGENE/DNA; Roche Biomedicals) in OptiMEM medium (Invitrogen). The transfection mixture was incubated at 37 °C for 6 hours, followed by the replacement of the OptiMEM transfection medium with DMEM. The cells were then incubated with rapamycin (10 nM) or **dRap** (5 nM) at 37 °C and 5% $CO_2$ overnight, followed by irradiation of selected wells for 5 min on a transilluminator (365 nm, 25 W) and replacement of medium with DMEM grow medium. Thirty-six hours post transfection, the cells were analyzed on a Carl Zeiss LSM 700 laser confocal microscope with a 20X plan-apochromat objective for the expression of GFP (excitation at 488 nm with an argon laser and emission at 493-545 nm) and DsRed (excitation at 561 nm with a solid state laser and emission at 574-659 nm) reporter proteins. Quantification of fluorescence was performed using Zen 2009 imaging software. Three independent integrations were performed.

**Membrane Localization Live-Cell Imaging.** HeLa cells were seeded in an 8-well chamber slide according to Section 6.5 and transfected according to Section 6.6. The day of imaging media was removed and replaced with DMEM without phenol red. Cells were placed in a stage top incubator (Tokai Hit) at 37 °C with 5% $CO_2$. Cells were imaged using a Nikon A1 confocal microscope using the lasers indicated in the caption.

# 6.0 GENERAL PROTOCOLS

## 6.1 PHUSION PCR

Combine all components of the reaction mixture (see below), adding Phusion polymerase (NEB) last, and mix thoroughly. Place reaction tubes in a thermocycler and program according to the temperatures and times in Table 5.[201] The temperature for the annealing step should be calculated based on the specific primers for insert amplification. The extension time should be calculated back on the length of the insert. After the program has been executed, add 11.1 µL of CutSmart buffer (NEB) and 1.1 µL of DpnI (NEB) to the reaction and incubate for 1 hour at 37 ˚C. Purify the DNA insert using a PCR purification kit (Qiagen or Omega Bio-Tek) and elute in 50 µL of warm (~42 ˚C) water.

**Reaction Mixture (100 µL)**
20 µL of 5X Phusion buffer
2 µL of dNTPs
5 µL of Primer A (10 µM stock)
5 µL of Primer B (10 µM stock)
1 µL of Template DNA
1 µL of Phusion polymerase
66 µL of water

**Table 5:** Thermocycler program for Phusion PCR

| Temperature | Time | # of cycles |
|---|---|---|
| **95 ˚C** | **30 sec.** | **1** |
| **95 ˚C** | **10 sec.** | **30** |
| **Primer $T_m$ – 5˚C** | **30 sec.** | |
| **72 ˚C** | **30 sec. per 1000 bp** | |
| **72 ˚C** | **10 min.** | **1** |
| **12 ˚C** | **hold** | |

## 6.2 DNA DIGESTION AND LIGATION

For single or double digestion of PCR products or up to 4 µg of backbone, mix DNA (up to 44 µL) with 5 µL of the appropriate 10X buffer from NEB, 0.5 µL of the enzyme(s), and the appropriate volume of water to make a 50 µL final volume. Incubate the reaction at 37 ˚C for 2 hours and then heat inactivate enzymes by incubating at 75 ˚C for 20 minutes.

DNA backbones were treated with Antarctic Phosphatase (AP) after digestion by adding 5.5 µL of 10X AP buffer, and 0.55 µL of AP to the 50 µL of heat-inactivated digestion reaction. This reaction was incubated at 37 ˚C for 1 hour and then gel purified with a Gel Extraction kit (Omgea).

To ligate DNA inserts into DNA backbones, the appropriate volumes were calculated using the equation below. Solving for *X* produced the ratio to determine the volumes of backbone and insert that were used in the ligation reaction. The ligation reaction mixture was 1 µL of 10X ligase buffer, 0.2 µL of ligase and the predetermined ratio of insert and backbone to equal up to 8.8 µL. If the volumes of insert and backbone do not equal 8.8 µL exactly, water was used to fill the reaction to 10 µL. The reaction was incubated at 4 ˚C overnight and transformed into bacteria the following day.

$$\frac{Concentration\ of\ backbone\ ({}^{ng}/_{\mu L}) \times 1}{Number\ of\ basepairs\ of\ backbone} \times 10 = \frac{Concentration\ of\ insert\ ({}^{ng}/_{\mu L}) \times X}{Number\ of\ basepairs\ of\ insert}$$

## 6.3 SITE-DIRECTED MUTAGENESIS

Primers for site-directed mutagenesis (SDM) were designed according to the diagram below and the following restrictions: (1) $T_m$(no) = $T_m$(pp) + 5-10 ˚C, (2) $T_m$ (forward) ≅ $T_m$ (reverse), (3) ΔG of 3' hairpins < –2.5.

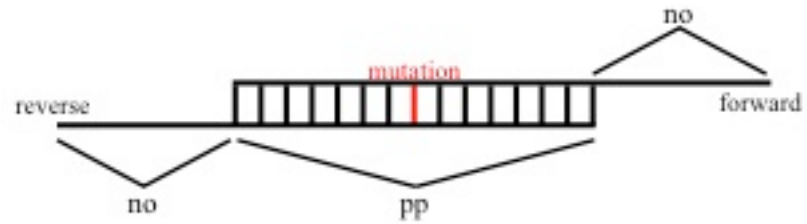


**Figure 65**: Schematic for designing site-directed mutatgenesis primers.

The reaction mixture was combined and Phusion polyermase (NEB) was added last The reaction was mixed thoroughly and placed in thermocycler and program according to the temperatures and times below.[202,203] After the program has been executed, add 3 µL of CutSmart buffer (NEB) and 0.3 µL of DpnI (NEB) to the reaction and incubate for 1 hour at 37 ˚C. DNA was then transformed according to the procedure below.

**Reaction Mixture (100 µL)**
5 µL of 5X Phusion buffer
1 µL of dNTPs
2.5 µL of Primer A (10 µM stock)
2.5 µL of Primer B (10 µM stock)
1 µL of Template DNA (5 ng/µL stock)
1 µL of Phusion polymerase
12 µL of water

**Table 6**: Thermocycler program for site-directed mutagenesis.

| Temperature | Time | # of cycles |
|---|---|---|
| **95 ˚C** | **5 min.** | **1** |
| **95 ˚C** | **1 min.** | **15** |
| **$T_m$ (whole) – 5˚C** | **1 min.** | |
| **72 ˚C** | **1 min. per 500 bp** | |
| **$T_m$ (pp) – 5 ˚C** | **1 min** | **1** |
| **72 ˚C** | **30 min.** | **1** |
| **12 ˚C** | **hold** | |

## 6.4 TRANSFORMATION

Thaw competent cell vial, typically 50 µL, on ice. Add 1 µL DNA for general amplification of plasmids and 10 µL of ligations of SDM reactions. Incubate on ice for 30 minutes. Heat shock in a 42 ˚C water bath for 45 seconds. Incubate on ice for 2 minutes. Add 500 µL SOC to each transformation and shake at 37 ˚C for 1 hour. Plate 100 µL on LB agar containing the appropriate antibiotic for general plasmid amplification and plate all of the transformation for ligations and SDM reactions. Incubate plates overnight at 37 ˚C upside down.

## 6.5 CELL CULTURE MAINTENANCE

Incubate mammalian cells at 37 ˚C/5% $CO_2$ in 10 cm plates with 10 mL of DMEM. Every two to three days passage the cells for continued growth by removing the media, adding 1 mL of TrypLE (Gibco) and incubating for 5-10 minutes. Passaging schedule depends on the growth rate of the cells. Cells were checked every day for confluency to ensure they did not overgrow. Typically HEK293T cells and HeLa cells were passaged every two days. Detach the cells from the plate by pippetting the solution over them with a 1000 µL pipet. Add 9 mL of fresh pre-warmed DMEM to the detached cells and mix gently by swirling the plate. For continued cell growth, add 1 mL of the newly resuspended cells to 9 mL of fresh DMEM. These plates should be labeled with cell type, passage number, date and initials, and incubated at 37 ˚C/5% $CO_2$ until the next passage is required. The cells remaining in the plate will be passaged into plates or chamber-slides for experiments if necessary. The volumes of cell-suspension and fresh DMEM for various plate sizes can be found below.

**Table 7**: Seeding volumes for vary sized plates.

| Plate Type | Volume of Cell-Suspension | Volume of Fresh DMEM | Total Volume |
|---|---|---|---|
| **8-well chamber slide** | **100 µL** | **200 µL** | **300 µL** |
| **96-well plate** | **50 µL** | **150 µL** | **200 µL** |
| **6-well plate** | **750 µL** | **1.25 mL** | **2 mL** |

## 6.6 TRANSFECTION

On the day of transfection, replace the DMEM with fresh media without antibiotics. Place plate with cells in incubator (37 ˚C/5% $CO_2$) while the transfection mixture is prepared. Combine OptiMEM, DNA, and LPEI according to the table below. Mix well and incubate for 10 minutes at room temperature. Add the transfection mixture to the appropriate wells and incubate overnight at 37 ˚C/5% $CO_2$.

**Table 8**: Transfection volumes for LPEI transfection in varying plate sizes.

| Plate Type | Volume of DMEM without antibiotics | Volume of OptiMEM | Volume of LPEI | Amount of total DNA |
|---|---|---|---|---|
| **8-well chamber slide** | **180 µL** | **20 µL** | **2 µL** | **200 ng** |
| **96-well plate** | **180 µL** | **20 µL** | **2 µL** | **200 ng** |
| **6-well plate** | **1.8 mL** | **200 µL** | **20 µL** | **2 µg** |

## 6.7 MAMMALIAN CELL LYSIS

Remove DMEM with the transfection mix and wash cells with 1 mL of cold PBS. Add 200 µL of appropriate lysis buffer directly to each well, place the plate on ice and rock for 20 minutes.

Transfer the lysates to microcentrifuge tubes and centrifuge at maximum speed (21,130 × *g*) for 20 minutes at 4 °C. Transfer supernatants to new microcentrifuge tubes and discard the debris pellets.

## 6.8 SDS-PAGE

Add 30 µL of supernatant to 10 µL of 4× SDS loading dye and mix by pipetting. Heat for 5 minutes at 95 °C. Load 15 µL of the protein solution from each well into 2 lanes of a 10-well SDS-PAGE gel. Two lanes are loaded in order to blot for the protein of interest and the GAPDH control in the Western blot protocol. Run gel at 60 V for 15 minutes and 150 V for 45 minutes to 1 hour until the dye front has run off the gel.

## 6.9 WESTERN BLOTTING

To transfer proteins from the gel to the PVDF membrane (GE Healthcare) using a Bio-Rad wet transfer system, start with the black side of the transfer cassette down in a dish with enough cold transfer buffer to cover the transfer cassette, stack the foam pad, 2 sheets of filter paper, and the SDS-PAGE gel. Soak the PVDF membrane in 15 mL of methanol for 1 minute and place it on top of the gel. Carefully remove any air bubbles from between the gel and the membrane. Add 2 sheets of filter paper and another foam pad on top of the membrane and close the transfer cassette. Place the transfer sandwich in the transfer apparatus and then into a gel tank that is filled with ice-cold transfer buffer. Add an ice pack to the tank and run the transfer at 80 V for 1

hour. Alternatively, the tank can be placed into an ice bath during transfer. Remove the membrane from the transfer sandwich and place it protein-side up in a suitable container (e.g., a 50 mL Falcon tube). The rest of the transfer sandwich can be discarded. Block the membrane with 25 mL of 2.5% milk in TBST for 1 hour while rocking at room temperature. Incubate the membrane with the appropriate antibody overnight at 4 °C while rocking. Antibody dilutions are typically 1:1000 in 15 mL TBST with 2.5% milk. Wash the membrane three times with 15 mL of TBST for 5 minutes each. Incubate the membrane with 15 mL of goat anti-rabbit-HRP conjugate antibody (1:30,000 dilution in TBST) for 1 hour while rocking at room temperature. Wash the membrane three times with 15 mL of TBST for 5 minutes each. Develop the membrane using the VisiGlo Prime HRP Chemiluminescent Substrate Kit (Amresco). Image the chemiluminescence signal using a ChemiDoc gel imaging system (Bio-Rad). Signal should be accumulated for 30 seconds using the chemiluminescent setting, "Chemi." If this does not result in a clear image of the Western blot bands, accumulation time can be increased. Alternative, if the signal is too high, the accumulation time can be decreased.

# APPENDIX A

Reagent recipes

10X Phosphate buffered saline (PBS) (250 mL)

20 g of sodium chloride

0.5 g of potassium chloride

3.6 g of sodium phosphate (dibasic)

0.6 g of potassium phosphate (monobasic)

Fill to 250 mL with MilliQ water. Adjust the pH to 7.4 +/– 0.2. Sterilize by autoclaving and store at room temperature of 4 ˚C. Dilute to 1X before use.

10X Tris buffered saline (TBS) (1 L)

87.6 g of sodium chloride

12.1 g of Tris-base

Fill to 900 mL with MilliQ water and adjust the pH to 7.6 +/– 0.2. This will take approximate 15 mL of 60% hydrochloric acid. Then fill to 1 L with MilliQ water. Store at room temperature.

Tris buffered saline with Tween-20 (TBST, 500 mL)

50 mL of 10X TBS

0.5 g of Tween-20

Add 450 mL of MilliQ water and mix thoroughly.

10X Western blot transfer buffer (1 L)

30.3 g of Tris-base

144 g of glycine

Fill to 1 L with MilliQ water and mix thoroughly. Store at 4 ˚C.

Western blot transfer buffer (2 L)

200 mL of 10X Western blot transfer buffer

400 mL of methanol

0.5 g of sodium dodecyl sulfate

Fill to 2 L with MilliQ water and mix thoroughly. Store at 4 ˚C. Western blot transfer buffer can be reused three times.

10X SDS-PAGE running buffer (1 L)

30 g of Tris-base

144 g of glycine

10 g of sodium dodecylsulfate

Fill to 1 L with MilliQ water and mix thoroughly. Store at room temperature. Dilute to 1X before use. Diluted SDS-PAGE running buffer can be reused up to 5 times.

Western blot stripping buffer

2% sodium dodecylsulfate (SDS)

100 mM β-mercaptoethanol (BME)

50 mM Tris, pH 6.8

4% SDS-PAGE stacking gel (2 mL)

1.458 mL of water

0.25 mL of 40% acrylamine

0.25 mL of 1 M Tris, pH 6.8

20 µL of 10% sodium dodecylsulfate (SDS)

20 µL of 10% ammonium persulfate (APS)

2 µL of Tetramethylethylenediamine (TEMED)

8% SDS-PAGE gel (5 mL)

2.645 mL of water

1 mL of 40% acrylamine

1.25 mL of 1 M Tris, pH 6.8

50 μL of 10% sodium dodecylsulfate (SDS)

50 μL of 10% ammonium persulfate (APS)

5 μL of Tetramethylethylenediamine (TEMED)

10% SDS-PAGE gel (5 mL)

2.4 mL of water

1.25 mL of 40% acrylamide

1.25 mL of 1.5 M Tris, pH 8.9

50 μL of 10% sodium dodecylsulfate (SDS)

50 μL of 10% ammonium persulfate (APS)

3 μL of Tetramethylethylenediamine (TEMED)

12% SDS-PAGE gel (5 mL)

2.15 mL of water

1.5 mL of 40% acrylamide

1.25 mL of 1.5 M Tris, pH 8.9

50 μL of 10% sodium dodecylsulfate (SDS)

50 μL of 10% ammonium persulfate (APS)

3 μL of Tetramethylethylenediamine (TEMED)

15% SDS-PAGE gel (5 mL)

1.775 mL of water

1.875 mL of 40% acrylamide

1.25 mL of 1.5 M Tris, pH 8.9

50 µL of 10% sodium dodecylsulfate (SDS)

50 µL of 10% ammonium persulfate (APS)

3 µL of Tetramethylethylenediamine (TEMED)

DMEM

5.89 g of DMEM powder

1.63 g of sodium bicarbonate

0.145 g of L-glutamine

Add 440 mL of MilliQ water and pH to 7.4 ± 0.2. Add 50 mL fetal bovine serum and 10 mL of penicillin/streptomycin in the biological safety cabinet. Filter media and store at 4 ˚C for up to two months. Before use, media should be warmed at room temperature for 30 minutes or in a 37 ˚C water bath until warm.

Kinase lysis buffer

20 mM Tris

10% glycerol

1% Triton-X100

200 mM sodium chloride

25 mM β-glycerophosphate

2 mM ethylenediaminetetraacetic acid (EDTA)

0.5 mM dithiothreitol (DTT)

1 mM sodium orthovanadate

2 mM sodium pyrophosphate

1 mM phenylmethanesulfonylfluoride (PMSF)

50 mM sodium fluoride

protease inhibitor (diluted to manufacturer's instructions)

Make fresh before use and keep on ice.

Phosphorylation lysis buffer (from Haugh Lab)

50 mM HEPES, pH 7.4

100 mM sodium chloride

10% (w/v) glycerol

1% (v/v) Triton X-100

1 mM sodium orthovanadate

50 mM β-glycerophosphate, pH 7.3

5 mM sodium fluoride

1 mM ethylene glycol tetraacetic acid

10 mM sodium pyrophosphate, pH 7.0

protease inhibitor (diluted to manufacturer's instructions)

Make fresh before use and keep on ice.

Kinase assay buffer

25 mM HEPES, pH 7.4

25 mM β-glycerophosphate

25 mM magnesium chloride

0.5 mM dithiothreitol (DTT)

0.1 mM sodium orthovanadate

Make fresh before use and keep on ice.

Kinase assay buffer II (from Haugh Lab)

20 mM Tris-HCl, pH 7.5

5 mM β-glycerophosphate, pH 7.3

1 mM ethylene glycol tetraacetic acid

0.2 mM dithiothreitol (DTT)

0.1 mg/mL bovine serum albumin

15 mM magnesium chloride

50 μM ATP

Make fresh before use and keep on ice.

4X SDS-PAGE loading dye

2 mL of 1 M Tris-HCl pH 6.8

0.8 g of sodium dodecylsulfate

4 mL of glycerol

400 μL of β-mercaptoethanol

8 mg of bromophenol blue

Add water to fill to 10 mL and store at room temperature.

## BIBLIOGRAPHY


1 Liu, C. C. & Schultz, P. G. Adding new chemistries to the genetic code. *Annu Rev Biochem* **79**, 413-444, doi:10.1146/annurev.biochem.052308.105824 (2010).

2 Noren, C., Anthony-Cahill, S., Griffith, M. & Schultz, P. A GENERAL-METHOD FOR SITE-SPECIFIC INCORPORATION OF UNNATURAL AMINO-ACIDS INTO PROTEINS. *Science* **244**, 182-188, doi:10.1126/science.2649980 (1989).

3 Nowak, M. W. *et al.* Nicotinic receptor binding site probed with unnatural amino acid incorporation in intact cells. *Science* **268**, 439-442 (1995).

4 Wang, L., Brock, A., Herberich, B. & Schultz, P. Expanding the genetic code of Escherichia coli. *Science* **292**, 498-500, doi:10.1126/science.1060077 (2001).

5 Wals, K. & Ovaa, H. Unnatural amino acid incorporation in E. coli: current and future applications in the design of therapeutic proteins. *Frontiers in chemistry* **2**, 15, doi:10.3389/fchem.2014.00015 (2014).

6 Chin, J. W. *et al.* An expanded eukaryotic genetic code. *Science* **301**, 964-967, doi:10.1126/science.1084772 (2003).

7 Hancock, S. M., Uprety, R., Deiters, A. & Chin, J. W. Expanding the genetic code of yeast for incorporation of diverse unnatural amino acids via a pyrrolysyl-tRNA synthetase/tRNA pair. *J Am Chem Soc* **132**, 14819-14824, doi:10.1021/ja104609m (2010).

8 Wang, Q. & Wang, L. New methods enabling efficient incorporation of unnatural amino acids in yeast. *J Am Chem Soc* **130**, 6066-6067, doi:10.1021/ja800894n (2008).

9 Sakamoto, K. *et al.* Site-specific incorporation of an unnatural amino acid into proteins in mammalian cells. *Nucleic Acids Res* **30**, 4692-4699 (2002).

10 Zhang, Z. *et al.* Selective incorporation of 5-hydroxytryptophan into proteins in mammalian cells. *Proc Natl Acad Sci U S A* **101**, 8882-8887, doi:10.1073/pnas.0307029101 (2004).

11 Mukai, T. *et al.* Adding l-lysine derivatives to the genetic code of mammalian cells with engineered pyrrolysyl-tRNA synthetases. *Biochem Biophys Res Commun* **371**, 818-822, doi:10.1016/j.bbrc.2008.04.164 (2008).

12 Srinivasan, G., James, C. M. & Krzycki, J. A. Pyrrolysine encoded by UAG in Archaea: charging of a UAG-decoding specialized tRNA. *Science* **296**, 1459-1462, doi:10.1126/science.1069588 (2002).

13 Neumann, H., Peak-Chew, S. & Chin, J. Genetically encoding N-epsilon-acetyllysine in recombinant proteins. *Nat Chem Biol* **4**, 232-234, doi:10.1038/nchembio.73 (2008).

14 Chen, P. *et al.* A Facile System for Encoding Unnatural Amino Acids in Mammalian Cells. *Angew. Chem. Int. Ed.* **48**, 4052-4055, doi:10.1002/anie.200900683 (2009).

15 Li, W. T. *et al.* Specificity of pyrrolysyl-tRNA synthetase for pyrrolysine and pyrrolysine analogs. *J Mol Biol* **385**, 1156-1164, doi:10.1016/j.jmb.2008.11.032 (2009).

16 Gautier, A. *et al.* Genetically Encoded Photocontrol of Protein Localization in Mammalian Cells. *J Am Chem Soc* **132**, 4086-4088, doi:10.1021/ja910688s (2010).

17 Bianco, A., Townsley, F. M., Greiss, S., Lang, K. & Chin, J. W. Expanding the genetic code of Drosophila melanogaster. *Nat Chem Biol* **8**, 748-750, doi:10.1038/nchembio.1043 (2012).
18 Greiss, S. & Chin, J. W. Expanding the genetic code of an animal. *J Am Chem Soc* **133**, 14196-14199, doi:10.1021/ja2054034 (2011).
19 Kang, J. Y. *et al.* In vivo expression of a light-activatable potassium channel using unnatural amino acids. *Neuron* **80**, 358-370, doi:10.1016/j.neuron.2013.08.016 (2013).
20 Parrish, A. R. *et al.* Expanding the genetic code of Caenorhabditis elegans using bacterial aminoacyl-tRNA synthetase/tRNA pairs. *ACS Chem Biol* **7**, 1292-1302, doi:10.1021/cb200542j (2012).
21 Bell, S. & Dutta, A. DNA replication in eukaryotic cells. *Annu Rev Biochem* **71**, 333-374, doi:10.1146/annurev.biochem.71.110601.135425|10.1146/annurev.biochem.71.110601.135425 (2002).
22 Csepanyi-Komi, R., Levay, M. & Ligeti, E. Small G proteins and their regulators in cellular signalling. *Mol Cell Endocrinol* **353**, 10-20, doi:10.1016/j.mce.2011.11.005 (2012).
23 Vale, R. The molecular motor toolbox for intracellular transport. *Cell* **112**, 467-480, doi:10.1016/S0092-8674(03)00111-9 (2003).
24 Merrick, W. Mechanism and Regulation of Eukaryotic Protein-Synthesis. *Microbiol Rev* **56**, 291-315 (1992).
25 Deiters, A. Principles and Applications of the Photochemical Control of Cellular Processes. *ChemBioChem* **11**, 47-53, doi:10.1002/cbic.200900529 (2010).
26 Golynskiy, M., Koay, M., Vinkenborg, J. & Merkx, M. Engineering Protein Switches: Sensors, Regulators, and Spare Parts for Biology and Biotechnology. *ChemBioChem* **12**, 353-361, doi:10.1002/cbic.201000642|10.1002/cbic.201000642 (2011).
27 Yu, H., Li, J., Wu, D., Qiu, Z. & Zhang, Y. Chemistry and biological applications of photo-labile organic molecules. *Chem Soc Rev* **39**, 464-473, doi:10.1039/b901255a (2010).
28 Fenno, L. *et al.* The Development and Application of Optogenetics. *Annu Rev Neurosci* **34**, 389-412, doi:10.1146/annurev-neuro-061010-113817 (2011).
29 Riggsbee, C. & Deiters, A. Recent advances in the photochemical control of protein function. *Trends Biotechnol* **28**, 468-475, doi:10.1016/j.tibtech.2010.06.001 (2010).
30 Baker, A. S. & Deiters, A. Optical Control of Protein Function through Unnatural Amino Acid Mutagenesis and Other Optogenetic Approaches. *Acs Chemical Biology* **9**, 1398-1407, doi:Doi 10.1021/Cb500176x (2014).
31 Gautier, A. *et al.* How to control proteins with light in living systems. *Nat Chem Biol* **10**, 533-541, doi:10.1038/nchembio.1534 (2014).
32 Crosson, S., Rajagopal, S. & Moffat, K. The LOV domain family: photoresponsive signaling modules coupled to diverse output domains. *Biochemistry* **42**, 2-10, doi:10.1021/bi026978l (2003).
33 van Bergeijk, P., Adrian, M., Hoogenraad, C. C. & Kapitein, L. C. Optogenetic control of organelle transport and positioning. *Nature* **518**, 111-114, doi:10.1038/nature14128 (2015).
34 Zhang, F. *et al.* The microbial opsin family of optogenetic tools. *Cell* **147**, 1446-1457, doi:10.1016/j.cell.2011.12.004 (2011).

35 Wen, L. *et al.* Opto-current-clamp actuation of cortical neurons using a strategically designed channelrhodopsin. *PLoS One* **5**, e12893, doi:10.1371/journal.pone.0012893 (2010).
36 Hegemann, P. & Moglich, A. Channelrhodopsin engineering and exploration of new optogenetic tools. *Nat Methods* **8**, 39-42, doi:10.1038/nmeth.f.327 (2011).
37 Yizhar, O., Fenno, L. E., Davidson, T. J., Mogri, M. & Deisseroth, K. Optogenetics in neural systems. *Neuron* **71**, 9-34, doi:10.1016/j.neuron.2011.06.004 (2011).
38 Levskaya, A., Weiner, O. D., Lim, W. A. & Voigt, C. A. Spatiotemporal control of cell signalling using a light-switchable protein interaction. *Nature* **461**, 997-1001, doi:10.1038/nature08446 (2009).
39 Kennedy, M. *et al.* Rapid blue-light-mediated induction of protein interactions in living cells. *Nat Methods* **7**, 973-U948, doi:10.1038/nmeth.1524|10.1038/NMETH.1524 (2010).
40 Konermann, S. *et al.* Optical control of mammalian endogenous transcription and epigenetic states. *Nature* **500**, 472-476, doi:10.1038/nature12466 (2013).
41 Lin, W., Albanese, C., Pestell, R. G. & Lawrence, D. S. Spatially discrete, light-driven protein expression. *Chem Biol* **9**, 1347-1353 (2002).
42 Young, D. D. & Deiters, A. Photochemical activation of protein expression in bacterial cells. *Angew Chem Int Ed Engl* **46**, 4290-4292, doi:10.1002/anie.200700057 (2007).
43 Cambridge, S. B., Geissler, D., Keller, S. & Curten, B. A caged doxycycline analogue for photoactivated gene expression. *Angew Chem Int Ed Engl* **45**, 2229-2231, doi:10.1002/anie.200503339 (2006).
44 Young, D. D., Garner, R. A., Yoder, J. A. & Deiters, A. Light-activation of gene function in mammalian cells via ribozymes. *Chemical communications*, 568-570, doi:10.1039/b819375d (2009).
45 Umeda, N., Ueno, T., Pohlmeyer, C., Nagano, T. & Inoue, T. A Photocleavable Rapamycin Conjugate for Spatiotemporal Control of Small GTPase Activity. *J Am Chem Soc* **133**, 12-14, doi:10.1021/ja108258d|10.1021/ja108258d (2011).
46 Karginov, A. V. *et al.* Light Regulation of Protein Dimerization and Kinase Activity in Living Cells Using Photocaged Rapamycin and Engineered FKBP. *J Am Chem Soc* **133**, 420-423, doi:10.1021/ja109630v (2011).
47 Lawrence, D. S. The preparation and in vivo applications of caged peptides and proteins. *Curr Opin Chem Biol* **9**, 570-575, doi:10.1016/j.cbpa.2005.09.002 (2005).
48 Lee, H. M., Larson, D. R. & Lawrence, D. S. Illuminating the chemistry of life: design, synthesis, and applications of "caged" and related photoresponsive compounds. *ACS Chem Biol* **4**, 409-427, doi:10.1021/cb900036s (2009).
49 Dawson, P. E. & Kent, S. B. Synthesis of native proteins by chemical ligation. *Annu Rev Biochem* **69**, 923-960, doi:10.1146/annurev.biochem.69.1.923 (2000).
50 Muir, T. W. Semisynthesis of proteins by expressed protein ligation. *Annu Rev Biochem* **72**, 249-289, doi:10.1146/annurev.biochem.72.121801.161900 (2003).
51 Ghosh, M., Ichetovkin, I., Song, X., Condeelis, J. S. & Lawrence, D. S. A new strategy for caging proteins regulated by kinases. *J Am Chem Soc* **124**, 2440-2441 (2002).
52 Ghosh, M. *et al.* Cofilin promotes actin polymerization and defines the direction of cell motility. *Science* **304**, 743-746, doi:10.1126/science.1094561 (2004).
53 Deiters, A., Groff, D., Ryu, Y., Xie, J. & Schultz, P. G. A genetically encoded photocaged tyrosine. *Angew Chem Int Ed Engl* **45**, 2728-2731, doi:10.1002/anie.200600264 (2006).

54 Arbely, E., Torres-Kolbus, J., Deiters, A. & Chin, J. W. Photocontrol of Tyrosine Phosphorylation in Mammalian Cells via Genetic Encoding of Photocaged Tyrosine. *J Am Chem Soc* **134**, 11912-11915, doi:10.1021/ja3046958 (2012).
55 Lemke, E. A., Summerer, D., Geierstanger, B. H., Brittain, S. M. & Schultz, P. G. Control of protein phosphorylation with a genetically encoded photocaged amino acid. *Nat Chem Biol* **3**, 769-772, doi:10.1038/nchembio.2007.44 (2007).
56 Wu, N., Deiters, A., Cropp, T. A., King, D. & Schultz, P. G. A genetically encoded photocaged amino acid. *J Am Chem Soc* **126**, 14306-14307, doi:10.1021/ja040175z (2004).
57 Nguyen, D. P. *et al.* Genetic encoding of photocaged cysteine allows photoactivation of TEV protease in live mammalian cells. *J Am Chem Soc* **136**, 2240-2243, doi:10.1021/ja412191m (2014).
58 Uprety, R. *et al.* Genetic encoding of caged cysteine and caged homocysteine in bacterial and mammalian cells. *Chembiochem* **15**, 1793-1799, doi:10.1002/cbic.201400073 (2014).
59 Meunier, J. R., Sarasin, A. & Marrot, L. Photogenotoxicity of mammalian cells: a review of the different assays for in vitro testing. *Photochemistry and photobiology* **75**, 437-447 (2002).
60 Forman, J., Dietrich, M. & Monroe, W. T. Photobiological and thermal effects of photoactivating UVA light doses on cell cultures. *Photochemical & photobiological sciences : Official journal of the European Photochemistry Association and the European Society for Photobiology* **6**, 649-658, doi:10.1039/b616979a (2007).
61 Robbins, J., Dilworth, S. M., Laskey, R. A. & Dingwall, C. Two interdependent basic domains in nucleoplasmin nuclear targeting sequence: identification of a class of bipartite nuclear targeting sequence. *Cell* **64**, 615-623 (1991).
62 Efthymiadis, A., Shao, H., Hubner, S. & Jans, D. A. Kinetic characterization of the human retinoblastoma protein bipartite nuclear localization sequence (NLS) in vivo and in vitro. A comparison with the SV40 large T-antigen NLS. *J Biol Chem* **272**, 22134-22139 (1997).
63 Luo, J. *et al.* Genetically encoded optochemical probes for simultaneous fluorescence reporting and light activation of protein function with two-photon excitation. *J Am Chem Soc* **136**, 15551-15558, doi:10.1021/ja5055862 (2014).
64 Hemphill, J., Chou, C., Chin, J. W. & Deiters, A. Genetically encoded light-activated transcription for spatiotemporal control of gene expression and gene silencing in mammalian cells. *J Am Chem Soc* **135**, 13433-13439, doi:10.1021/ja4051026 (2013).
65 Gautier, A., Deiters, A. & Chin, J. W. Light-activated kinases enable temporal dissection of signaling networks in living cells. *J Am Chem Soc* **133**, 2124-2127, doi:10.1021/ja1109979 (2011).
66 Cheng, H. C., Qi, R. Z., Paudel, H. & Zhu, H. J. Regulation and function of protein kinases and phosphatases. *Enzyme research* **2011**, 794089, doi:10.4061/2011/794089 (2011).
67 Manning, G., Whyte, D. B., Martinez, R., Hunter, T. & Sudarsanam, S. The protein kinase complement of the human genome. *Science* **298**, 1912-1934, doi:10.1126/science.1075762 (2002).
68 Banaszynski, L. A. & Wandless, T. J. Conditional control of protein function. *Chem Biol* **13**, 11-21, doi:10.1016/j.chembiol.2005.10.010 (2006).

69 Rakhit, R., Navarro, R. & Wandless, T. J. Chemical biology strategies for posttranslational control of protein function. *Chem Biol* **21**, 1238-1252, doi:10.1016/j.chembiol.2014.08.011 (2014).
70 Stein, V. & Alexandrov, K. Synthetic protein switches: design principles and applications. *Trends Biotechnol* **33**, 101-110, doi:10.1016/j.tibtech.2014.11.010 (2015).
71 Wu, Y. I. *et al.* A genetically encoded photoactivatable Rac controls the motility of living cells. *Nature* **461**, 104-108, doi:10.1038/nature08241 (2009).
72 McCubrey, J. A. *et al.* Roles of the Raf/MEK/ERK pathway in cell growth, malignant transformation and drug resistance. *Biochim Biophys Acta* **1773**, 1263-1284, doi:10.1016/j.bbamcr.2006.10.001 (2007).
73 Kim, E. K. & Choi, E. J. Pathological roles of MAPK signaling pathways in human diseases. *Biochim Biophys Acta* **1802**, 396-405, doi:10.1016/j.bbadis.2009.12.009 (2010).
74 Shaul, Y. D. & Seger, R. The MEK/ERK cascade: from signaling specificity to diverse functions. *Biochim Biophys Acta* **1773**, 1213-1226, doi:10.1016/j.bbamcr.2006.10.005 (2007).
75 Perrimon, N. & McMahon, A. P. Negative feedback mechanisms and their roles during pattern formation. *Cell* **97**, 13-16 (1999).
76 Cirit, M., Wang, C. C. & Haugh, J. M. Systematic quantification of negative feedback mechanisms in the extracellular signal-regulated kinase (ERK) signaling network. *J Biol Chem* **285**, 36736-36744, doi:10.1074/jbc.M110.148759 (2010).
77 Toettcher, J. E., Weiner, O. D. & Lim, W. A. Using optogenetics to interrogate the dynamic control of signal transmission by the Ras/Erk module. *Cell* **155**, 1422-1434, doi:10.1016/j.cell.2013.11.004 (2013).
78 Bishop, A. & Hall, A. Rho GTPases and their effector proteins. *Biochemical Journal* **348**, 241-255, doi:10.1042/0264-6021:3480241 (2000).
79 Rougerie, P. & Delon, J. Rho GTPases: Masters of T lymphocyte migration and activation. *Immunology Letters* **142**, 1-13, doi:10.1016/j.imlet.2011.12.003 (2012).
80 Kim, T. H. *et al.* Network-based identification of feedback modules that control RhoA activity and cell migration. *Journal of molecular cell biology* **7**, 242-252, doi:10.1093/jmcb/mjv017 (2015).
81 Ihara, K. *et al.* Crystal structure of human RhoA in a dominantly active form complexed with a GTP analogue. *Journal of Biological Chemistry* **273**, 9656-9666, doi:10.1074/jbc.273.16.9656 (1998).
82 Gautier, A. *et al.* Genetically Encoded Photocontrol of Protein Localization in Mammalian Cells. *Journal of the American Chemical Society* **132**, 4086-4088, doi:10.1021/ja910688s (2010).
83 Bokoch, G. Biology of the p21-activated kinases. *Annual Review of Biochemistry* **72**, 743-781, doi:10.1146/annurev.biochem.72.121801.161742 (2003).
84 Sells, M. A. *et al.* Human p21-activated kinase (Pak1) regulates actin organization in mammalian cells. *Curr Biol* **7**, 202-210 (1997).
85 Nayal, A. *et al.* Paxillin phosphorylation at ser273 localizes a GIT1-PIX-PAK complex and regulates adhesion and protrusion dynamics. *J Cell Biol* **173**, 587-599, doi:10.1083/jcb.200509075 (2006).
86 Delorme, V. *et al.* Cofilin activity downstream of Pak1 regulates cell protrusion efficiency by organizing lamellipodium and lamella actin networks. *Dev Cell* **13**, 646-662, doi:10.1016/j.devcel.2007.08.011 (2007).

87 Delorme-Walker, V. D. *et al.* Pak1 regulates focal adhesion strength, myosin IIA distribution, and actin dynamics to optimize cell migration. *J Cell Biol* **193**, 1289-1303, doi:10.1083/jcb.201010059 (2011).
88 Dhillon, A. S., Hagan, S., Rath, O. & Kolch, W. MAP kinase signalling pathways in cancer. *Oncogene* **26**, 3279-3290, doi:10.1038/sj.onc.1210421 (2007).
89 *Signal Transduction: Pathways, Mechanisms and Diseases*. 429 (Springer, 2010).
90 Ng, Y. W. *et al.* Why an A-loop phospho-mimetic fails to activate PAK1: understanding an inaccessible kinase state by molecular dynamics simulations. *Structure* **18**, 879-890, doi:10.1016/j.str.2010.04.011 (2010).
91 Zhang, S. *et al.* Rho family GTPases regulate p38 mitogen-activated protein kinase through the downstream mediator Pak1. *J Biol Chem* **270**, 23934-23936 (1995).
92 Nayal, A. *et al.* Paxillin phosphorylation at Ser273 localizes a GIT1-PIX-PAK complex and regulates adhesion and protrusion dynamics. *J Cell Biol* **173**, 587-589, doi:10.1083/jcb.200509075 (2006).
93 Emrick, M. A., Hoofnagle, A. N., Miller, A. S., Ten Eyck, L. F. & Ahn, N. G. Constitutive activation of extracellular signal-regulated kinase 2 by synergistic point mutations. *J Biol Chem* **276**, 46469-46479, doi:10.1074/jbc.M107708200 (2001).
94 Diskin, R., Askari, N., Capone, R., Engelberg, D. & Livnah, O. Active mutants of the human p38alpha mitogen-activated protein kinase. *J Biol Chem* **279**, 47040-47049, doi:10.1074/jbc.M404595200 (2004).
95 Robinson, M. J. *et al.* Mutation of position 52 in ERK2 creates a nonproductive binding mode for adenosine 5'-triphosphate. *Biochemistry* **35**, 5641-5646, doi:10.1021/bi952723e (1996).
96 Vandromme, M., Gauthier-Rouviere, C., Lamb, N. & Fernandez, A. Regulation of transcription factor localization: fine-tuning of gene expression. *Trends in biochemical sciences* **21**, 59-64 (1996).
97 Resh, M. D. Trafficking and signaling by fatty-acylated and prenylated proteins. *Nat Chem Biol* **2**, 584-590, doi:nchembio834 [pii]
10.1038/nchembio834 (2006).
98 Hediger, M. A. *et al.* The ABCs of solute carriers: physiological, pathological and therapeutic implications of human membrane transport proteinsIntroduction. P*flugers Archiv : European journal of physiology* 4**47,** 465-468, doi:10.1007/s00424-003-1192-y (2004).
99 Katritch, V., Cherezov, V. & Stevens, R. C. Structure-function of the G protein-coupled receptor superfamily. A*nnual review of pharmacology and toxicology* 5**3,** 531-556, doi:10.1146/annurev-pharmtox-032112-135923 (2013).
100 Abankwa, D., Gorfe, A. A. & Hancock, J. F. Mechanisms of Ras membrane organization and signalling: Ras on a rocker. C*ell cycle* 7**,** 2667-2673 (2008).
101 Mellman, I. & Nelson, W. J. Coordinated protein sorting, targeting and distribution in polarized cells. N*at Rev Mol Cell Biol* 9**,** 833-845, doi:10.1038/nrm2525 (2008).
102 Hung, M. C. & Link, W. Protein localization in disease and therapy. J *Cell Sci* 1**24,** 3381-3392, doi:10.1242/jcs.089110 (2011).
103 Skach, W. R. Defects in processing and trafficking of the cystic fibrosis transmembrane conductance regulator. K*idney international* 5**7,** 825-831, doi:10.1046/j.1523-1755.2000.00921.x (2000).

104 Schaeffer, C., Creatore, A. & Rampoldi, L. Protein trafficking defects in inherited kidney diseases. N*ephrology, dialysis, transplantation : official publication of the European Dialysis and Transplant Association - European Renal Association* **29 Suppl 4,** iv33-44, doi:10.1093/ndt/gfu231 (2014).
105 Wang, X. & Li, S. Protein mislocalization: mechanisms, functions and clinical applications in cancer. B*iochim Biophys Acta* **1846,** 13-25, doi:10.1016/j.bbcan.2014.03.006 (2014).
106 Alberts, B. M*olecular biology of the cell.* 4th edn, (Garland Science, 2002).
107 Gao, J., Liao, J. & Yang, G. Y. CAAX-box protein, prenylation process and carcinogenesis. A*merican journal of translational research* 1**,** 312-325 (2009).
108 Wright, L. P. & Philips, M. R. Thematic review series: lipid posttranslational modifications. CAAX modification and membrane targeting of Ras. J *Lipid Res* **47,** 883-891, doi:R600004-JLR200 [pii]
10.1194/jlr.R600004-JLR200 (2006).
109 Prior, I. A. & Hancock, J. F. Compartmentalization of Ras proteins. J *Cell Sci 1*1**4,** 1603-1608 (2001).
110 Hancock, J. F., Magee, A. I., Childs, J. E. & Marshall, C. J. All ras proteins are polyisoprenylated but only some are palmitoylated. C*ell 5*7**,** 1167-1177, doi:0092-8674(89)90054-8 [pii] (1989).
111 Apolloni, A., Prior, I. A., Lindsay, M., Parton, R. G. & Hancock, J. F. H-ras but not K-ras traffics to the plasma membrane through the exocytic pathway. Mo*l Cell Biol 2*0**,** 2475-2487 (2000).
112 Quilliam, L. A., Khosravi-Far, R., Huff, S. Y. & Der, C. J. Guanine nucleotide exchange factors: activators of the Ras superfamily of proteins. Bi*oessays 1*7**,** 395-404, doi:10.1002/bies.950170507 (1995).
113 Bourne, H. R., Sanders, D. A. & McCormick, F. The GTPase superfamily: conserved structure and molecular mechanism. Na*ture 3*4**9,** 117-127, doi:10.1038/349117a0 (1991).
114 Campbell, S. L., Khosravi-Far, R., Rossman, K. L., Clark, G. J. & Der, C. J. Increasing complexity of Ras signaling. On*cogene 1*7**,** 1395-1413, doi:10.1038/sj.onc.1202174 (1998).
115 Brunsveld, L. e*t al. L*ipidated ras and rab peptides and proteins--synthesis, structure, and function. An*gew Chem Int Ed Engl 4*5**,** 6622-6646, doi:10.1002/anie.200600855 (2006).
116 Repasky, G. A., Chenette, E. J. & Der, C. J. Renewing the conspiracy theory debate: does Raf function alone to mediate Ras oncogenesis? Tr*ends Cell Biol 1*4**,** 639-647, doi:S0962-8924(04)00265-X [pii]
10.1016/j.tcb.2004.09.014 (2004).
117 Konstantinopoulos, P. A., Karamouzis, M. V. & Papavassiliou, A. G. Post-translational modifications and regulation of the RAS superfamily of GTPases as anticancer targets. Nat *Rev Drug Discov 6,* **5**41-555, doi:nrd2221 [pii]
10.1038/nrd2221 (2007).
118 Hancock, J. F. Ras proteins: different signals from different locations. Nat *Rev Mol Cell Biol 4,* 3**7**3-384, doi:nrm1105 [pii]
10.1038/nrm1105 (2003).
119 Buday, L. & Downward, J. Many faces of Ras activation. Bioch*im Biophys Acta 1786*, **178-**187, doi:S0304-419X(08)00024-3 [pii]
10.1016/j.bbcan.2008.05.001 (2008).

120 Khosravi-Far, R. et al. *Ras (*CXXX) and Rab (CC/CXC) prenylation signal sequences are unique and functionally distinct. J Biol *Chem 267, 2***436**3-24368 (1992).
121 Roy, S. et al. *Domin*ant-negative caveolin inhibits H-Ras function by disrupting cholesterol-rich plasma membrane domains. Nat Ce*ll Biol 1, 98-***1**05, doi:10.1038/10067 (1999).
122 Prior, I. A. et al. *GTP-d*ependent segregation of H-ras from lipid rafts is required for biological activity. Nat Ce*ll Biol 3, 36*8-375, doi:35070050 [pii]
10.1038/35070050 (2001).
123 Ahearn, I. M., Haigis, K., Bar-Sagi, D. & Philips, M. R. Regulating the regulator: post-translational modification of RAS. Nat Rev *Mol Cell Biol 13, 39-***51**, doi:10.1038/nrm3255 (2012).
124 Inoue, T., Heo, W. D., Grimley, J. S., Wandless, T. J. & Meyer, T. An inducible translocation strategy to rapidly activate and inhibit small GTPase signaling pathways. Nat Met*hods 2, 415-***4**18, doi:10.1038/nmeth763 (2005).
125 Kennedy, M. J. et al. *Rapid* blue-light-mediated induction of protein interactions in living cells. Nat Met*hods 7, 973-***9**75, doi:10.1038/nmeth.1524 (2010).
126 Abate-Pella, D. et al. *Photoc*hemical modulation of Ras-mediated signal transduction using caged farnesyltransferase inhibitors: activation by one- and two-photon excitation. Chembio*chem 13, 10***9-**1016, doi:10.1002/cbic.201200063 (2012).
127 Misaki, R. et al. *Palmit*oylated Ras proteins traffic through recycling endosomes to the plasma membrane during exocytosis. J Cell *Biol 191, 2*3**-29**, doi:jcb.200911143 [pii]
10.1083/jcb.200911143 (2010).
128 Yasuda, R. et al. *Supers*ensitive Ras activation in dendrites and spines revealed by two-photon fluorescence lifetime imaging. Nat Neur*osci 9, 283-*2**9**1, doi:nn1635 [pii]
10.1038/nn1635 (2006).
129 Ahearn, I. M. et al. F*KBP12 b*inds to acylated H-ras and promotes depalmitoylation. Mol Cell *41, 173-*1**85**, doi:S1097-2765(11)00002-5 [pii]
10.1016/j.molcel.2011.01.001 (2011).
130 Ali, B. R., Nouvel, I., Leung, K. F., Hume, A. N. & Seabra, M. C. A novel statin-mediated "prenylation block-and-release" assay provides insight into the membrane targeting mechanisms of small GTPases. Biochem Bi*ophys Res Commun 397, 34-4*1**,** **d**oi:S0006-291X(10)00936-8 [pii]
10.1016/j.bbrc.2010.05.045 (2010).
131 Hancock, J. F., Cadwallader, K., Paterson, H. & Marshall, C. J. A CAAX or a CAAL motif and a second signal are sufficient for plasma membrane targeting of ras proteins. EMBO J 10, *4033-4*0**39** (1991).
132 Axelrod, D. in Methods in *cell biology Vol. 89 (*eds John J. Correia & H. William Detrich, III) Ch. 7, 169-221 (Elsevier, 2008).
133 Furfine, E. S., Leban, J. J., Landavazo, A., Moomaw, J. F. & Casey, P. J. Protein farnesyltransferase: kinetics of farnesyl pyrophosphate binding and product release. Biochemistr*y 34, 6857-6*8**62** (1995).
134 Rocks, O. et al. The *palmit*oylation machinery is a spatially organizing system for peripheral membrane proteins. Cell 141, 4*58-47***1,** doi:S0092-8674(10)00381-8 [pii]
10.1016/j.cell.2010.04.007 (2010).
135 Long, S. B., Casey, P. J. & Beese, L. S. Reaction path of protein farnesyltransferase at atomic resolution. Nature 419, *645-65***0,** doi:nature00986 [pii]

10.1038/nature00986 (2002).
136 Hougland, J. L. et al. Iden*tificat*ion of novel peptide substrates for protein farnesyltransferase reveals two substrate classes with distinct sequence selectivities. J Mol Biol 3*95, 176-19*0**, d**oi:S0022-2836(09)01278-9 [pii]
10.1016/j.jmb.2009.10.038 (2010).
137 DeGraw, A. J. et al. Caged *protei*n prenyltransferase substrates: tools for understanding protein prenylation. Chem Biol Drug *Des 72, 171-181,* **do**i:10.1111/j.1747-0285.2008.00698.x (2008).
138 DeGraw, A. J. et al. Evalu*ation o*f alkyne-modified isoprenoids as chemical reporters of protein prenylation. Chem Biol Drug *Des 76, 460-471,* **do**i:10.1111/j.1747-0285.2010.01037.x (2010).
139 Tatosyan, A. G. & Mizenina, O. A. Kinases of the Src family: structure and functions. Biochemistry *(Mosc) 65, 49-58, d*o**i:**BCM65010057 [pii] (2000).
140 Boggon, T. J. & Eck, M. J. Structure and regulation of Src family kinases. Oncogene 23, *7918-7927***,** doi:1208081 [pii]
10.1038/sj.onc.1208081 (2004).
141 Thomas, S. M. & Brugge, J. S. Cellular functions regulated by Src family kinases. Annu Rev Cell *Dev Biol 13, 513-609,* d**oi**:10.1146/annurev.cellbio.13.1.513 (1997).
142 Alland, L., Peseckis, S. M., Atherton, R. E., Berthiaume, L. & Resh, M. D. Dual myristylation and palmitylation of Src family member p59fyn affects subcellular localization. J Biol Chem 26*9, 16701-167***05** (1994).
143 McCabe, J. B. & Berthiaume, L. G. Functional roles for fatty acylated amino-terminal domains in subcellular localization. Mol Biol Cell *10, 3771-3786* **(1**999).
144 van't Hof, W. & Resh, M. D. Dual fatty acylation of p59(Fyn) is required for association with the T cell receptor zeta chain through phosphotyrosine-Src homology domain-2 interactions. J Cell Biol 14*5, 377-389* (**199**9).
145 Kaplan, J. M., Mardon, G., Bishop, J. M. & Varmus, H. E. The first seven amino acids encoded by the v-src oncogene act as a myristylation signal: lysine 7 is a critical determinant. Mol Cell Biol *8, 2435-2441* (**1**988).
146 Liang, X., Lu, Y., Wilkes, M., Neubert, T. A. & Resh, M. D. The N-terminal SH4 region of the Src family kinase Fyn is modified by methylation and heterogeneous fatty acylation: role in membrane targeting, cell adhesion, and spreading. J Biol Chem 27*9, 8133-8139***, d**oi:M311180200 [pii]
10.1074/jbc.M311180200 (2004).
147 Sato, I. et al. Differe*ntial t*rafficking of Src, Lyn, Yes and Fyn is specified by the state of palmitoylation in the SH4 domain. J Cell Sci 122, *965-975,* d**oi:**10.1242/jcs.034843 (2009).
148 Ossovskaya, V. S. & Bunnett, N. W. Protease-activated receptors: contribution to physiology and disease. Physiol Rev 84, *579-621, d*o**i:**84/2/579 [pii]
10.1152/physrev.00028.2003 (2004).
149 Sharony, R. et al. Protein *targets* of inflammatory serine proteases and cardiovascular disease. J Inflamm (Lond) *7, 45, doi:1476-***9**255-7-45 [pii]
10.1186/1476-9255-7-45 (2010).
150 Déry, O., Thoma, M. S., Wong, H., Grady, E. F. & Bunnett, N. W. Trafficking of proteinase-activated receptor-2 and beta-arrestin-1 tagged with green fluorescent protein.

beta-Arrestin-dependent endocytosis of a proteinase receptor. J Biol Chem 274, *18524-18535* **(19**99).

151 Shpacovitch, V., Feld, M., Bunnett, N. W. & Steinhoff, M. Protease-activated receptors: novel PARtners in innate immunity. Trends Immunol 28*, 541-550, doi*:**S1**471-4906(07)00234-7 [pii]
10.1016/j.it.2007.09.001 (2007).

152 Al-Ani, B., Wijesuriya, S. J. & Hollenberg, M. D. Proteinase-activated receptor 2: differential activation of the receptor by tethered ligand and soluble peptide analogs. J Pharmacol Exp Th*er 302, 1046-1054 (2*0**02)**.

153 Böhm, S. K. et al. Mechanisms *of des*ensitization and resensitization of proteinase-activated receptor-2. J Biol Chem 271, 2*2003-22016* (**199**6).

154 Al-Ani, B., Hansen, K. K. & Hollenberg, M. D. Proteinase-activated receptor-2: key role of amino-terminal dipeptide residues of the tethered ligand for receptor activation. Mol Pharmacol 65, *149-156, doi:*6**5/**1/149 [pii]
10.1124/mol.65.1.149 (2004).

155 Rutkowska, A. & Schultz, C. Protein tango: the toolbox to capture interacting partners. Angew Chem Int Ed E*ngl 51, 8166-8176, doi*:**10**.1002/anie.201201717 (2012).

156 Blau, C. A., Peterson, K. R., Drachman, J. G. & Spencer, D. M. A proliferation switch for genetically modified cells. Proc Natl Acad Sci *U S A 94, 3076-3081 (199*7**).**

157 Spencer, D. M. et al. Functional *analysi*s of Fas signaling in vivo using synthetic inducers of dimerization. Curr Biol 6, 839-84*7 (1996).*

**1**58 Gross, A., Jockel, J., Wei, M. C. & Korsmeyer, S. J. Enforced dimerization of BAX results in its translocation, mitochondrial dysfunction and apoptosis. EMBO J 17, 3878-388*5, doi*:**10**.1093/emboj/17.14.3878 (1998).

159 Jin, L. et al. Targeted ex*pansion* of genetically modified bone marrow cells. Proc Natl Acad Sci *U S A 95, 8093-8097 (199*8**).**

160 Miyamoto, T. et al. Rapid and o*rthogon*al logic gating with a gibberellin-induced dimerization system. Nat Chem Biol 8, 46*5-470, doi:10*.**1**038/nchembio.922 (2012).

161 Lin, Y. C. et al. Rapidly rev*ersible* manipulation of molecular activity with dual chemical dimerizers. Angew Chem Int Ed E*ngl 52, 6450-6454, doi*:**10**.1002/anie.201301219 (2013).

162 Lin, Y. C. et al. Chemically *induci*ble diffusion trap at cilia reveals molecular sieve-like barrier. Nat Chem Biol 9, 43*7-443, doi:10*.**1**038/nchembio.1252 (2013).

163 Farrar, M. A., Olson, S. H. & Perlmutter, R. M. Coumermycin-induced dimerization of GyrB-containing fusion proteins. Methods Enzymol 327*, 421-429 (2000*)**.**

**1**64 Perron, A. et al. Agonist-ind*epende*nt desensitization and internalization of the human platelet-activating factor receptor by coumermycin-gyrase B-induced dimerization. J Biol Chem 278, 27*956-27965,* d**oi:**10.1074/jbc.M212302200 (2003).

165 Farrar, M. A., Alberol-Ila, J. & Perlmutter, R. M. Activation of the Raf-1 kinase cascade by coumermycin-induced dimerization. Nature 383, 178-181*, doi:*1**0.1**038/383178a0 (1996).

166 O'Farrell, A. M., Liu, Y., Moore, K. W. & Mui, A. L. IL-10 inhibits macrophage activation and proliferation by distinct signaling mechanisms: evidence for Stat3-dependent and -independent pathways. EMBO J 17, 1006-101*8, doi*:**10**.1093/emboj/17.4.1006 (1998).

167 Huang, S., Bjornsti, M. & Houghton, P. Rapamycins - Mechanism of action and cellular resistance. Cancer Biol Ther 2, *222-232 (2003).*
168 Choi, J., Chen, J., Schreiber, S. & Clardy, J. Structure of the FKBP12-rapamycin complex interacting with the binding domain of human FRAP. Science 273, 239-24*2, doi:*1**0.1**126/science.273.5272.239 (1996).
169 Pollock, R. & Clackson, T. Dimerizer-regulated gene expression. Curr Opin Biotechno*l 13, 459-467 (2002)*.
170 Williams, D. J., Puhl, H. L. & Ikeda, S. R. Rapid Modification of Proteins Using a Rapamycin-Inducible Tobacco Etch Virus Protease System. PLoS One 4, doi:e74*74 10.137***1**/journal.pone.0007474 (2009).
171 Jullien, N., Sampieri, F., Enjalbert, A. & Herman, J. P. Regulation of Cre recombinase by ligand-induced complementation of inactive fragments. Nucleic Acids Res 3*1, doi:e131 10.109***3**/nar/gng131 (2003).
172 Zhu, S., Zhang, H. & Matunis, M. SUMO modification through rapamycin-mediated heterodimerization reveals a dual role for Ubc9 in targeting RanGAP1 to nuclear pore complexes. Exp Cell Res 312, 1*042-1049, do*i**:10**.1016/j.yexcr.2005.12.031 (2006).
173 Ho, S., Biggar, S., Spencer, D., Schreiber, S. & Crabtree, G. Dimeric ligands define a role for transcriptional activation domains in reinitiation. Nature 382, 822-826*, doi:*1**0.1**038/382822a0 (1996).
174 Komatsu, T. et al. Organelle-s*pecific*, rapid induction of molecular activities and membrane tethering. Nat Methods 7, 206-*U261, doi:1***0.**1038/NMETH.1428 (2010).
175 Pratt, M., Schwartz, E. & Muir, T. Small-molecule-mediated rescue of protein function by an inducible proteolytic shunt. Proc Natl Acad Sci *USA 104, 11209-11214,* d**oi:**10.1073/pnas.0700816104|10.1073/pnas.070081610 (2007).
176 Putyrski, M. & Schultz, C. Protein Translocation as a Tool: The Current Rapamycin Story. Fed Eur Biochem Soc *Lett 586, 2097-2105 (20*1**2).**
177 Boeckeler, K., Rosse, C., Howell, M. & Parker, P. Manipulating signal delivery - plasma-membrane ERK activation in aPKC-dependent migration. J Cell Sci 123, 2*725-2732, do*i**:10**.1242/jcs.062299 (2010).
178 Bayle, J. H. et al. Rapamycin A*nalogs* with Differential Binding Specificity Permit Orthogonal Control of Protein Activity. Chem Biol 13, 99-10*7 (2006).*
179 Liberles, S., Diver, S., Austin, D. & Schreiber, S. Inducible gene expression and protein translocation using nontoxic ligands identified by a mammalian three-hybrid screen. Proc Natl Acad Sci *USA 94, 7825-7830, doi*:**10**.1073/pnas.94.15.7825 (1997).
180 Sadovski, O. et al. A collectio*n of ca*ged compounds for probing roles of local translation in neurobiology. Bioorg Med Chem 18, *7746-7752, doi*:**10**.1016/j.bmc.2010.04.005 (2010).
181 Laplante, M. & Sabatini, D. M. mTOR signaling at a glance. J Cell Sci 122, 358*9-3594, do*i**:10**.1242/jcs.051011 (2009).
182 Guadliana, M. A. & Truesdell, S. J. (Google Patents, 1996).
183 Karginov, A., Ding, F., Kota, P., Dokholyan, N. & Hahn, K. Engineered allosteric activation of kinases in living cells. Nat Biotechnol 28, *743-U1756, doi*:**10**.1038/nbt.1639 (2010).
184 Harwood, K. & Miller, S. Leveraging a Small-Molecule Modification to Enable the Photoactivation of Rho GTPases. Chembiochem 10, 285*5-2857, doi*:**10**.1002/cbic.200900546 (2009).

185 Brown, K. A. et al. Light-cleav*able ra*pamycin dimer as an optical trigger for protein dimerization. Chemical communicat*ions 51, 5702-5705, doi*:**10**.1039/c4cc09442e (2015).
186 Kapust, R. B. & Waugh, D. S. Controlled Intracellular Processing of Fusion Proteins by TEV Protease. Protein Expression *Purifi 19, 312-318 (2000)*.
**1**87 Tolbert, T., Franke, D. & Wong, C. A new strategy for glycoprotein synthesis: ligation of synthetic glycopeptides with truncated proteins expressed in E-coli as TEV protease cleavable fusion protein. Bioorg Med Chem 13, *909-915, doi:1*0**.1**016/j.bmc.2004.06.047|10.1016/j.bmc.2004.06.047 (2005).
188 Knuesel, M. et al. Identificat*ion of* novel protein-protein interactions using a versatile mammalian tandem affinity purification expression system. Mol Cell Proteomics *2, 1225-1233, doi:*1**0**.1074/mcp.T300007-MCP200|10.1074/mcp.T300007-MCP200 (2003).
189 Yang, X., Gregan, J., Lindner, K., Young, H. & Kearsey, S. Nuclear distribution and chromatin association of DNA polymerase alpha-primase is affected by TEV protease cleavage of Cdc23 (Mcm10) in fission yeast. BMC Mol Biol 6, doi*:10.1186/147*1-2199-6-13|10.1186/1471-2199-6-13 (2005).
190 Wigdal, S. S. et al. A novel bio*lumines*cent protease assay using engineered firefly luciferase. Curr Chem Genomics *2, 16-28, doi:10.2*17**4**/1875397300802010016 (2008).
191 Adams, D., Bliska, J. & Cozzarelli, N. Cre-Lox Recombination in Escherichia-Coli-Cells - Mechanistic Differences from the invitro Reation. J of Mol Biol 226, *661-673, doi:*1**0.1**016/0022-2836(92)90623-R (1992).
192 Laplaza, J., Torres, B., Jin, Y. & Jeffries, T. Sh ble and Cre adapted for functional genomics and metabolic engineering of Pichia stipitis. Enzyme Microb Techn*ol 38, 741-747, doi:1*0**.1**016/j.enzmictec.2005.07.024|10.1016/j.enzmictec.2005.07.024 (2006).
193 Lyznik, L., Gordon-Kamm, W. & Tao, Y. Site-specific recombination for genetic engineering in plants. Plant Cell Rep 21, *925-932, doi:1*0**.1**007/s00299-003-0616-7 (2003).
194 Nagy, A. Cre recombinase: The universal reagent for genome tailoring. Genesis 26, 99-109, *doi:10*.**10**02/(SICI)1526-968X(200002)26:2<99::AID-GENE1>3.0.CO;2-B (2000).
195 Lakso, M. et al. Targeted On*cogene* Activation by Site-Specific Recombination in Transgenic Mice. Proc Natl Acad Sci *USA 89, 6232-6236, doi*:**10**.1073/pnas.89.14.6232 (1992).
196 van der Weyden, L. & Bradley, A. Mouse chromosome engineering for modeling human disease. Annu Rev Genomics H*um Genet 7, 247-276, doi:10*.**1**146/annurev.genom.7.080505.115741|10.1146/annurev.genom.7.080505.115741 (2006).
197 Link, K., Shi, Y. & Koh, J. Light activated recombination. J Am Chem Soc 127, *13088-13089,* d**oi:**10.1021/ja0531226|10.1021/ja0531226 (2005).
198 Edwards, W., Young, D. & Deiters, A. Light-Activated Cre Recombinase as a Tool for the Spatial and Temporal Control of Gene Function in Mammalian Cells. ACS Chem Biol 4, 44*1-445, doi:10*.**1**021/cb900041s (2009).
199 Yang, Y. S. & Hughes, T. E. Cre stoplight: A red/green fluorescent reporter of Cre recombinase expression in living cells. Biotechniques 31, 1*036 (2001)*.
*20***0** Fulton, K., Jackson, S. & Buckle, A. Energetic and structural analysis of the role of tryptophan 59 in FKBP12. Biochemistry 42, 2*364-2372, doi*:**10**.1021/bi020564a (2003).
201 <https://www.neb.com/protocols/1/01/01/pcr-protocol-m0530> (

202 Zheng, L., Baumann, U. & Reymond, J. L. An efficient one-step site-directed and site-saturation mutagenesis protocol. Nucleic Acids Res 3*2, e115, doi:10.1*0**93**/nar/gnh110 (2004).

203 Liu, H. & Naismith, J. H. An efficient one-step site-directed deletion, insertion, single and multiple-site plasmid mutagenesis protocol. BMC biotechnology 8*, 91, doi:10.1186/***1**472-6750-8-91 (2008).